



Accuracy versus precision in boosted top tagging with the ATLAS detector

The ATLAS Collaboration

The identification of top quark decays where the top quark has a large momentum transverse to the beam axis, known as *top tagging*, is a crucial component in many measurements of Standard Model processes and searches for beyond the Standard Model physics at the Large Hadron Collider. Machine learning techniques have improved the performance of top tagging algorithms, but the size of the systematic uncertainties for all proposed algorithms has not been systematically studied. This paper presents the performance of several machine learning based top tagging algorithms on a dataset constructed from simulated proton–proton collision events measured with the ATLAS detector at $\sqrt{s} = 13$ TeV. The systematic uncertainties associated with these algorithms are estimated through an approximate procedure that is not meant to be used in a physics analysis, but is appropriate for the level of precision required for this study. The most performant algorithms are found to have the largest uncertainties, motivating the development of methods to reduce these uncertainties without compromising performance. To enable such efforts in the wider scientific community, the datasets used in this paper are made publicly available.

Contents

1	Introduction	2
2	Monte carlo simulation samples	4
3	Jet reconstruction, selection, and pre-processing	4
4	Top quark taggers	7
4.1	High-level-quantity baseline	8
4.2	Densely connected neural network	8
4.3	Energy flow network	8
4.4	Particle flow network	8
4.5	ResNet 50	9
4.6	ParticleNet	10
5	Tagger performance	10
6	Systematic uncertainties	12
6.1	Experimental uncertainties	13
6.2	Theoretical uncertainties	15
6.3	Validation of uncertainties	17
6.4	Total uncertainties	18
7	Conclusion	19

1 Introduction

Collisions at the Large Hadron Collider (LHC) [1] can produce short-lived heavy Standard Model (SM) particles such as the W and Z bosons, the Higgs boson, and the top quark. These particles often decay to quarks, which later hadronize and are detected as collimated sprays of particles called jets. In the case that the originating particle's momentum transverse to the beam axis (p_T) is large compared to its mass (i.e. it is *boosted*), the decay products are highly collimated in the laboratory frame and are reconstructed as a single jet. The task of distinguishing jets resulting from the decays of heavy particles from the much more numerous jets resulting from light quarks and gluons is known as *boosted jet tagging*. There is a rich history of boosted jet tagging methods at the LHC [2–4]. Recently, the adoption of machine-learning-based algorithms for boosted jet tagging has provided large performance improvements [5, 6]. These algorithms, often called *jet taggers*, have been used in two ways. The first is to make use of *high-level quantities*, which are observables designed to produce different values when the jet is due to the decay of a heavy particle versus due to light quarks and gluons. These are always functions of the kinematic properties of the constituent particles (called *jet constituents*) within a jet, which are experimentally reconstructed from inner detector tracks, calorimeter energy deposits, or some non-trivial combination of the two. A set of high-level quantities is calculated for a given jet, and then used as input to a neural network. The second approach is to directly use the kinematic properties of the constituent particles as input to a neural network (see Ref. [7]). The information contained in a set of high-level quantities is a subset of the information contained in the kinematic properties of the constituent particles, so the second approach has the potential

for higher performance. However, it requires the use of more complex neural networks as there are a varying and possibly large number of constituent particles within a jet.

The performance of the constituent-based approach has been demonstrated [8–13] in the context of highly detailed simulation of the ATLAS [14–16] and CMS [17] detectors, and used to enhance the sensitivity of several physics analyses at the LHC [18–20]. However, open questions remain about the relative size of the systematic uncertainties associated with various constituent-based jet tagging algorithms. The simulated datasets on which ATLAS and CMS train and evaluate ML-based jet tagging algorithms are a useful, but limited approximation of the experimental data gathered by the experiments. There are important differences that can produce different jet tagging efficiencies between simulated and experimental data. These differences in efficiency are accounted for through a measurement of *scale factors*, defined as the ratio of the efficiency in simulated data to the efficiency in experimental data, and its associated uncertainties. These scale factors are required for interpreting the results of any physics analysis in the context of the SM or any beyond the Standard Model (BSM) physics model, so it is crucial to consider the size of scale-factor uncertainties when comparing jet tagging algorithms. Scale-factor measurements are a significant bottleneck in the development of new jet tagging algorithms, as they require access to experimental data and must be independently repeated for each algorithm. As a result they have only been carried out for a few constituent-based taggers [21, 22], and most studies on constituent-based jet tagging have not considered the uncertainties associated with the application of the tagger to experimental data.

This paper presents the performance of several constituent-based taggers, compared to the performance of a baseline high-level-quantity-based tagger, on a benchmark jet tagging task that involves identifying jets originating from the decay of a boosted top quark. This task, known as *top tagging*, is a crucial component of many measurements of SM processes that involve the production of top quarks [23–30] and searches for BSM physics that contain top quarks in their final state [31–36]. It is used as a benchmark jet tagging task since the three-body decay of the top quark produces jets with a distinctive three-subjet radiation pattern, which can be used to distinguish them from the background of jets originating from light quarks and gluons.

Following the performance comparison, the systematic uncertainties associated with the application of each tagger to experimental data are assessed by applying systematic variations directly to the kinematics of the jet constituents used as inputs to the neural networks. The resulting variations in tagger efficiency are used to estimate the size of the systematic uncertainties associated with each tagger. This approach does not require experimental data, and can be easily repeated for an arbitrary tagger by measuring performance on the testing set with the systematic variations. applied, allowing the first comparison of the systematic uncertainties produced by various jet tagging algorithms. However, as will be discussed, there are many simplifying assumptions made in this approach. The resulting systematic uncertainties lack the precision needed for use in a physics analysis, but they do provide a useful estimate of the size of the systematic uncertainties associated with each tagger.

The rest of this paper is organized as follows. The samples of simulated collision events used in this study are described in Section 2, and the subsequent jet reconstruction and event selections are described in Section 3. The various jet taggers considered are described in Section 4, and the performance of the taggers is compared in Section 5. Section 6 describes the procedure used to estimate the systematic uncertainties associated with each tagger, and presents the results. Finally, conclusions are drawn in Section 7.

2 Monte carlo simulation samples

Simulated proton–proton collisions at $\sqrt{s} = 13$ TeV using Monte Carlo (MC) methods are used throughout this study. The nominal samples are generated at leading-order (LO) with PYTHIA8 [37] using the NNPDF2.3LO [38] set of parton distribution functions (PDFs) and the A14 [39] set of tuned parameters. The effects of pile-up are simulated by overlaying inelastic interactions on top of the underlying hard scattering process. All simulated samples are passed through a GEANT4 [40]-based simulation of the ATLAS detector. For more details on the ATLAS detector, see Ref. [14]. Boosted top quarks are selected from simulated events containing the decay of a heavy BSM Z' boson ($Z' \rightarrow t\bar{t}$), with $m_{Z'} = 2$ TeV [41]. The cross section of this process is reweighted to produce an approximately flat jet p_T distribution to efficiently populate the kinematic region $[0.35, 5]$ TeV. Light-quark and gluon jets are selected from simulated events containing the production of high p_T light quarks and gluons through quantum chromodynamic (QCD) processes.

Additional samples of simulated collisions are utilized to assess the uncertainties from the modeling of the parton shower and hadronization processes as described in Section 6.2. These uncertainties for boosted top-quark jets are assessed using simulated collision events containing the production of boosted top quarks through SM processes. Two samples are generated with matrix element calculations performed by the POWHEG BOX v2 [42–45] generator at NLO with the NNPDF3.0NLO [46] PDF set and the h_{damp} parameter¹ set to 1.5 times the mass of the top quark [47]. For both samples the decays of bottom and charm hadrons were performed by EVTGEN 1.6.0 [48]. In one sample the parton shower and hadronization is then modeled with PYTHIA8 [37], and in the other it is modeled with HERWIG7 [49, 50].

The uncertainties from the modeling of the parton shower and hadronization processes in the production of light-quark and gluon jets are assessed using four samples of simulated collisions. All of these samples are generated with matrix element calculations at LO using the NNPDF3.0LO [46] PDF set. The parton shower modeling uncertainty is estimated by comparing performance between samples generated with HERWIG7, one produced with the default angular ordered parton shower model, and the other produced with an alternative dipole parton shower model. The default cluster-based hadronization model is used for both samples [51]. The hadronization model uncertainty is estimated by comparing performance between samples generated with SHERPA2.2 [52], one produced with the default cluster-based hadronization model [51], and the other produced with the SHERPA interface to the Lund string fragmentation model of PYTHIA 6 [53] and its decay tables. The default p_T ordered parton shower model is used for both SHERPA generated samples.

3 Jet reconstruction, selection, and pre-processing

Unified Flow Objects (UFOs) [54] are jet clustering input objects that make use of different ATLAS sub-systems in different kinematic ranges². At low p_T , the inner tracking detector provides exceptional

¹ The h_{damp} parameter is a resummation damping factor and one of the parameters that controls the matching of POWHEG matrix elements to the parton shower and thus effectively regulates the high- p_T radiation against which the $t\bar{t}$ system recoils.

² ATLAS uses a right-handed coordinate system with its origin at the nominal interaction point (IP) in the centre of the detector and the z -axis along the beam pipe. The x -axis points from the IP to the centre of the LHC ring, and the y -axis points upwards. Polar coordinates (r, ϕ) are used in the transverse plane, ϕ being the azimuthal angle around the z -axis. The pseudorapidity is defined in terms of the polar angle θ as $\eta = -\ln \tan(\theta/2)$ and is equal to the rapidity $y = \frac{1}{2} \ln \left(\frac{E+p_z c}{E-p_z c} \right)$ in the relativistic limit. Angular distance is measured in units of $\Delta R \equiv \sqrt{(\Delta y)^2 + (\Delta \phi)^2}$.

Table 1: A summary of the requirements applied on all of the jets in the simulation samples to produce the training and testing sets. The additional top-quark jet requirements constitute the truth labeling strategy, and are only applied to jets taken from the $Z' \rightarrow t\bar{t}$ and SM $t\bar{t}$ samples of simulated events.

Jet requirements	Top-quark jet requirements
$\Delta R(\text{jet}, \text{truth jet}) < 0.75$	$\Delta R(\text{truth jet}, \text{top parton}) < 0.75$
Jet $ \eta_{\text{true}} < 2.0$	Ungroomed truth jet mass > 140 GeV
Jet $p_{\text{T,truth}} > 350$ GeV	Number ghost-associated b -hadrons ≥ 1
Number of constituents ≥ 3	Truth jet $\sqrt{d_{23}} > \exp(3.3 - 6.98 \times 10^{-4} \times \text{truth jet } p_{\text{T}} [\text{GeV}])$
Jet mass > 40 GeV	

spatial and momentum resolution, so low- p_{T} charged constituents are reconstructed from tracks using charged Particle Flow objects (PFO) [55]. At high transverse momentum, the tracking detector’s momentum resolution degrades but it retains high spatial resolution, and so high- p_{T} charged constituents are reconstructed using energy measurements from the calorimeters and spatial measurements from the tracking detector using Track Calo Clusters (TCC) [56]. Electrically neutral constituents are reconstructed as neutral PFOs using measurements from the electromagnetic and hadronic calorimeters. This scheme provides accurate reconstruction of constituent particles across a wide kinematic range.

Both the leading and sub-leading jets in p_{T} in each event are used in these studies. Jets are clustered using the anti- k_r algorithm [57] with a radius parameter of $R = 1.0$, as implemented in the FASTJET package [58]. The Constituent Subtraction [59, 60] and Soft-Killer [61] (CSSK) algorithms are applied to the neutral UFOs to mitigate contamination from any radiation that comes from pile-up collisions rather than the quarks or gluons that initiated the jet. Further, the Soft-Drop algorithm [62] (SD) is applied with parameters $\beta = 1.0$ and $z_{\text{cut}} = 0.1$ to remove soft and wide-angle radiation resulting from pile-up or the underlying event.

Some requirements in the jet selection are placed on the *truth jet*, which is a jet formed from stable particles³ in the simulated event before the detector response is modeled. All jets are required to have a matched truth jet with $\Delta R(\text{jet}, \text{truth jet}) < 0.75$. The jet itself is required to have a mass of at least 40 GeV, and at least three constituents. This last requirement is included to ensure the preprocessing scheme described below is well defined.

Jets in the signal sample must satisfy additional requirements which ensure the jet is due to the decay of a top quark, and the decay products of the top quark are fully contained within the jet. They require that the truth jet be spatially aligned with the observed jet, have a mass greater than 140 GeV, have a ghost-associated bottom hadron [63], and satisfy a p_{T} -dependent requirement on the k_r splitting scale $\sqrt{d_{23}}$ [64]. For more details on these requirements, see Ref. [65]. All of the requirements are summarized in Table 1.

The training and performance of ML models can often be improved by applying *pre-processing* to the data to eliminate irrelevant features and capitalize on well-known symmetries. One set of irrelevant features is the unphysical bumps in the p_{T} spectrum of the background light-quark and gluon jets, which result from

³ The stable particles are required to have a lifetime greater than 10 ps and muons and neutrinos are excluded as they only leave minimal energy within the calorimeter.

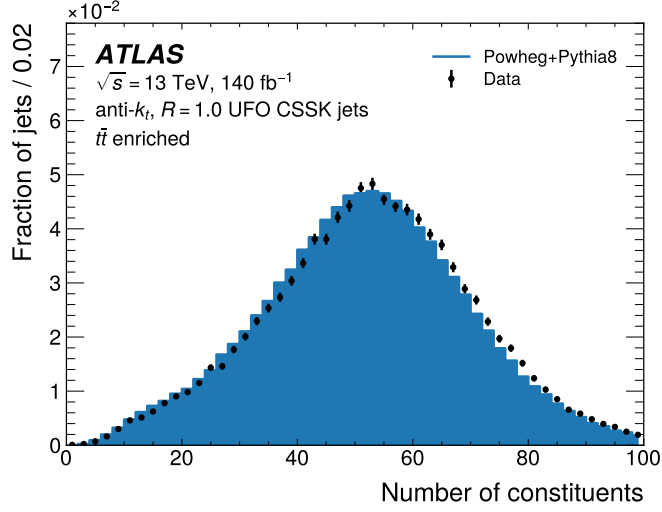


Figure 1: The number of constituents in a sample of jets obtained from the $t\bar{t}$ enriched region described in Ref. [66]. The number of constituents is shown for both the POWHEG BOX v2 +PYTHIA 8 MC sample and experimental data.

the simulation of QCD multijet events in intervals of jet p_T to allow for efficient generation of high- p_T events. A physical p_T spectrum is not required for tagger training. It is only important that the tagger is trained to classify jets from across the desired kinematic range. To achieve this, the background jet p_T spectrum is re-weighted to match the approximately flat signal jet p_T spectrum. Additionally, to a good approximation the probability of a jet to be due to a top quark or to a light quark or gluon is invariant under translations of the jet in the η - ϕ plane, and rotations of the jet about the jet axis. In this study, a pre-processing of the angular coordinates modeled after that used in Ref. [7] is applied to the η and ϕ coordinates of all jet constituents to remove this approximate translational and rotational symmetry. First the coordinates of the jet constituents are shifted such that the highest p_T constituent is located at the origin of the η - ϕ plane. Then the jet is rotated such that the second highest p_T constituent is located on the negative ϕ axis. Finally if the third highest p_T constituent is located in the negative η half-plane, the jet is reflected about the ϕ axis to place it in the positive η half-plane. It is also advantageous to pre-process the constituent p_T and energy values to place them on an $O(1)$ scale. This is done by taking the logarithm of these values. Three other constituent-level quantities are calculated and used as inputs to the constituent-based taggers. The first is the angular distance of the constituent from the jet axis, calculated as

$$R = \sqrt{\eta^2 + \phi^2}, \quad (1)$$

where η and ϕ are taken after the pre-processing. The second (third) is calculated by dividing the constituent p_T (energy) by the total p_T (energy) in the jet, and then taking the logarithm of this fraction. All together, seven constituent-level quantities are used as inputs to the constituent-based taggers: the preprocessed η and ϕ coordinates, the logarithm of the p_T and energy of the constituent, the logarithm of the fraction of the constituent p_T and energy to the total p_T and energy of the jet, and the angular distance of the constituent from the jet axis.

The number of constituents for a selection of jets from the $t\bar{t}$ enriched region described in Ref. [66] is shown in Figure 1 comparing the simulation to a data sample of proton-proton collisions at $\sqrt{s} = 13$ TeV recorded

with the ATLAS detector during Run 2 of the LHC and corresponding to an integrated luminosity of 140 fb^{-1} [67, 68]. Despite the complexity of the ATLAS detector’s calorimetry the number of constituents in data is well modeled by simulation. The jets in this histogram are representative of those entering the signal regions of most analyses targeting boosted top quarks. Each constituent is characterized by a four-vector, so there is an average of around 200 dimensions used as input to the constituent-based taggers. To reduce the memory and compute requirements for training the constituent-based taggers, the number of constituents used as input is limited to 80. Most boosted top jets have fewer than 80 constituents, but those with more are truncated. The effects of this truncation are mitigated by first sorting the constituents by decreasing p_T , ensuring that only the softest constituents are removed.

4 Top quark taggers

The top quark taggers considered in this study are described below. The constituent-based taggers use the four-vectors of the UFOs used to reconstruct the jet as inputs, while the high-level-quantity-based tagger uses the 15 high-level quantities listed in Table 3 as inputs. Information useful for identifying heavy-flavor decays, such as the presence of displaced-vertices, is not used as input to any of the taggers. Instead the taggers are trained to identify the “3-pronged” substructure of boosted top-quark jets. Inclusion of displaced-vertex information in the inputs would likely improve the taggers’ performance, but maximizing performance is not the goal of this study and so this is left for future work. The number of trainable parameters and inference time, defined as the amount of time required to run inference for a batch of 256 jets on an NVIDIA Tesla V100 GPU, are shown for each tagger considered in this study in Table 2. Many other proposed jet tagging algorithms have shown promising performance in the context of simplified jet reconstruction and detector simulation [69–74], but these are not considered in this study. The training, validation, and testing sets consisted of about 9 million, 1 million, and 3.8 million jets respectively, each with equal parts signal and background jets. The taggers were trained and the hyper-parameters were chosen as described in Ref. [8].

Table 2: The number of trainable parameters and inference time for each tagger considered in this study. The inference time is measured using a NVIDIA Tesla V100 GPU.

Tagger	Number of parameters	Inference time
hIDNN	133,381	3 ms
DNN	876,641	3 ms
EFN	959,251	4 ms
PFN	754,501	3 ms
ResNet 50	1,499,585	20 ms
ParticleNet	764,887	143 ms

Table 3: A listing of the 15 quantities used to train the baseline high-level-quantity-based tagger.

Quantity	Symbols	References
N-subjettiness	$\tau_1, \tau_2, \tau_3, \tau_4$	[76] [77]
k_t Splitting Scales	$\sqrt{d_{12}}, \sqrt{d_{23}}$	[78]
Generalized Energy Correlation Functions	$ECF_1, ECF_2, ECF_3, C_2, D_2, L_2, L_3$	[79] [80] [81]
Minimum Pair-wise Invariant Mass	Q_w	[78]
Thrust Major	T_m	[82]

4.1 High-level-quantity baseline

The high-level quantity densely connected neural network tagger (hlDNN) is trained on the 15 high-level quantities listed in Table 3. This tagger is modeled after Ref. [65], and serves as the baseline against which the constituent-based taggers are compared. The network is a standard multi-layer perceptron [75] (MLP).

4.2 Densely connected neural network

The simplest constituent-based tagger is the densely connected neural network (DNN), which is a multi-layer perceptron operating directly on a vector of the constituent information [83]. When there are less than 80 constituents in a jet, this vector contains zero padding which is used as input to the DNN. The DNN has no mechanism for masking these zero padded inputs, meaning it has no *inductive bias*, or specialization to the top tagging task, that naturally accounts for the variable number of jet constituents. The DNN uses all 7 of the pre-processed constituent-level quantities described in Section 3 as inputs.

4.3 Energy flow network

The Energy Flow Network [84] (EFN) is a model specifically engineered for jet tagging. It uses the DeepSets structure [85], which ensures permutation invariance across the jet constituents used as input and naturally handles the variable number of jet constituents. The EFN also uses a p_T weighting mechanism to ensure that lower p_T constituents have lower impact on the output of the network. This p_T weighting can be interpreted as enforcing infrared and collinear (IRC) safety [86]. The output for any of the other networks considered in this study is not IRC safe. The EFN uses the logarithm of the constituent p_T as input to the p_T weighting mechanism, and does not use the constituent energy as input.

4.4 Particle flow network

The particle flow network [84] (PFN) has a very similar structure to the EFN that naturally deals with the variable number of jet constituents and enforces permutation invariance. However it does not use the p_T weighting mechanism, and uses the constituent energy and all other constituent-level quantities described in Section 3 as inputs.

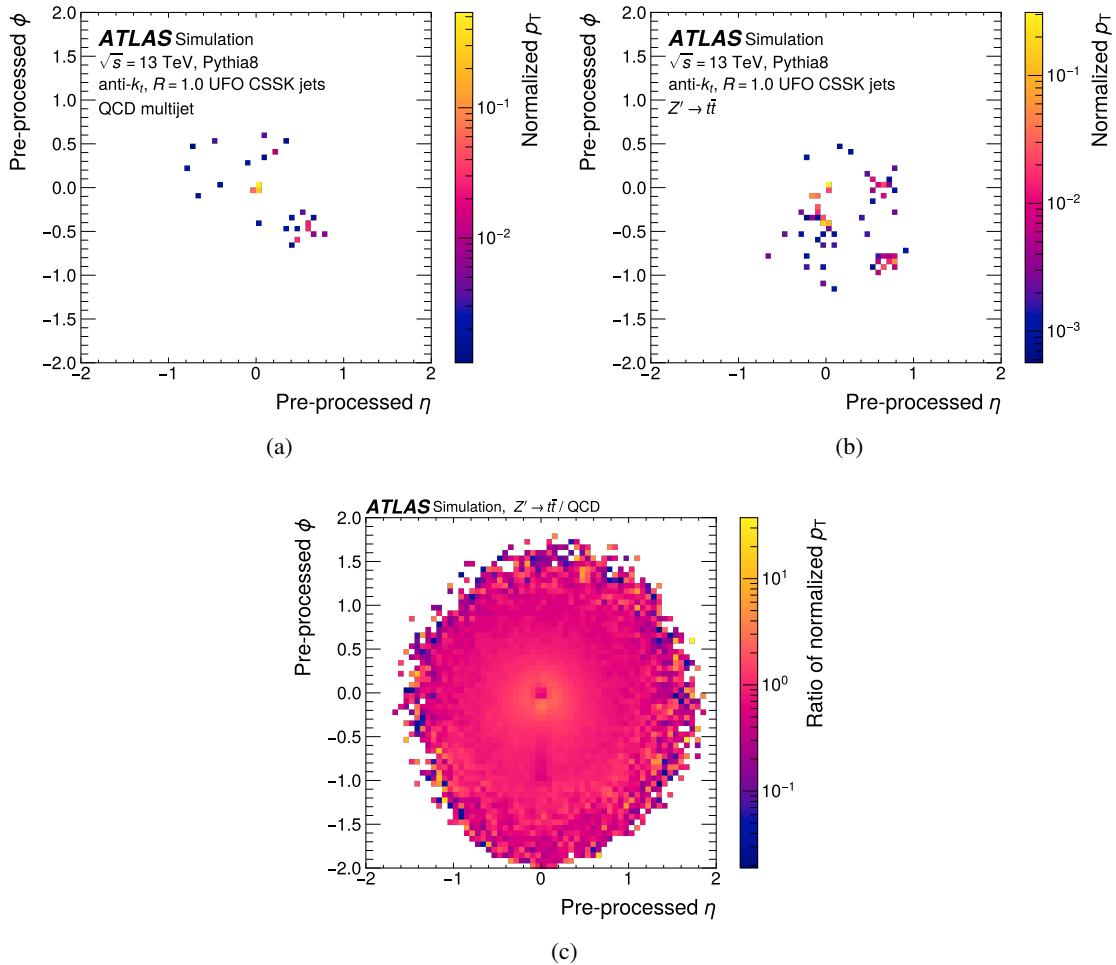


Figure 2: (a) An example background jet image. (b) An example signal jet image. (c) The ratio of the average signal and background jet images.

4.5 ResNet 50

ResNet 50 [87] is a large-scale convolutional neural network (CNN) designed for image classification tasks. CNNs operate on two dimensional arrays whose values give pixel intensity. Noting the similarity between energy deposits in the ATLAS calorimeter and standard two-dimensional images [88–92], the jets are converted into “jet images” by binning each constituent’s η and ϕ coordinates into 64 bins, equally spaced in the range of $[-2, 2]$. The image is then a 64×64 square array where the pixel values are the sum of the raw p_T of the constituents within the pixel, normalized such that the sum of the pixel intensity over the image is one. Pixel intensities are then rescaled by $\log(1 + 100 \times p_T)$ to make lower p_T patterns in the jet substructure visible.

Typically the images produced for single jets are very sparse, with most pixels containing no constituents. Example signal and background jet images are shown in Figure 2, along with an image which shows the ratio of the average signal and background jets. The differences between the average radiation patterns for signal and background jets can be seen in deviations of the ratio from one. An excess of transverse

momentum concentrated just below the origin on the negative ϕ -axis results from the second prong of boosted top jets which is preprocessed to align with this axis. The diffuse excess of transverse momentum distributed around the center is due to the third prong of the boosted top jets. Finally the deficit of transverse momentum in the center of the image is due to the more collimated nature of light-quark and gluon jets.

4.6 ParticleNet

ParticleNet [93] is a graph neural network (GNN) which represents each jet as a graph composed of nodes and edges. Each constituent in a jet is associated with a node, where all of the input quantities are taken as features of the node. In this study, these are the 7 constituent-level quantities defined in Section 3. Each node is connected by an edge to its k nearest neighbors in the η - ϕ plane, where k is a network hyper-parameter. ParticleNet applies a specialized form of the EdgeConv operation [94] to this graph. This operation is similar to the two dimensional convolution used in CNNs, but defined on graphs instead of images.

Like the EFN and PFN, ParticleNet naturally handles the variable lengths of jets and enforces permutation invariance. However the EdgeConv operation acts on the feature vectors of pairs of constituents that are spatially close to each other, rather than each constituent separately. These paired inputs allow ParticleNet to exploit the local relations between constituents.

5 Tagger performance

Performance metrics for the six taggers evaluated on the testing set are shown in Table 4. The metrics are the area under the receiving-operator-characteristic curve (AUC) [95], the fraction of correct predictions (ACC), and the inverse of the background efficiency (background rejection) at two different working points that fix the signal efficiencies to 50% and 80%. The uncertainties in the performance metrics are the quadrature sum of the uncertainty from the finite size of the testing set (statistical uncertainty), and the uncertainty from the random initialization of the weights and the stochastic nature of network training (training uncertainty). The statistical uncertainty is calculated as the standard error of the performance metrics over 100 bootstrap replicas of the testing set [96]. The training uncertainty is calculated by training each network 10 times on the same training set with different weight initializations and batching of training data, and then evaluating the standard error of the performance metrics over the 10 training runs. The differences in the performance metrics between the taggers are larger than the uncertainties in the performance metrics. In all metrics, ParticleNet achieves the best performance, followed by the PFN, the DNN, and the high-level-quantity-based tagger. The EFN and ResNet50 fail to outperform the hIDNN, despite access to the constituent information. The structure of the EFN ensures it is insensitive to low p_T jet constituents, but at the expense of not fully exploiting the available information. The weaker relative performance of ResNet50 is more surprising, given its strong performance on datasets generated with a parametric detector simulation [7]. The parametric detector simulation assumes uniform calorimeter cell granularity. Realistic calorimeters like those used in ATLAS have a non-uniform granularity, which is captured in the high quality simulation used to produce ATLAS simulated data. Building jet images by applying a uniform pixelization to jet constituents in the context of a non-uniform calorimeter granularity could produce non-physical distortions that are not present in simulated events generated with a parametric detector simulation. This could explain the weaker performance of ResNet50 on ATLAS simulated data.

Table 4: The performance of each top quark tagger is measured with several metrics evaluated on the testing set. AUC is the area under the receiving-operator-characteristic curve, ACC is the accuracy, and ε_{bkg}^{-1} is the inverse background efficiency (or background rejection) evaluated at working points which yield a given signal efficiency (ε_{sig}) across the entire testing set. For all metrics, a higher value means better performance, and the table is sorted by increasing AUC. The uncertainty reported on the metrics is the quadrature sum of the uncertainty from the finite statistics of the testing set and the error from the random initialization of network weights and the stochastic nature of network training.

Tagger	AUC	ACC	$\varepsilon_{bkg}^{-1} @ \varepsilon_{sig} = 0.5$	$\varepsilon_{bkg}^{-1} @ \varepsilon_{sig} = 0.8$
ResNet 50	0.872 ± 0.006	0.787 ± 0.006	18.4 ± 1.1	4.63 ± 0.2
EFN	0.894 ± 0.001	0.810 ± 0.001	23.8 ± 0.5	5.74 ± 0.07
hIDNN	0.9374 ± 0.0001	0.8628 ± 0.0002	47.2 ± 0.4	10.36 ± 0.03
DNN	0.9447 ± 0.0004	0.8715 ± 0.0008	73.0 ± 1.3	12.5 ± 0.1
PFN	0.9502 ± 0.0004	0.878 ± 0.001	92.7 ± 1.8	14.6 ± 0.2
ParticleNet	0.9614 ± 0.0005	0.895 ± 0.001	155.8 ± 3.8	20.6 ± 0.4

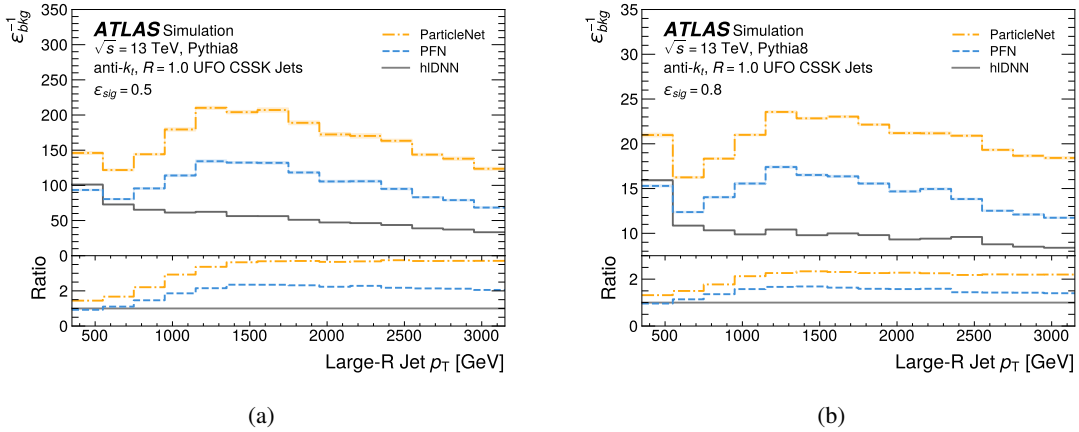


Figure 3: Background rejection, or inverse background efficiency (ε_{bkg}^{-1}), of the hIDNN, PFN, and ParticleNet top quark taggers as a function of the jet p_T at the (a) 50% signal efficiency and (b) 80% signal efficiency working points. Shaded error bands are the quadrature sum of the error from the finite size of the testing set and the error from the random initialization of network weights and the stochastic nature of network training.

The background rejection at the 50% and 80% signal efficiency working points is shown as a function of the jet p_T in Figure 3 for the hIDNN, PFN, and ParticleNet taggers. Unlike the high-level-quantity-based tagger, the constituent-based taggers' performances are best in the mid- p_T range around 1-2 TeV. The high p_T decrease in background rejection is expected, since the higher collimation of jets at high- p_T makes it harder for the tracking detector and calorimeters to resolve the 3-pronged substructure of boosted top jets. The low- p_T increase in background rejection appears for all constituent-based taggers.

6 Systematic uncertainties

Samples of simulated events generated with Monte Carlo methods are a useful model of the experimental data collected by the ATLAS detector for a given physics process, but as important differences between simulated and experimental data can exist, the efficiency of a tagger in experimental data cannot be assumed to be the same as the efficiency in simulated data. To establish the sensitivity of a physics analysis to a SM or BSM process, this difference in efficiency must be known. The standard method to establish this difference is to measure a *scale-factor* and the accompanying uncertainties. Scale-factor measurements are made using samples of signal and background jets collected from experimental data. These samples are not obtainable for difficult-to-isolate SM or any BSM signature in jet substructure, meaning scale-factors cannot be derived in many applications of jet tagging. Scale-factor measurements are also time intensive, making it difficult to measure scale factors for two taggers and then compare the size of the scale factors and their uncertainties.

An alternative approach to constraining the difference in tagger efficiency between simulated and experimental data is to apply a set of *systematic variations* directly to simulated data, which alter the tagger inputs within their uncertainties. These variations produce many systematic varied datasets, and a tagger is then trained on the nominal and evaluated on the nominal and systematic varied datasets. The differences in tagger efficiency between the nominal and systematic varied datasets can then be used to set an uncertainty in the tagger's efficiency in simulated data. Provided the systematic variations account for all possible differences between simulated and experimental data at the level of the tagger inputs, the uncertainty provides an estimate of the expected size of the difference in tagger efficiency.

Differences can be classified into two types: possible mis-modeling of the measurements of the kinematic properties of jet constituents by the ATLAS detector (which produce *experimental uncertainties*), and possible mis-modeling of the underlying physical processes that produce the jets (which produce *theoretical uncertainties*). In this paper, the theoretical uncertainties are assessed by evaluating the tagger efficiency over samples of jets generated with alternative models of the underlying physics processes that produce light quarks, gluons, and top quarks. This is similar to the procedure used in evaluating theoretical uncertainties in scale-factor measurements [66]. The experimental uncertainties are assessed by varying the kinematic properties of the jet constituents within the uncertainties of the ATLAS detector's measurements. These uncertainties are established through auxiliary measurements such as Refs. [97, 98]. This is termed the "bottom-up" approach to experimental uncertainties, which has been used to produce several measurements of jet substructure observables [27, 99, 100]. In practice it is difficult to construct a set of variations that cover all possible experimental uncertainties without over-covering some uncertainties and disregarding others. For this reason the approach of applying systematic variations directly to simulated data is generally less precise than scale-factor measurements, but it offers several advantages. Once the systematically varied datasets are constructed, it is very easy to set uncertainties on the efficiency of an arbitrary tagger, as it only requires running inference over additional datasets. Further, the approach requires no samples of signal and background jets taken from experimental data. This is particularly useful for analyses which use a jet tagger to identify BSM physics signatures.

In this section, the standard approach to theoretical uncertainties is combined with the bottom-up approach to set uncertainties on the background rejection of the taggers. In a realistic physics analysis, scale factors and their uncertainties would be derived for the signal efficiency. This study derives uncertainties on the background rejection to have a single performance metric and its associated uncertainty which can be compared between taggers. Several assumptions are made to simplify the experimental uncertainties assigned in this study which will be mentioned explicitly in the following sections. As a result the

experimental uncertainties are only intended to be an estimate of the relative size of the experimental uncertainties associated with each tagger, and are not meant to be used in a physics analysis.

6.1 Experimental uncertainties

The UFOs used as inputs to the constituent-based taggers can be classified into three types: charged, neutral, and merged [54]. Charged UFOs are simply charged PFOs where an inner detector track [101] is matched to a topological cluster [102] and used to subtract the expected calorimeter energy from the cluster in a process called *cell subtraction*. The properties of charged UFOs are determined by the underlying inner detector track, so a set of systematic variations covering track uncertainties are applied to these objects [103, 104].

Neutral UFOs are the topological clusters which remain after both the cell subtraction procedure in the Particle Flow algorithm, and the splitting procedure in the TCC algorithm. Their properties are primarily determined by the underlying topological cluster, but the inner detector tracks can also affect them through the cell subtraction and TCC splitting procedures. In this paper, the simplifying assumption is made that neutral UFOs are only affected by the underlying topological cluster, and so a set of systematic variations covering topological cluster uncertainties are applied to these objects [27, 98, 100].

Merged UFOs start as charged PFOs where the cell subtraction procedure is disabled due to a large amount of calorimeter activity in the vicinity of the track. The TCC algorithm is then run with these charged PFOs as input. The UFOs this algorithm outputs have their p_T determined by the properties of the underlying topological cluster, and their η and ϕ determined by the properties of the underlying inner detector track. Since merged UFOs have their properties set by a combination of the properties of the underlying inner detector tracks and topological clusters, a selection of the track and topological cluster systematic variations are applied to these objects. This paper makes the simplifying assumption that the η and ϕ coordinates of merged UFOs are determined solely by the properties of the underlying inner detector track, and the p_T and energy of merged UFOs are determined solely by the properties of the underlying topological cluster. This is not strictly true because of the complex interplay between the inner detector tracks and topological clusters in the particle flow and TCC algorithms.

The track uncertainties are covered by three systematic variations: the track fake rate, the tracking efficiency, and the track bias. The track fake rate systematic variation accounts for uncertainty in the rate of tracks produced by chance alignment of signals in the tracking detector. The size of this uncertainty is estimated by studying the non-linear component of the evolution of the number of inner detector tracks with increasing pile-up in experimental data collected through random triggers [101]. The systematic variation selectively drops charged or merged UFOs, which has the effect of decreasing the track fake rate by its uncertainty. An increase in the track fake rate is then covered by symmetrizing the uncertainty in the tagger background rejection.

The tracking efficiency systematic variation accounts for uncertainty in the efficiency of finding true tracks. It contains components that account for limited knowledge of the inner detector material [101], and the merging of tracks within dense tracking environments such as the cores of jets [105]. Like the track fake rate systematic variation, the track efficiency systematic variation drops charged or merged UFOs, but with different probabilities. This has the effect of decreasing the tracking efficiency, and an increase in the efficiency is covered by symmetrizing the uncertainty in the tagger background rejection.

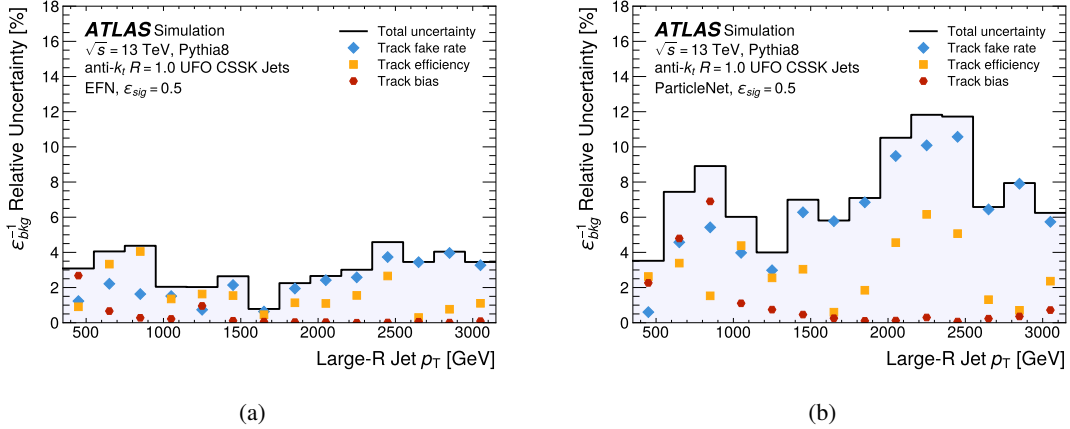


Figure 4: The relative uncertainty in the background rejection due to the track systematic uncertainties as a function of the jet p_T for (a) the EFN and (b) ParticleNet taggers. The total uncertainty is the quadrature sum of all track uncertainties. The fluctuations in the uncertainty result from the finite statistics of the nominal and systematic varied datasets. All uncertainties are evaluated at the 50% signal efficiency working point.

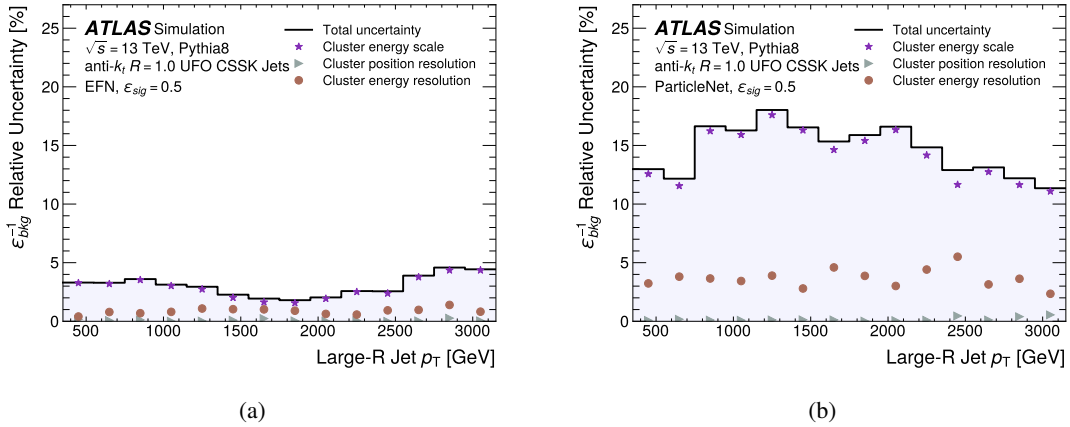


Figure 5: The relative uncertainty in the background rejection due to the cluster systematic uncertainties as a function of the jet p_T for (a) the EFN and (b) ParticleNet taggers. The total uncertainty is the quadrature sum of all cluster uncertainties. All uncertainties are evaluated at the 50% signal efficiency working point.

The track bias systematic variation accounts for possible biases in track p_T measurements due to residual misalignments in the ATLAS tracking detector [106]. This systematic variation biases the ratio of the track's charge to its momentum for charged UFOs, which in turn shifts the UFO p_T . It is only applied to charged UFOs, since merged UFOs have their p_T set by the properties of the underlying topological cluster.

The relative uncertainty in background rejection due to the track uncertainties as a function of the jet p_T is shown in Figure 4 for the EFN and ParticleNet taggers. Fluctuations in the track uncertainties result from the finite statistics of the nominal and systematic varied datasets. For both taggers the track fake rate is the dominant uncertainty in most p_T bins. ParticleNet is found to be more sensitive to the track systematic uncertainties than the EFN.

The cluster uncertainties are covered by three systematic variations: the cluster energy scale, the cluster energy resolution, and the cluster position resolution. The cluster reconstruction efficiency is a negligible source of uncertainty at the p_T scale of the clusters contained within the jets in this study. The cluster energy scale systematic variation accounts for uncertainty in the response of the ATLAS calorimeter. A difference in the cluster energy scale between simulated and experimental data would produce a coherent shift in the energy and p_T measurements of topological clusters toward higher or lower energy. The size of these possible differences is estimated by matching topological clusters to isolated inner detector tracks, and studying the differences between the ratio of the topological cluster’s energy to the inner detector track’s momentum (this quantity is often termed E/p) between simulated and experimental data [97]. The difference in the mean of the E/p distributions between simulated and experimental data gives the cluster energy scale uncertainty. The energy and p_T measurements of the neutral and merged UFOs are then shifted either up or down by an amount within the cluster energy scale uncertainty to create the systematic varied datasets. The final uncertainty is then the maximum of the differences in background rejection between the nominal and the cluster energy scale varied up and down datasets.

The cluster energy resolution systematic variation accounts for uncertainty in the energy resolution of the ATLAS calorimeter. The size of this uncertainty is estimated by comparing the standard deviations of the distributions of E/p between simulated and experimental data. The cluster energy resolution is varied up by an amount within the uncertainty by applying Gaussian smearing to the energy and p_T measurements. It is then varied down by symmetrizing the uncertainty in the tagger efficiency.

Finally, the cluster position resolution systematic variation accounts for uncertainty in the position resolution of the ATLAS calorimeter. The size of this uncertainty is set by comparing the angular coordinates between isolated tracks matched to isolated clusters. Like the cluster energy resolution systematic, the cluster position resolution is varied up by applying Gaussian noise, but it acts on the η and ϕ coordinates instead of the energy and p_T . It is varied down by symmetrizing the uncertainty in the tagger efficiency. This variation is applied only to neutral UFOs since the η and ϕ coordinates of merged UFOs are set by the underlying inner detector track.

In addition to these systematic variations, the taggers may be sensitive to the splitting and merging of topological clusters, where a single particle is reconstructed as two or more clusters, or two or more particles are reconstructed as single cluster. This paper makes the simplifying assumption that this effect, and any other effects that may bias the reconstruction of jet constituents, is negligible.

The relative uncertainty in background rejection due to the cluster uncertainties as a function of the jet p_T is shown in Figure 5 for the EFN and ParticleNet taggers. For both taggers the cluster energy scale uncertainty is dominant in all p_T bins.

6.2 Theoretical uncertainties

Quarks and gluons produced in proton–proton collisions undergo a parton shower and hadronization before they form jets. Given the strongly coupled nature of QCD, the description of the parton shower and hadronization processes within the MC simulation is not exact. The possible differences between simulated and experimental data that result are covered by parton shower and hadronization modeling uncertainties. For the $Z' \rightarrow t\bar{t}$ process used to obtain a sample of boosted top jets, these uncertainties are estimated by evaluating the tagger background rejection with jets obtained from the two samples of simulated SM $t\bar{t}$ events described in Section 2. These are pure signal jets, so to set an uncertainty in the background rejection the requirements which produce a 50% signal efficiency are re-calculated using the jets obtained

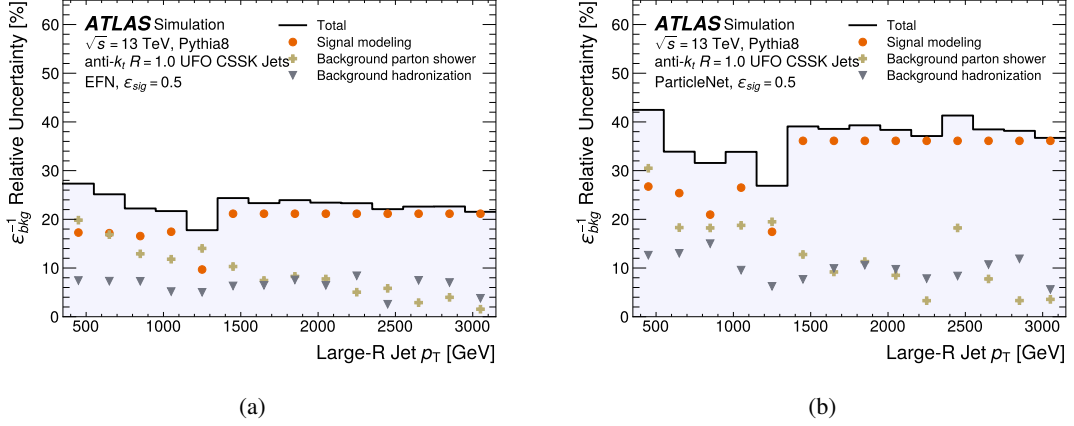


Figure 6: The relative uncertainty in the background rejection due to the parton shower and hadronization modeling as a function of the jet p_T for (a) the EFN and (b) ParticleNet taggers. The total uncertainty is the quadrature sum of all parton shower and hadronization modeling uncertainties. All uncertainties are evaluated at the 50% signal efficiency working point. The uncertainty due to the modeling in the signal process is larger than for the background process, but the signal process uncertainty covers both the parton shower and hadronization modeling uncertainties together.

from the SM $t\bar{t}$ events, and then the background rejection is re-calculated using these requirements. The difference between the background rejections calculated with the two sets of requirements is taken as the uncertainty. Since the SM $t\bar{t}$ process only produces jets in a limited kinematic range, the uncertainty is extrapolated to high p_T by assigning the maximum measured uncertainty to all p_T bins above 1.5 TeV.

For the QCD multijet process used to obtain light-quark and gluon jets, the uncertainty due to the parton shower and hadronization modeling is estimated by comparing background rejections between the four alternative samples described in Section 2. The parton shower modeling uncertainty is estimated by comparing background rejections between the two HERWIG generated samples which differ only by the parton shower model. The hadronization modeling uncertainty is likewise estimated by comparing background rejections between the SHERPA generated samples which differ only by the hadronization model. In both cases the difference in background rejection between the two samples is taken as the uncertainty. In a realistic physics analysis involving top quarks, backgrounds would typically be estimated with data-driven methods instead of with simulated data, so the parton shower and hadronization modeling uncertainties for the QCD multijet process would not be relevant. However the taggers are trained on simulated data, so it is useful to know how the tagger performance is affected by these uncertainties.

The relative uncertainty in background rejection due to the parton shower and hadronization uncertainties as a function of the jet p_T is shown in Figure 6 for the EFN and ParticleNet taggers. Overall the signal process modeling uncertainties are larger than the background process modeling uncertainties. However the signal process uncertainty covers both the parton shower and hadronization modeling uncertainties together. The modeling uncertainties for the background process tend to decrease with increasing jet p_T . The fluctuations in the uncertainties at high p_T , where the uncertainties are small, are due to the finite statistics of the nominal and systematic varied datasets. It is difficult to discern a trend for the modeling uncertainties for the signal process due to the limited kinematic range of the SM $t\bar{t}$ process. As with the experimental uncertainties, ParticleNet is much more sensitive to the parton shower and hadronization modeling uncertainties than the EFN.

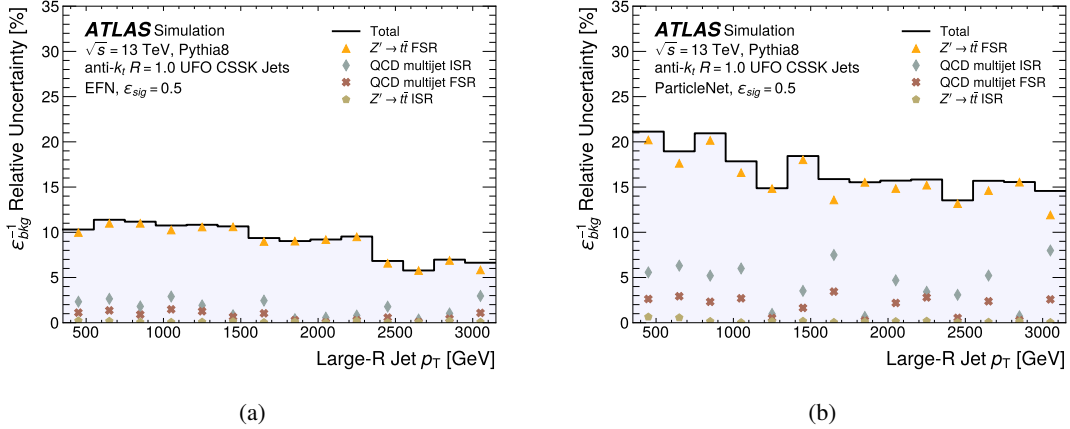


Figure 7: The relative uncertainty in the background rejection due to the choice of renormalization and factorization scales as a function of the jet p_T for (a) the EFN and (b) ParticleNet taggers. The total uncertainty is the quadrature sum of all renormalization and factorization scale uncertainties. All uncertainties are evaluated at the 50% signal efficiency working point.

The fixed-order matrix element calculations used in the simulation of the $Z' \rightarrow t\bar{t}$ and QCD multijet processes require a choice of factorization and renormalization scales to remove divergences. The choice of this scale is unphysical and should not affect the final result of the calculation, but in practice this can happen due to the truncation of the perturbative series. The scale uncertainties cover possible mis-modeling of the underlying physical processes due to the choice of these scales. It is assessed by applying PYTHIA parton shower weights [107] which vary the renormalization and factorization scales for both the initial state radiation (ISR) and final state radiation (FSR) up and down by factors of two. The uncertainty is then estimated by comparing the background rejection of the taggers calculated with the nominal sample to the background rejection calculated with each jet weighted by the relevant shower weight. The uncertainties are then symmetrized by taking the envelope over the up and down variations. This process is performed separately for the $Z' \rightarrow t\bar{t}$ and QCD multijet simulation samples. The relative uncertainty in the background rejection due to the choice of renormalization and factorization scales as a function of the jet p_T is shown in Figure 7 for the EFN and ParticleNet taggers. The fluctuations in these uncertainties are due to the finite statistics of the testing set. Again, ParticleNet is associated with larger uncertainties than the EFN. Both taggers show much larger sensitivity to the FSR scales used in generating the $Z' \rightarrow t\bar{t}$ sample compared to the other scales.

6.3 Validation of uncertainties

To place the uncertainties derived in this study in the context of the scale factor approach utilized by realistic physics analyses, a comparison is made between the two methods for the hIDNN tagger. For comparing uncertainties between taggers, it is useful to calculate uncertainties on the background rejection so that a single metric can be used to characterize both tagger performance and the size of the uncertainties. However physics analyses targeting boosted top-quarks are interested in the uncertainties on the signal efficiency, since backgrounds are typically estimated with data-driven methods. Therefore boosted top tagger scale factors are derived for the signal efficiency, so the uncertainties in this study must be transferred to this quantity for a direct comparison. This excludes the parton shower and hadronization modeling

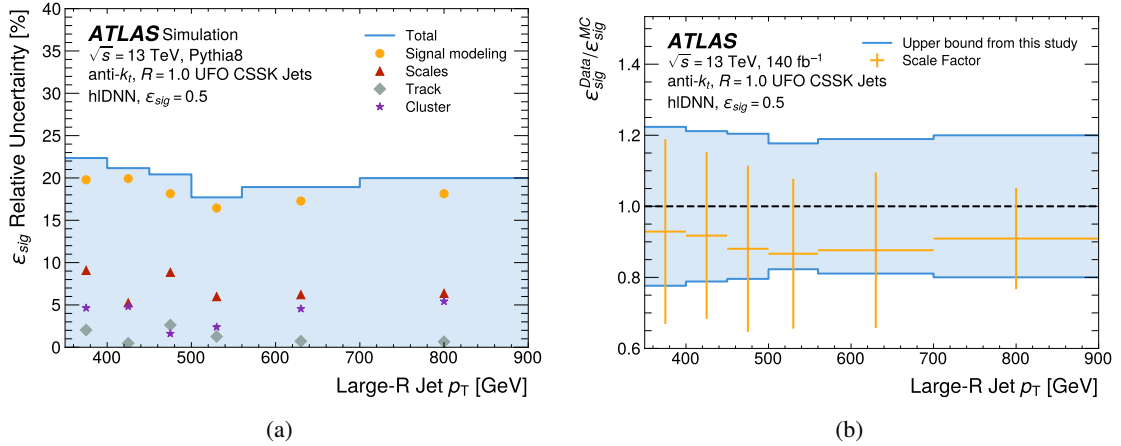


Figure 8: (a) The uncertainty in the signal efficiency for the hIDNN tagger, calculated as the quadrature sum of all uncertainties considered in this study except the parton shower and hadronization modeling uncertainty for the QCD multijet process. (b) A comparison between the total uncertainty derived in this study and the scale factor and its uncertainty for the hIDNN tagger. The scale factor is measured using the same methods as described in Ref. [66]

uncertainty for the QCD multijet process, since it is not relevant for the signal efficiency. The uncertainty budget for the signal efficiency is shown for the hIDNN tagger in Figure 8(a). Within the jet p_T range of [350 – 1000] GeV in which scale factors are derived, the parton shower and hadronization modeling uncertainty for the $Z' \rightarrow t\bar{t}$ process is the dominant uncertainty.

To calculate the scale factor, the signal efficiency in experimental data is measured using the highest p_T large-radius jet in events taken from a semi-leptonic $t\bar{t}$ enriched signal region. The uncertainty in the scale factor is calculated by propagating experimental and theoretical uncertainties through the template fit used to extract the signal efficiency. For details on scale-factor measurements see Ref. [66]. The scale factor is a measurement of the ratio of the signal efficiencies in simulated and experimental data, along with the uncertainty in this ratio. In contrast the uncertainties derived in this study provide an upper bound, or maximum possible value, for the magnitude of the difference in tagger efficiency between simulated and experimental data. The deviation of the scale factors from one should then be smaller than the uncertainties derived in this study. Figure 8(b) shows a comparison between the upper bound on the magnitude of the difference in efficiency derived in this study and the scale factor and its uncertainty for the hIDNN tagger. The upper bound covers the central value of the scale factor in all p_T bins, providing good validation of the approach.

6.4 Total uncertainties

The total uncertainty, calculated as the quadrature sum of all sources of uncertainty described above, is shown as a function of the jet p_T for the EFN and ParticleNet taggers in Figure 9. For both the EFN and ParticleNet, the parton shower and hadronization modeling uncertainties for the $Z' \rightarrow t\bar{t}$ process are the largest in most p_T bins. These are followed by the factorization and renormalization scales and background parton shower and hadronization modeling uncertainties. The total uncertainty as a function of the jet p_T is shown for all constituent-based taggers in Figure 10(a). All taggers have the largest uncertainties at low jet p_T where the theoretical uncertainties produce large and equal contributions to the total uncertainty. Figure 10(b) shows the total uncertainty in the background rejection across the entire p_T range plotted against the

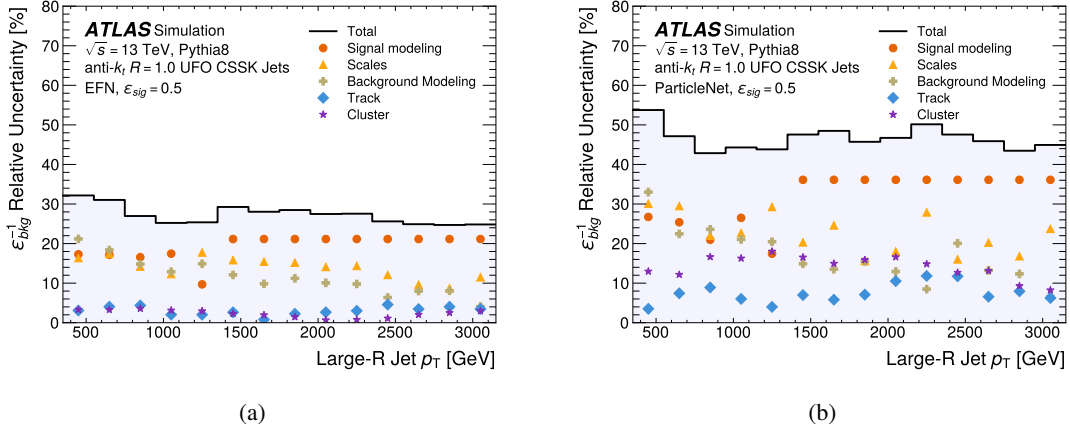


Figure 9: The total uncertainty budget in the background rejection as a function of the jet p_T for (a) the EFN and (b) ParticleNet taggers. All uncertainties are evaluated at the 50% signal efficiency working point.

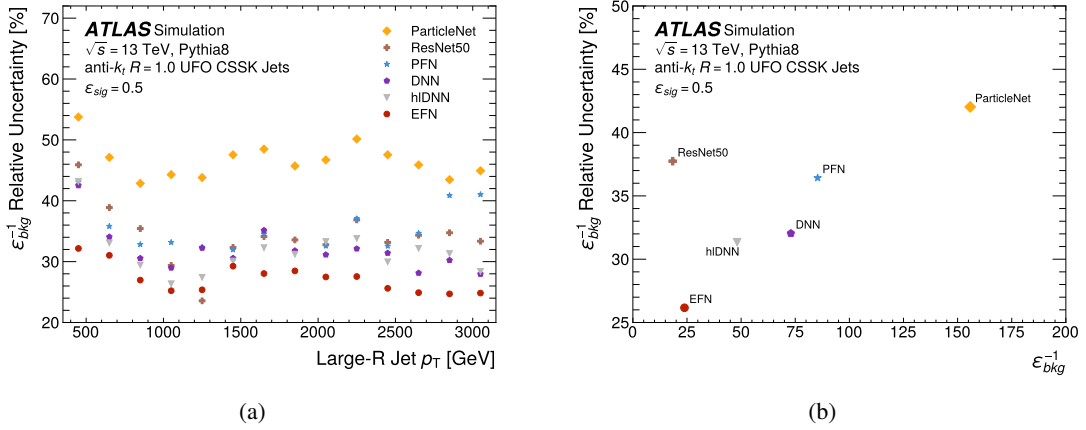


Figure 10: (a) The total uncertainty for each of the constituent-based taggers considered in this study, and (b) the total uncertainty in the background rejection across the entire testing set plotted against the background point for each constituent-based tagger. All uncertainties are evaluated at the 50% signal efficiency working point.

background rejection for all taggers considered. A clear correlation between background rejection and uncertainty in the background rejection is visible, with the most powerful taggers producing the largest uncertainties. The exception to this correlation is ResNet50, which is associated with large uncertainties while also having poor performance.

7 Conclusion

This paper presents the performance of selected constituent-based jet taggers on a top tagging task. Several constituent-based taggers (DNN, PFN, and ParticleNet) outperform the high-level-quantity-based baseline tagger, while the EFN and ResNet50 underperform. This underperformance was not observed in studies

performed with a parametric detector simulation [7], highlighting the importance of developing taggers in the context of realistic detector simulation.

The systematic uncertainties that would result from the application of taggers to experimental data are then probed by applying systematic variations directly to the simulated data. A strong correlation between tagger performance and the size of the uncertainties is observed. The theoretical uncertainties were found to be dominant for all taggers considered. In particular the parton shower and hadronization modeling uncertainties are dominant in most p_T bins for all taggers. Compared with the theoretical uncertainties, the experimental uncertainties are found to be small. The uncertainties derived in this study are not a scale-factor measurement, or uncertainties on a scale factor. The experimental uncertainties rely on simplifying assumptions which ignore possible differences between simulated and experimental data. They should be considered as an illustration of the bottom-up approach to experimental systematic uncertainties, rather than a set of uncertainties that could be used in a physics analysis. However they are useful for establishing the sensitivity of the different taggers to possible differences between simulated and experimental data.

The systematic uncertainties derived in this study stem from performance differences between the nominal and systematic varied datasets. Therefore large uncertainties suggest that large performance differences between the nominal datasets and experimental data are possible. The highly performant jet taggers that produce large systematic uncertainties in this study could have lower performance in experimental data than in simulated data, meaning they would not deliver the sensitivity improvements expected from performance studies which do not consider systematic uncertainties. Even if these performance differences are accounted for by scale-factor measurements, such a degradation in tagger performance is not recoverable. Additionally scale-factor measurements also have uncertainties which are expected to correlate with the uncertainties derived in this study. This was verified by comparing the size of the uncertainties derived for the hiDNN in this study to scale factors and scale-factor uncertainties derived using semi-leptonic $t\bar{t}$ events with the methods described in Ref. [66], and finding good agreement. Scale-factor uncertainties will be included as a systematic uncertainty in any physics analysis which uses a jet tagger, so larger scale-factor uncertainties will also degrade the sensitivity improvements from a more performant tagger.

The size of scale-factor uncertainties relative to other uncertainties in a physics analysis will be highly dependent on the context, so it is difficult to predict if larger scale-factor uncertainties would be limiting for a given physics analysis. In some cases larger scale-factor uncertainties could present a limitation in the sensitivity improvements expected from ML-based jet tagging techniques. Reducing the size of these systematic uncertainties without compromising the tagger performance is then an important direction for future research. Two possible directions are to design taggers which are robust against, or aware of systematic effects [70–74, 108–112], or to train taggers directly on experimental data in a weakly supervised setting [113–115]. To support progress in the first direction and to allow a more realistic assessment of the performance of other existing taggers, the datasets used in this study are made publicly available [116]. This includes all nominal and systematic varied datasets, including the alternative Monte Carlo samples used to assess the parton shower and hadronization modeling uncertainties. Additional documentation is provided, which details how to use the datasets to assess the uncertainties associated with an arbitrary tagger.

Acknowledgements

We thank CERN for the very successful operation of the LHC and its injectors, as well as the support staff at CERN and at our institutions worldwide without whom ATLAS could not be operated efficiently.

The crucial computing support from all WLCG partners is acknowledged gratefully, in particular from CERN, the ATLAS Tier-1 facilities at TRIUMF/SFU (Canada), NDGF (Denmark, Norway, Sweden), CC-IN2P3 (France), KIT/GridKA (Germany), INFN-CNAF (Italy), NL-T1 (Netherlands), PIC (Spain), RAL (UK) and BNL (USA), the Tier-2 facilities worldwide and large non-WLCG resource providers. Major contributors of computing resources are listed in Ref. [117].

We gratefully acknowledge the support of ANPCyT, Argentina; YerPhI, Armenia; ARC, Australia; BMWF and FWF, Austria; ANAS, Azerbaijan; CNPq and FAPESP, Brazil; NSERC, NRC and CFI, Canada; CERN; ANID, Chile; CAS, MOST and NSFC, China; Minciencias, Colombia; MEYS CR, Czech Republic; DNR and DNSRC, Denmark; IN2P3-CNRS and CEA-DRF/IRFU, France; SRNSFG, Georgia; BMBF, HGF and MPG, Germany; GSRI, Greece; RGC and Hong Kong SAR, China; ISF and Benozzi Center, Israel; INFN, Italy; MEXT and JSPS, Japan; CNRST, Morocco; NWO, Netherlands; RCN, Norway; MNiSW, Poland; FCT, Portugal; MNE/IFA, Romania; MESTD, Serbia; MSSR, Slovakia; ARIS and MVZI, Slovenia; DSI/NRF, South Africa; MICIU/AEI, Spain; SRC and Wallenberg Foundation, Sweden; SERI, SNSF and Cantons of Bern and Geneva, Switzerland; NSTC, Taipei; TENMAK, Türkiye; STFC/UKRI, United Kingdom; DOE and NSF, United States of America.

Individual groups and members have received support from BCKDF, CANARIE, CRC and DRAC, Canada; CERN-CZ, FORTE and PRIMUS, Czech Republic; COST, ERC, ERDF, Horizon 2020, ICSC-NextGenerationEU and Marie Skłodowska-Curie Actions, European Union; Investissements d’Avenir Labex, Investissements d’Avenir Idex and ANR, France; DFG and AvH Foundation, Germany; Herakleitos, Thales and Aristeia programmes co-financed by EU-ESF and the Greek NSRF, Greece; BSF-NSF and MINERVA, Israel; NCN and NAWA, Poland; La Caixa Banking Foundation, CERCA Programme Generalitat de Catalunya and PROMETEO and GenT Programmes Generalitat Valenciana, Spain; Göran Gustafssons Stiftelse, Sweden; The Royal Society and Leverhulme Trust, United Kingdom.

In addition, individual members wish to acknowledge support from Armenia: Yerevan Physics Institute (FAPERJ); CERN: European Organization for Nuclear Research (CERN PJAS); Chile: Agencia Nacional de Investigación y Desarrollo (FONDECYT 1230812, FONDECYT 1230987, FONDECYT 1240864); China: Chinese Ministry of Science and Technology (MOST-2023YFA1605700), National Natural Science Foundation of China (NSFC - 12175119, NSFC 12275265, NSFC-12075060); Czech Republic: Czech Science Foundation (GACR - 24-11373S), Ministry of Education Youth and Sports (FORTE CZ.02.01.01/00/22_008/0004632), PRIMUS Research Programme (PRIMUS/21/SCI/017); EU: H2020 European Research Council (ERC - 101002463); European Union: European Research Council (ERC - 948254, ERC 101089007), Horizon 2020 Framework Programme (MUCCA - CHIST-ERA-19-XAI-00), European Union, Future Artificial Intelligence Research (FAIR-NextGenerationEU PE00000013), Italian Center for High Performance Computing, Big Data and Quantum Computing (ICSC, NextGenerationEU); France: Agence Nationale de la Recherche (ANR-20-CE31-0013, ANR-21-CE31-0013, ANR-21-CE31-0022, ANR-22-EDIR-0002), Investissements d’Avenir Labex (ANR-11-LABX-0012); Germany: Baden-Württemberg Stiftung (BW Stiftung-Postdoc Eliteprogramme), Deutsche Forschungsgemeinschaft (DFG - 469666862, DFG - CR 312/5-2); Italy: Istituto Nazionale di Fisica Nucleare (ICSC, NextGenerationEU), Ministero dell’Università e della Ricerca (PRIN - 20223N7F8K - PNRR M4.C2.1.1); Japan: Japan Society for the Promotion of Science (JSPS KAKENHI JP22H01227, JSPS

KAKENHI JP22H04944, JSPS KAKENHI JP22KK0227, JSPS KAKENHI JP23KK0245); Netherlands: Netherlands Organisation for Scientific Research (NWO Veni 2020 - VI.Veni.202.179); Norway: Research Council of Norway (RCN-314472); Poland: Ministry of Science and Higher Education (IDUB AGH, POB8, D4 no 9722), Polish National Agency for Academic Exchange (PPN/PPO/2020/1/00002/U/00001), Polish National Science Centre (NCN 2021/42/E/ST2/00350, NCN OPUS nr 2022/47/B/ST2/03059, NCN UMO-2019/34/E/ST2/00393, UMO-2020/37/B/ST2/01043, UMO-2021/40/C/ST2/00187, UMO-2022/47/O/ST2/00148, UMO-2023/49/B/ST2/04085); Slovenia: Slovenian Research Agency (ARIS grant J1-3010); Spain: Generalitat Valenciana (Artemisa, FEDER, IDIFEDER/2018/048), Ministry of Science and Innovation (MCIN & NextGenEU PCI2022-135018-2, MICIN & FEDER PID2021-125273NB, RYC2019-028510-I, RYC2020-030254-I, RYC2021-031273-I, RYC2022-038164-I), PROMETEO and GenT Programmes Generalitat Valenciana (CIDEAGENT/2019/027); Sweden: Swedish Research Council (Swedish Research Council 2023-04654, VR 2018-00482, VR 2022-03845, VR 2022-04683, VR 2023-03403, VR grant 2021-03651), Knut and Alice Wallenberg Foundation (KAW 2018.0157, KAW 2018.0458, KAW 2019.0447, KAW 2022.0358); Switzerland: Swiss National Science Foundation (SNSF - PCEFP2_194658); United Kingdom: Leverhulme Trust (Leverhulme Trust RPG-2020-004), Royal Society (NIF-R1-231091); United States of America: U.S. Department of Energy (ECA DE-AC02-76SF00515), Neubauer Family Foundation.

References

- [1] L. Evans and P. Bryant, *LHC Machine*, *JINST* **3** (2008) S08001.
- [2] A. Abdesselam et al., *Boosted Objects: A Probe of Beyond the Standard Model Physics*, *Eur. Phys. J. C* **71** (2011) 1661, arXiv: [1012.5412](https://arxiv.org/abs/1012.5412) [hep-ph].
- [3] A. Altheimer et al., *Jet Substructure at the Tevatron and LHC: New results, new tools, new benchmarks*, *J. Phys. G* **39** (2012) 063001, arXiv: [1201.0008](https://arxiv.org/abs/1201.0008) [hep-ph].
- [4] A. Altheimer et al., *Boosted objects and jet substructure at the LHC. Report of BOOST2012, held at IFIC Valencia, 23rd–27th of July 2012*, *Eur. Phys. J. C* **74** (2014) 2792, arXiv: [1311.2708](https://arxiv.org/abs/1311.2708).
- [5] A. J. Larkoski, I. Moult and B. Nachman, *Jet Substructure at the Large Hadron Collider: A Review of Recent Advances in Theory and Machine Learning*, *Phys. Rept.* **841** (2020) 1, arXiv: [1709.04464](https://arxiv.org/abs/1709.04464) [hep-ph].
- [6] D. Guest, K. Cranmer and D. Whiteson, *Deep Learning and its Application to LHC Physics*, *Ann. Rev. Nucl. Part. Sci.* **68** (2018) 161, arXiv: [1806.11484](https://arxiv.org/abs/1806.11484) [hep-ex].
- [7] G. Kasieczka et al., *The Machine Learning landscape of top taggers*, *SciPost Phys.* **7** (2019) 014, arXiv: [1902.09914](https://arxiv.org/abs/1902.09914) [hep-ph].
- [8] ATLAS Collaboration, *Constituent-Based Top-Quark Tagging with the ATLAS Detector*, ATL-PHYS-PUB-2022-039, 2022, URL: <https://cds.cern.ch/record/2825328>.
- [9] ATLAS Collaboration, *Constituent-Based W-boson Tagging with the ATLAS Detector*, ATL-PHYS-PUB-2023-020, 2023, URL: <https://cds.cern.ch/record/2860189>.
- [10] ATLAS Collaboration, *Tagging boosted W bosons applying machine learning to the Lund Jet Plane*, ATL-PHYS-PUB-2023-017, 2023, URL: <https://cds.cern.ch/record/2864131>.

- [11] ATLAS Collaboration, *Transformer Neural Networks for Identifying Boosted Higgs Bosons decaying into $b\bar{b}$ and $c\bar{c}$ in ATLAS*, ATL-PHYS-PUB-2023-021, 2023, URL: <https://cds.cern.ch/record/2866601>.
- [12] ATLAS Collaboration, *Constituent-Based Quark Gluon Tagging using Transformers with the ATLAS detector*, ATL-PHYS-PUB-2023-032, 2023, URL: <https://cds.cern.ch/record/2878932>.
- [13] CMS Collaboration, *Identification of heavy, energetic, hadronically decaying particles using machine-learning techniques*, *JINST* **15** (2020) P06005, arXiv: [2004.08262](https://arxiv.org/abs/2004.08262) [[hep-ex](#)].
- [14] ATLAS Collaboration, *The ATLAS Experiment at the CERN Large Hadron Collider*, *JINST* **3** (2008) S08003.
- [15] ATLAS Collaboration, *The ATLAS Simulation Infrastructure*, *Eur. Phys. J. C* **70** (2010) 823, arXiv: [1005.4568](https://arxiv.org/abs/1005.4568) [[physics.ins-det](#)].
- [16] ATLAS Collaboration, *Software and computing for Run 3 of the ATLAS experiment at the LHC*, (2024), arXiv: [2404.06335](https://arxiv.org/abs/2404.06335) [[hep-ex](#)].
- [17] CMS Collaboration, *The CMS Experiment at the CERN LHC*, *JINST* **3** (2008) S08004.
- [18] CMS Collaboration, *Search for Higgs Boson Decay to a Charm Quark-Antiquark Pair in Proton-Proton Collisions at $\sqrt{s} = 13$ TeV*, *Phys. Rev. Lett.* **131** (2023) 061801, arXiv: [2205.05550](https://arxiv.org/abs/2205.05550) [[hep-ex](#)].
- [19] CMS Collaboration, *Search for Nonresonant Pair Production of Highly Energetic Higgs Bosons Decaying to Bottom Quarks*, *Phys. Rev. Lett.* **131** (2023) 041803, arXiv: [2205.06667](https://arxiv.org/abs/2205.06667) [[hep-ex](#)].
- [20] CMS Collaboration, *Search for a massive scalar resonance decaying to a light scalar and a Higgs boson in the four b quarks final state with boosted topology*, *Phys. Lett. B* **842** (2023) 137392, arXiv: [2204.12413](https://arxiv.org/abs/2204.12413) [[hep-ex](#)].
- [21] ATLAS Collaboration, *Identification of high transverse momentum top quarks in pp collisions at $\sqrt{s} = 8$ TeV with the ATLAS detector*, *JHEP* **06** (2016) 093, arXiv: [1603.03127](https://arxiv.org/abs/1603.03127) [[hep-ex](#)].
- [22] CMS Collaboration, *Performance of heavy-flavour jet identification in boosted topologies in proton-proton collisions at $\sqrt{s} = 13$ TeV*, (2023), URL: <https://cds.cern.ch/record/2866276>.
- [23] ATLAS Collaboration, *Measurement of the charge asymmetry in highly boosted top-quark pair production in $\sqrt{s} = 8$ TeV pp collision data collected by the ATLAS experiment*, *Phys. Lett. B* **756** (2016) 52, arXiv: [1512.06092](https://arxiv.org/abs/1512.06092) [[hep-ex](#)].
- [24] ATLAS Collaboration, *Differential $t\bar{t}$ cross-section measurements using boosted top quarks in the all-hadronic final state with 139 fb^{-1} of ATLAS data*, *JHEP* **04** (2023) 080, arXiv: [2205.02817](https://arxiv.org/abs/2205.02817) [[hep-ex](#)].
- [25] ATLAS Collaboration, *Measurement of jet substructure in boosted $t\bar{t}$ events with the ATLAS detector using 140 fb^{-1} of 13 TeV pp collisions*, (2023), arXiv: [2312.03797](https://arxiv.org/abs/2312.03797) [[hep-ex](#)].
- [26] ATLAS Collaboration, *Measurement of the energy asymmetry in $t\bar{t}j$ production at 13 TeV with the ATLAS experiment and interpretation in the SMEFT framework*, *Eur. Phys. J. C* **82** (2022) 374, arXiv: [2110.05453](https://arxiv.org/abs/2110.05453) [[hep-ex](#)].
- [27] ATLAS Collaboration, *Measurement of jet-substructure observables in top quark, W boson and light jet production in proton-proton collisions at $\sqrt{s} = 13$ TeV with the ATLAS detector*, *JHEP* **08** (2019) 033, arXiv: [1903.02942](https://arxiv.org/abs/1903.02942) [[hep-ex](#)].

- [28] CMS Collaboration, *Measurement of the jet mass in highly boosted $t\bar{t}$ events from pp collisions at $\sqrt{s} = 8$ TeV*, [Eur. Phys. J. C **77** \(2017\) 467](#), arXiv: [1703.06330 \[hep-ex\]](#).
- [29] CMS Collaboration, *Measurement of differential $t\bar{t}$ production cross sections using top quarks at large transverse momenta in pp collisions at $\sqrt{s} = 13$ TeV*, [Phys. Rev. D **103** \(2021\) 052008](#), arXiv: [2008.07860 \[hep-ex\]](#).
- [30] CMS Collaboration, *Measurement of the $t\bar{t}$ charge asymmetry in events with highly Lorentz-boosted top quarks in pp collisions at $\sqrt{s} = 13$ TeV*, [Phys. Lett. B **846** \(2023\) 137703](#), arXiv: [2208.02751 \[hep-ex\]](#).
- [31] CMS Collaboration, *Search for electroweak production of a vector-like quark decaying to a top quark and a Higgs boson using boosted topologies in fully hadronic final states*, [JHEP **04** \(2017\) 136](#), arXiv: [1612.05336 \[hep-ex\]](#).
- [32] ATLAS Collaboration, *Search for single production of a vectorlike T quark decaying into a Higgs boson and top quark with fully hadronic final states using the ATLAS detector*, [Phys. Rev. D **105** \(2022\) 092012](#), arXiv: [2201.07045 \[hep-ex\]](#).
- [33] ATLAS Collaboration, *Search for $t\bar{t}$ resonances in fully hadronic final states in pp collisions at $\sqrt{s} = 13$ TeV with the ATLAS detector*, [JHEP **10** \(2020\) 061](#), arXiv: [2005.05138 \[hep-ex\]](#).
- [34] CMS Collaboration, *Search for a W' boson decaying to a vector-like quark and a top or bottom quark in the all-jets final state at $\sqrt{s} = 13$ TeV*, [JHEP **09** \(2022\) 088](#), arXiv: [2202.12988 \[hep-ex\]](#).
- [35] CMS Collaboration, *Search for single production of a vector-like T quark decaying to a top quark and a Z boson in the final state with jets and missing transverse momentum at $\sqrt{s} = 13$ TeV*, [JHEP **05** \(2022\) 093](#), arXiv: [2201.02227 \[hep-ex\]](#).
- [36] CMS Collaboration, *Search for a heavy resonance decaying to a top quark and a W boson at $\sqrt{s} = 13$ TeV in the fully hadronic final state*, [JHEP **12** \(2021\) 106](#), arXiv: [2104.12853 \[hep-ex\]](#).
- [37] T. Sjöstrand et al., *An introduction to PYTHIA 8.2*, [Comput. Phys. Commun. **191** \(2015\) 159](#), arXiv: [1410.3012 \[hep-ph\]](#).
- [38] NNPDF Collaboration, R. D. Ball et al., *Parton distributions with LHC data*, [Nucl. Phys. B **867** \(2013\) 244](#), arXiv: [1207.1303 \[hep-ph\]](#).
- [39] ATLAS Collaboration, *ATLAS Pythia 8 tunes to 7 TeV data*, ATL-PHYS-PUB-2014-021, 2014, URL: <https://cds.cern.ch/record/1966419>.
- [40] S. Agostinelli et al., *GEANT4 – a simulation toolkit*, [Nucl. Instrum. Meth. A **506** \(2003\) 250](#).
- [41] G. Altarelli, B. Mele and M. Ruiz-Altaba, *Searching for New Heavy Vector Bosons in $p\bar{p}$ Colliders*, [Z. Phys. C **45** \(1989\) 109](#), [Erratum: [Z.Phys.C 47, 676 \(1990\)](#)].
- [42] S. Frixione, G. Ridolfi and P. Nason, *A positive-weight next-to-leading-order Monte Carlo for heavy flavour hadroproduction*, [JHEP **09** \(2007\) 126](#), arXiv: [0707.3088 \[hep-ph\]](#).
- [43] P. Nason, *A new method for combining NLO QCD with shower Monte Carlo algorithms*, [JHEP **11** \(2004\) 040](#), arXiv: [hep-ph/0409146](#).

- [44] S. Frixione, P. Nason and C. Oleari, *Matching NLO QCD computations with parton shower simulations: the POWHEG method*, *JHEP* **11** (2007) 070, arXiv: [0709.2092 \[hep-ph\]](#).
- [45] S. Alioli, P. Nason, C. Oleari and E. Re, *A general framework for implementing NLO calculations in shower Monte Carlo programs: the POWHEG BOX*, *JHEP* **06** (2010) 043, arXiv: [1002.2581 \[hep-ph\]](#).
- [46] NNPDF Collaboration, R. D. Ball et al., *Parton distributions for the LHC run II*, *JHEP* **04** (2015) 040, arXiv: [1410.8849 \[hep-ph\]](#).
- [47] ATLAS Collaboration, *Studies on top-quark Monte Carlo modelling for Top2016*, ATL-PHYS-PUB-2016-020, 2016, URL: <https://cds.cern.ch/record/2216168>.
- [48] D. J. Lange, *The EvtGen particle decay simulation package*, *Nucl. Instrum. Meth. A* **462** (2001) 152.
- [49] J. Bellm et al., *Herwig 7.0/Herwig++ 3.0 release note*, *Eur. Phys. J. C* **76** (2016) 196, arXiv: [1512.01178 \[hep-ph\]](#).
- [50] M. Bähr et al., *Herwig++ Physics and Manual*, *Eur. Phys. J. C* **58** (2008) 639, arXiv: [0803.0883 \[hep-ph\]](#).
- [51] J.-C. Winter, F. Krauss and G. Soff, *A modified cluster-hadronisation model*, *Eur. Phys. J. C* **36** (2004) 381, arXiv: [hep-ph/0311085](#).
- [52] E. Bothmann et al., *Event Generation with Sherpa 2.2*, *SciPost Phys.* **7** (2019) 034, arXiv: [1905.09127 \[hep-ph\]](#).
- [53] T. Sjöstrand, S. Mrenna and P. Skands, *PYTHIA 6.4 physics and manual*, *JHEP* **05** (2006) 026, arXiv: [hep-ph/0603175](#).
- [54] ATLAS Collaboration, *Optimisation of large-radius jet reconstruction for the ATLAS detector in 13 TeV proton–proton collisions*, *Eur. Phys. J. C* **81** (2021) 334, arXiv: [2009.04986 \[hep-ex\]](#).
- [55] ATLAS Collaboration, *Jet reconstruction and performance using particle flow with the ATLAS Detector*, *Eur. Phys. J. C* **77** (2017) 466, arXiv: [1703.10485 \[hep-ex\]](#).
- [56] ATLAS Collaboration, *Improving jet substructure performance in ATLAS using Track-CaloClusters*, ATL-PHYS-PUB-2017-015, 2017, URL: <https://cds.cern.ch/record/2275636>.
- [57] M. Cacciari, G. P. Salam and G. Soyez, *The anti- k_t jet clustering algorithm*, *JHEP* **04** (2008) 063, arXiv: [0802.1189 \[hep-ph\]](#).
- [58] M. Cacciari, G. P. Salam and G. Soyez, *FastJet User Manual*, *Eur. Phys. J. C* **72** (2012) 1896, arXiv: [1111.6097 \[hep-ph\]](#).
- [59] P. Berta, M. Spousta, D. W. Miller and R. Leitner, *Particle-level pileup subtraction for jets and jet shapes*, *JHEP* **06** (2014) 092, arXiv: [1403.3108 \[hep-ex\]](#).
- [60] P. Berta, L. Masetti, D. W. Miller and M. Spousta, *Pileup and Underlying Event Mitigation with Iterative Constituent Subtraction*, *JHEP* **08** (2019) 175, arXiv: [1905.03470 \[hep-ph\]](#).
- [61] M. Cacciari, G. P. Salam and G. Soyez, *SoftKiller, a particle-level pileup removal method*, *Eur. Phys. J. C* **75** (2015) 59, arXiv: [1407.0408 \[hep-ph\]](#).

- [62] A. J. Larkoski, S. Marzani, G. Soyez and J. Thaler, *Soft Drop*, **JHEP** **05** (2014) 146, arXiv: [1402.2657 \[hep-ph\]](#).
- [63] M. Cacciari, G. P. Salam and G. Soyez, *The Catchment Area of Jets*, **JHEP** **04** (2008) 005, arXiv: [0802.1188 \[hep-ph\]](#).
- [64] ATLAS Collaboration, *Measurement of k_T splitting scales in $W \rightarrow \ell\nu$ events at $\sqrt{s} = 7$ TeV with the ATLAS detector*, **Eur. Phys. J. C** **73** (2013) 2432, arXiv: [1302.1415 \[hep-ex\]](#).
- [65] ATLAS Collaboration, *Identification of hadronically-decaying top quarks using UFO jets with ATLAS in Run 2*, ATL-PHYS-PUB-2021-028, 2021, URL: <https://cds.cern.ch/record/2776782>.
- [66] ATLAS Collaboration, *Performance of top-quark and W-boson tagging with ATLAS in Run 2 of the LHC*, **Eur. Phys. J. C** **79** (2019) 375, arXiv: [1808.07858 \[hep-ex\]](#).
- [67] ATLAS Collaboration, *Luminosity determination in pp collisions at $\sqrt{s} = 13$ TeV using the ATLAS detector at the LHC*, **Eur. Phys. J. C** **83** (2023) 982, arXiv: [2212.09379 \[hep-ex\]](#).
- [68] G. Avoni et al., *The new LUCID-2 detector for luminosity measurement and monitoring in ATLAS*, **JINST** **13** (2018) P07017.
- [69] H. Qu, C. Li and S. Qian, *Particle Transformer for Jet Tagging*, (2024), arXiv: [2202.03772 \[hep-ph\]](#).
- [70] A. Bogatskiy, T. Hoffman, D. W. Miller and J. T. Offermann, *PELICAN: Permutation Equivariant and Lorentz Invariant or Covariant Aggregator Network for Particle Physics*, (2022), arXiv: [2211.00454 \[hep-ph\]](#).
- [71] A. Bogatskiy, T. Hoffman, D. W. Miller, J. T. Offermann and X. Liu, *Explainable equivariant neural networks for particle physics: PELICAN*, **JHEP** **03** (2024) 113, arXiv: [2307.16506 \[hep-ph\]](#).
- [72] A. Bogatskiy, T. Hoffman and J. T. Offermann, *19 Parameters Is All You Need: Tiny Neural Networks for Particle Physics*, Advances in neural information processing systems (2023), arXiv: [2310.16121 \[hep-ph\]](#).
- [73] S. Gong et al., *An efficient Lorentz equivariant graph neural network for jet tagging*, **JHEP** **07** (2022) 030, arXiv: [2201.08187 \[hep-ph\]](#).
- [74] C. Li et al., *Does Lorentz-symmetric design boost network performance in jet physics?*, **Phys. Rev. D** **109** (2024) 056003, arXiv: [2208.07814 \[hep-ph\]](#).
- [75] D. E. Rumelhart, G. E. Hinton and R. J. Williams, *Learning representations by back-propagating errors*, **Nature** **323** (1986) 533.
- [76] J. Thaler and K. Van Tilburg, *Identifying Boosted Objects with N-subjettiness*, **JHEP** **03** (2011) 015, arXiv: [1011.2268 \[hep-ph\]](#).
- [77] J. Thaler and K. Van Tilburg, *Maximizing Boosted Top Identification by Minimizing N-subjettiness*, **JHEP** **02** (2012) 093, arXiv: [1108.2701 \[hep-ph\]](#).
- [78] J. Thaler and L.-T. Wang, *Strategies to Identify Boosted Tops*, **JHEP** **07** (2008) 092, arXiv: [0806.0023 \[hep-ph\]](#).

- [79] A. J. Larkoski, G. P. Salam and J. Thaler, *Energy Correlation Functions for Jet Substructure*, [JHEP **06** \(2013\) 108](#), arXiv: [1305.0007 \[hep-ph\]](#).
- [80] I. Moutl, L. Necib and J. Thaler, *New Angles on Energy Correlation Functions*, [JHEP **12** \(2016\) 153](#), arXiv: [1609.07483 \[hep-ph\]](#).
- [81] A. J. Larkoski, I. Moutl and D. Neill, *Power Counting to Better Jet Observables*, [JHEP **12** \(2014\) 009](#), arXiv: [1409.6298 \[hep-ph\]](#).
- [82] C. Chen, *New approach to identifying boosted hadronically decaying particles using jet substructure in its center-of-mass frame*, [Phys. Rev. D **85** \(2012\) 034007](#), arXiv: [1112.2567 \[hep-ph\]](#).
- [83] J. Pearkes, W. Fedorko, A. Lister and C. Gay, *Jet Constituents for Deep Neural Network Based Top Quark Tagging*, (2017), arXiv: [1704.02124 \[hep-ex\]](#).
- [84] P. T. Komiske, E. M. Metodiev and J. Thaler, *Energy Flow Networks: Deep Sets for Particle Jets*, [JHEP **01** \(2019\) 121](#), arXiv: [1810.05165 \[hep-ph\]](#).
- [85] M. Zaheer et al., *Deep sets*, Advances in neural information processing systems (2018), arXiv: [1703.06114 \[cs.LG\]](#).
- [86] P. T. Komiske, E. M. Metodiev and J. Thaler, *Energy flow polynomials: A complete linear basis for jet substructure*, [JHEP **04** \(2018\) 013](#), arXiv: [1712.07124 \[hep-ph\]](#).
- [87] K. He, X. Zhang, S. Ren and J. Sun, *Deep Residual Learning for Image Recognition*, (2015), arXiv: [1512.03385](#).
- [88] J. Cogan, M. Kagan, E. Strauss and A. Schwartzman, *Jet-Images: Computer Vision Inspired Techniques for Jet Tagging*, [JHEP **02** \(2015\) 118](#), arXiv: [1407.5675 \[hep-ph\]](#).
- [89] P. Baldi, K. Bauer, C. Eng, P. Sadowski and D. Whiteson, *Jet Substructure Classification in High-Energy Physics with Deep Neural Networks*, [Phys. Rev. D **93** \(2016\) 094034](#), arXiv: [1603.09349 \[hep-ex\]](#).
- [90] L. de Oliveira, M. Kagan, L. Mackey, B. Nachman and A. Schwartzman, *Jet-images — deep learning edition*, [JHEP **07** \(2016\) 069](#), arXiv: [1511.05190 \[hep-ph\]](#).
- [91] S. Macaluso and D. Shih, *Pulling Out All the Tops with Computer Vision and Deep Learning*, [JHEP **10** \(2018\) 121](#), arXiv: [1803.00107 \[hep-ph\]](#).
- [92] G. Kasieczka, T. Plehn, M. Russell and T. Schell, *Deep-learning Top Taggers or The End of QCD?*, [JHEP **05** \(2017\) 006](#), arXiv: [1701.08784 \[hep-ph\]](#).
- [93] H. Qu and L. Gouskos, *Jet Tagging via Particle Clouds*, [Phys. Rev. D **101** \(2020\) 056019](#), arXiv: [1902.08570 \[hep-ph\]](#).
- [94] Y. Wang et al., *Dynamic Graph CNN for Learning on Point Clouds*, [ACM Transactions On Graphics **38** \(2019\)](#), arXiv: [1801.07829](#).
- [95] F. Melo, ‘Area under the ROC Curve’, *Encyclopedia of Systems Biology*, ed. by W. Dubitzky, O. Wolkenhauer, K.-H. Cho and H. Yokota, New York, NY: Springer New York, 2013 38, ISBN: 978-1-4419-9863-7.

- [96] ATLAS Collaboration, *Evaluating statistical uncertainties and correlations using the bootstrap method*, ATL-PHYS-PUB-2021-011, 2021, URL: <https://cds.cern.ch/record/2759945>.
- [97] ATLAS Collaboration, *A measurement of the calorimeter response to single hadrons and determination of the jet energy scale uncertainty using LHC Run-1 pp-collision data with the ATLAS detector*, *Eur. Phys. J. C* **77** (2017) 26, arXiv: [1607.08842](https://arxiv.org/abs/1607.08842) [hep-ex].
- [98] ATLAS Collaboration, *Measurement of the energy response of the ATLAS calorimeter to charged pions from $W^\pm \rightarrow \tau^\pm(\rightarrow \pi^\pm\nu_\tau)\nu_\tau$ events in Run 2 data*, *Eur. Phys. J. C* **82** (2022) 223, arXiv: [2108.09043](https://arxiv.org/abs/2108.09043) [hep-ex].
- [99] ATLAS Collaboration, *Measurement of the Soft-Drop Jet Mass in pp Collisions at $\sqrt{s} = 13$ TeV with the ATLAS detector*, *Phys. Rev. Lett.* **121** (2018) 092001, arXiv: [1711.08341](https://arxiv.org/abs/1711.08341) [hep-ex].
- [100] ATLAS Collaboration, *Measurement of soft-drop jet observables in pp collisions with the ATLAS detector at $\sqrt{s} = 13$ TeV*, *Phys. Rev. D* **101** (2020) 052007, arXiv: [1912.09837](https://arxiv.org/abs/1912.09837) [hep-ex].
- [101] ATLAS Collaboration, *Early Inner Detector Tracking Performance in the 2015 Data at $\sqrt{s} = 13$ TeV*, ATL-PHYS-PUB-2015-051, 2015, URL: <https://cds.cern.ch/record/2110140>.
- [102] ATLAS Collaboration, *Topological cell clustering in the ATLAS calorimeters and its performance in LHC Run 1*, *Eur. Phys. J. C* **77** (2017) 490, arXiv: [1603.02934](https://arxiv.org/abs/1603.02934) [hep-ex].
- [103] ATLAS Collaboration, *Measurement of the Lund Jet Plane Using Charged Particles in 13 TeV Proton-Proton Collisions with the ATLAS Detector*, *Phys. Rev. Lett.* **124** (2020) 222002, arXiv: [2004.03540](https://arxiv.org/abs/2004.03540) [hep-ex].
- [104] ATLAS Collaboration, *Measurements of Lund subjet multiplicities in 13 TeV proton-proton collisions with the ATLAS detector*, (2024), arXiv: [2402.13052](https://arxiv.org/abs/2402.13052) [hep-ex].
- [105] ATLAS Collaboration, *Performance of the ATLAS track reconstruction algorithms in dense environments in LHC Run 2*, *Eur. Phys. J. C* **77** (2017) 673, arXiv: [1704.07983](https://arxiv.org/abs/1704.07983) [hep-ex].
- [106] ATLAS Collaboration, *Alignment of the ATLAS Inner Detector in Run 2*, *Eur. Phys. J. C* **80** (2020) 1194, arXiv: [2007.07624](https://arxiv.org/abs/2007.07624) [hep-ex].
- [107] S. Mrenna and P. Skands, *Automated Parton-Shower Variations in Pythia 8*, *Phys. Rev. D* **94** (2016) 074005, arXiv: [1605.08352](https://arxiv.org/abs/1605.08352) [hep-ph].
- [108] S. Bright-Thonney, B. Nachman and J. Thaler, *Safe but Incalculable: Energy-weighting is not all you need*, (2024), arXiv: [2311.07652](https://arxiv.org/abs/2311.07652) [hep-ph].
- [109] A. Ghosh, B. Nachman and D. Whiteson, *Uncertainty-aware machine learning for high energy physics*, *Phys. Rev. D* **104** (2021) 056026, arXiv: [2105.08742](https://arxiv.org/abs/2105.08742) [physics.data-an].
- [110] A. Stein, X. Coubez, S. Mondal, A. Novak and A. Schmidt, *Improving Robustness of Jet Tagging Algorithms with Adversarial Training*, *Comput. Softw. Big Sci.* **6** (2022) 15, arXiv: [2203.13890](https://arxiv.org/abs/2203.13890) [physics.data-an].

- [111] A. Butter, B. M. Dillon, T. Plehn and L. Vogel,
Performance versus resilience in modern quark-gluon tagging, *SciPost Phys. Core* **6** (2023) 085,
arXiv: [2212.10493](https://arxiv.org/abs/2212.10493) [[hep-ph](#)].
- [112] A. Ghosh and B. Nachman, *A cautionary tale of decorrelating theory uncertainties*,
Eur. Phys. J. C **82** (2022) 46, arXiv: [2109.08159](https://arxiv.org/abs/2109.08159) [[hep-ph](#)].
- [113] E. M. Metodiev, B. Nachman and J. Thaler,
Classification without labels: Learning from mixed samples in high energy physics,
JHEP **10** (2017) 174, arXiv: [1708.02949](https://arxiv.org/abs/1708.02949) [[hep-ph](#)].
- [114] M. J. Dolan, J. Gargalionis and A. Ore,
Quark-versus-gluon tagging in CMS Open Data with CWoLa and TopicFlow, (2023),
arXiv: [2312.03434](https://arxiv.org/abs/2312.03434) [[hep-ph](#)].
- [115] CMS Collaboration, *Measurement of the $t\bar{t}b\bar{b}$ production cross section in the all-jet final state in pp collisions at $\sqrt{s} = 13$ TeV*, *Phys. Lett. B* **803** (2020) 135285, arXiv: [1909.05306](https://arxiv.org/abs/1909.05306) [[hep-ex](#)].
- [116] ATLAS Collaboration, *ATLAS top tagging open data set with systematic uncertainties*,
URL: <http://doi.org/10.7483/OPENDATA.ATLAS.SOAY.LABE>.
- [117] ATLAS Collaboration, *ATLAS Computing Acknowledgements*, ATL-SOFT-PUB-2023-001, 2023,
URL: <https://cds.cern.ch/record/2869272>.

The ATLAS Collaboration

G. Aad ¹⁰⁴, E. Aakvaag ¹⁷, B. Abbott ¹²³, S. Abdelhameed ^{119a}, K. Abeling ⁵⁶, N.J. Abicht ⁵⁰, S.H. Abidi ³⁰, M. Aboeela ⁴⁵, A. Abouhorma ^{36e}, H. Abramowicz ¹⁵⁴, H. Abreu ¹⁵³, Y. Abulaiti ¹²⁰, B.S. Acharya ^{70a,70b,1}, A. Ackermann ^{64a}, C. Adam Bourdarios ⁴, L. Adamczyk ^{87a}, S.V. Addepalli ²⁷, M.J. Addison ¹⁰³, J. Adelman ¹¹⁸, A. Adiguzel ^{22c}, T. Adye ¹³⁷, A.A. Affolder ¹³⁹, Y. Afik ⁴⁰, M.N. Agaras ¹³, J. Agarwala ^{74a,74b}, A. Aggarwal ¹⁰², C. Agheorghiesei ^{28c}, F. Ahmadov ^{39,x}, W.S. Ahmed ¹⁰⁶, S. Ahuja ⁹⁷, X. Ai ^{63e}, G. Aielli ^{77a,77b}, A. Aikot ¹⁶⁶, M. Ait Tamlhat ^{36e}, B. Aitbenkikh ^{36a}, M. Akbiyik ¹⁰², T.P.A. Åkesson ¹⁰⁰, A.V. Akimov ³⁸, D. Akiyama ¹⁷¹, N.N. Akolkar ²⁵, S. Aktas ^{22a}, K. Al Houry ⁴², G.L. Alberghi ^{24b}, J. Albert ¹⁶⁸, P. Albicocco ⁵⁴, G.L. Albouy ⁶¹, S. Alderweireldt ⁵³, Z.L. Alegria ¹²⁴, M. Aleksa ³⁷, I.N. Aleksandrov ³⁹, C. Alexa ^{28b}, T. Alexopoulos ¹⁰, F. Alfonsi ^{24b}, M. Algren ⁵⁷, M. Alhroob ¹⁷⁰, B. Ali ¹³⁵, H.M.J. Ali ⁹³, S. Ali ³², S.W. Alibocus ⁹⁴, M. Aliev ^{34c}, G. Alimonti ^{72a}, W. Alkahi ⁵⁶, C. Allaire ⁶⁷, B.M.M. Allbrooke ¹⁴⁹, J.F. Allen ⁵³, C.A. Allendes Flores ^{140f}, P.P. Allport ²¹, A. Aloisio ^{73a,73b}, F. Alonso ⁹², C. Alpigiani ¹⁴¹, Z.M.K. Alsolami ⁹³, M. Alvarez Estevez ¹⁰¹, A. Alvarez Fernandez ¹⁰², M. Alves Cardoso ⁵⁷, M.G. Alvigi ^{73a,73b}, M. Aly ¹⁰³, Y. Amaral Coutinho ^{84b}, A. Ambler ¹⁰⁶, C. Amelung ³⁷, M. Amerl ¹⁰³, C.G. Ames ¹¹¹, D. Amidei ¹⁰⁸, B. Amini ⁵⁵, K.J. Amirie ¹⁵⁸, S.P. Amor Dos Santos ^{133a}, K.R. Amos ¹⁶⁶, S. An ⁸⁵, V. Ananiev ¹²⁸, C. Anastopoulos ¹⁴², T. Andeen ¹¹, J.K. Anders ³⁷, A.C. Anderson ⁶⁰, S.Y. Andreev ^{48a,48b}, A. Andreatza ^{72a,72b}, S. Angelidakis ⁹, A. Angerami ⁴², A.V. Anisenkov ³⁸, A. Annovi ^{75a}, C. Antel ⁵⁷, E. Antipov ¹⁴⁸, M. Antonelli ⁵⁴, F. Anulli ^{76a}, M. Aoki ⁸⁵, T. Aoki ¹⁵⁶, M.A. Aparo ¹⁴⁹, L. Aperio Bella ⁴⁹, C. Appelt ¹⁹, A. Apyan ²⁷, S.J. Arbiol Val ⁸⁸, C. Arcangeletti ⁵⁴, A.T.H. Arce ⁵², J-F. Arguin ¹¹⁰, S. Argyropoulos ⁵⁵, J.-H. Arling ⁴⁹, O. Arnaez ⁴, H. Arnold ¹⁴⁸, G. Artoni ^{76a,76b}, H. Asada ¹¹³, K. Asai ¹²¹, S. Asai ¹⁵⁶, N.A. Asbah ³⁷, R.A. Ashby Pickering ¹⁷⁰, K. Assamagan ³⁰, R. Astalos ^{29a}, K.S.V. Astrand ¹⁰⁰, S. Atashi ¹⁶², R.J. Atkin ^{34a}, M. Atkinson ¹⁶⁵, H. Atmani ^{36f}, P.A. Atlasiddha ¹³¹, K. Augsten ¹³⁵, S. Auricchio ^{73a,73b}, A.D. Auriol ²¹, V.A. Austrup ¹⁰³, G. Avolio ³⁷, K. Axiotis ⁵⁷, G. Azuelos ^{110,ac}, D. Babal ^{29b}, H. Bachacou ¹³⁸, K. Bachas ^{155,p}, A. Bachiu ³⁵, F. Backman ^{48a,48b}, A. Badea ⁴⁰, T.M. Baer ¹⁰⁸, P. Bagnaia ^{76a,76b}, M. Bahmani ¹⁹, D. Bahner ⁵⁵, K. Bai ¹²⁶, J.T. Baines ¹³⁷, L. Baines ⁹⁶, O.K. Baker ¹⁷⁵, E. Bakos ¹⁶, D. Bakshi Gupta ⁸, L.E. Balabram Filho ^{84b}, V. Balakrishnan ¹²³, R. Balasubramanian ¹¹⁷, E.M. Baldin ³⁸, P. Balek ^{87a}, E. Ballabene ^{24b,24a}, F. Balli ¹³⁸, L.M. Baltes ^{64a}, W.K. Balunas ³³, J. Balz ¹⁰², I. Bamwidhi ^{119b}, E. Banas ⁸⁸, M. Bandieramonte ¹³², A. Bandyopadhyay ²⁵, S. Bansal ²⁵, L. Barak ¹⁵⁴, M. Barakat ⁴⁹, E.L. Barberio ¹⁰⁷, D. Barberis ^{58b,58a}, M. Barbero ¹⁰⁴, M.Z. Barel ¹¹⁷, T. Barillari ¹¹², M-S. Barisits ³⁷, T. Barklow ¹⁴⁶, P. Baron ¹²⁵, D.A. Baron Moreno ¹⁰³, A. Baroncelli ^{63a}, A.J. Barr ¹²⁹, J.D. Barr ⁹⁸, F. Barreiro ¹⁰¹, J. Barreiro Guimarães da Costa ¹⁴, U. Barron ¹⁵⁴, M.G. Barros Teixeira ^{133a}, S. Barsov ³⁸, F. Bartels ^{64a}, R. Bartoldus ¹⁴⁶, A.E. Barton ⁹³, P. Bartos ^{29a}, A. Basan ¹⁰², M. Baselga ⁵⁰, A. Bassalat ^{67,b}, M.J. Basso ^{159a}, S. Bataju ⁴⁵, R. Bate ¹⁶⁷, R.L. Bates ⁶⁰, S. Batlamous ¹⁰¹, B. Batool ¹⁴⁴, M. Battaglia ¹³⁹, D. Battulga ¹⁹, M. Bauce ^{76a,76b}, M. Bauer ⁸⁰, P. Bauer ²⁵, L.T. Bazzano Hurrell ³¹, J.B. Beacham ⁵², T. Beau ¹³⁰, J.Y. Beaucamp ⁹², P.H. Beauchemin ¹⁶¹, P. Bechtel ²⁵, H.P. Beck ^{20,o}, K. Becker ¹⁷⁰, A.J. Beddall ⁸³, V.A. Bednyakov ³⁹, C.P. Bee ¹⁴⁸, L.J. Beemster ¹⁶, T.A. Beermann ³⁷, M. Begalli ^{84d}, M. Begel ³⁰, A. Behera ¹⁴⁸, J.K. Behr ⁴⁹, J.F. Beirer ³⁷, F. Beisiegel ²⁵, M. Belfkir ^{119b}, G. Bella ¹⁵⁴, L. Bellagamba ^{24b}, A. Bellerive ³⁵, P. Bellos ²¹, K. Beloborodov ³⁸, D. Benckekroun ^{36a}, F. Bendebba ^{36a}, Y. Benhammou ¹⁵⁴,

K.C. Benkendorfer ⁶², L. Beresford ⁴⁹, M. Beretta ⁵⁴, E. Bergeaas Kuutmann ¹⁶⁴, N. Berger ⁴,
 B. Bergmann ¹³⁵, J. Beringer ^{18a}, G. Bernardi ⁵, C. Bernius ¹⁴⁶, F.U. Bernlochner ²⁵,
 F. Bernon ^{37,104}, A. Berrocal Guardia ¹³, T. Berry ⁹⁷, P. Berta ¹³⁶, A. Berthold ⁵¹, S. Bethke ¹¹²,
 A. Betti ^{76a,76b}, A.J. Bevan ⁹⁶, N.K. Bhalla ⁵⁵, S. Bhatta ¹⁴⁸, D.S. Bhattacharya ¹⁶⁹,
 P. Bhattarai ¹⁴⁶, K.D. Bhide ⁵⁵, V.S. Bhopatkar ¹²⁴, R.M. Bianchi ¹³², G. Bianco ^{24b,24a},
 O. Biebel ¹¹¹, R. Bielski ¹²⁶, M. Biglietti ^{78a}, C.S. Billingsley ⁴⁵, Y. Bimgdi ^{36f}, M. Bindi ⁵⁶,
 A. Bingul ^{22b}, C. Bini ^{76a,76b}, G.A. Bird ³³, M. Birman ¹⁷², M. Biros ¹³⁶, S. Biryukov ¹⁴⁹,
 T. Bisanz ⁵⁰, E. Bisceglie ^{44b,44a}, J.P. Biswal ¹³⁷, D. Biswas ¹⁴⁴, I. Bloch ⁴⁹, A. Blue ⁶⁰,
 U. Blumenschein ⁹⁶, J. Blumenthal ¹⁰², V.S. Bobrovnikov ³⁸, M. Boehler ⁵⁵, B. Boehm ¹⁶⁹,
 D. Bogavac ³⁷, A.G. Bogdanchikov ³⁸, C. Bohm ^{48a}, V. Boisvert ⁹⁷, P. Bokan ³⁷, T. Bold ^{87a},
 M. Bomben ⁵, M. Bona ⁹⁶, M. Boonekamp ¹³⁸, C.D. Booth ⁹⁷, A.G. Borbély ⁶⁰,
 I.S. Bordulev ³⁸, G. Borissov ⁹³, D. Bortoletto ¹²⁹, D. Boscherini ^{24b}, M. Bosman ¹³,
 J.D. Bossio Sola ³⁷, K. Bouaouda ^{36a}, N. Bouchhar ¹⁶⁶, L. Boudet ⁴, J. Boudreau ¹³²,
 E.V. Bouhova-Thacker ⁹³, D. Boumediene ⁴¹, R. Bouquet ^{58b,58a}, A. Boveia ¹²², J. Boyd ³⁷,
 D. Boye ³⁰, I.R. Boyko ³⁹, L. Bozianu ⁵⁷, J. Bracinik ²¹, N. Brahimi ⁴, G. Brandt ¹⁷⁴,
 O. Brandt ³³, F. Braren ⁴⁹, B. Brau ¹⁰⁵, J.E. Brau ¹²⁶, R. Brenner ¹⁷², L. Brenner ¹¹⁷,
 R. Brenner ¹⁶⁴, S. Bressler ¹⁷², G. Brianti ^{79a,79b}, D. Britton ⁶⁰, D. Britzger ¹¹², I. Brock ²⁵,
 G. Brooijmans ⁴², E.M. Brooks ^{159b}, E. Brost ³⁰, L.M. Brown ¹⁶⁸, L.E. Bruce ⁶²,
 T.L. Bruckler ¹²⁹, P.A. Bruckman de Renstrom ⁸⁸, B. Brüers ⁴⁹, A. Bruni ^{24b}, G. Bruni ^{24b},
 M. Bruschi ^{24b}, N. Bruscinò ^{76a,76b}, T. Buanes ¹⁷, Q. Buat ¹⁴¹, D. Buchin ¹¹², A.G. Buckley ⁶⁰,
 O. Bulekov ³⁸, B.A. Bullard ¹⁴⁶, S. Burdin ⁹⁴, C.D. Burgard ⁵⁰, A.M. Burger ³⁷,
 B. Burghgrave ⁸, O. Burlayenko ⁵⁵, J. Burleson ¹⁶⁵, J.T.P. Burr ³³, J.C. Burzynski ¹⁴⁵,
 E.L. Busch ⁴², V. Büscher ¹⁰², P.J. Bussey ⁶⁰, J.M. Butler ²⁶, C.M. Buttar ⁶⁰,
 J.M. Butterworth ⁹⁸, W. Buttinger ¹³⁷, C.J. Buxo Vazquez ¹⁰⁹, A.R. Buzykaev ³⁸,
 S. Cabrera Urbán ¹⁶⁶, L. Cadamuro ⁶⁷, D. Caforio ⁵⁹, H. Cai ¹³², Y. Cai ^{14,114c}, Y. Cai ^{114a},
 V.M.M. Cairo ³⁷, O. Cakir ^{3a}, N. Calace ³⁷, P. Calafiura ^{18a}, G. Calderini ¹³⁰, P. Calfayan ⁶⁹,
 G. Callea ⁶⁰, L.P. Caloba ^{84b}, D. Calvet ⁴¹, S. Calvet ⁴¹, M. Calvetti ^{75a,75b}, R. Camacho Toro ¹³⁰,
 S. Camarda ³⁷, D. Camarero Munoz ²⁷, P. Camarri ^{77a,77b}, M.T. Camerlingo ^{73a,73b},
 D. Cameron ³⁷, C. Camincher ¹⁶⁸, M. Campanelli ⁹⁸, A. Camplani ⁴³, V. Canale ^{73a,73b},
 A.C. Canbay ^{3a}, E. Canonero ⁹⁷, J. Cantero ¹⁶⁶, Y. Cao ¹⁶⁵, F. Capocasa ²⁷, M. Capua ^{44b,44a},
 A. Carbone ^{72a,72b}, R. Cardarelli ^{77a}, J.C.J. Cardenas ⁸, G. Carducci ^{44b,44a}, T. Carli ³⁷,
 G. Carlino ^{73a}, J.I. Carlotto ¹³, B.T. Carlson ^{132,q}, E.M. Carlson ^{168,159a}, J. Carmignani ⁹⁴,
 L. Carminati ^{72a,72b}, A. Carnelli ¹³⁸, M. Carnesale ^{76a,76b}, S. Caron ¹¹⁶, E. Carquin ^{140f},
 S. Carrá ^{72a}, G. Carratta ^{24b,24a}, A.M. Carroll ¹²⁶, T.M. Carter ⁵³, M.P. Casado ^{13,i},
 M. Caspar ⁴⁹, F.L. Castillo ⁴, L. Castillo Garcia ¹³, V. Castillo Gimenez ¹⁶⁶, N.F. Castro ^{133a,133e},
 A. Catinaccio ³⁷, J.R. Catmore ¹²⁸, T. Cavaliere ⁴, V. Cavaliere ³⁰, N. Cavalli ^{24b,24a},
 L.J. Caviedes Betancourt ^{23b}, Y.C. Cekmecelioglu ⁴⁹, E. Celebi ⁸³, S. Cella ³⁷, F. Celli ¹²⁹,
 M.S. Centonze ^{71a,71b}, V. Cepaitis ⁵⁷, K. Cerny ¹²⁵, A.S. Cerqueira ^{84a}, A. Cerri ¹⁴⁹,
 L. Cerrito ^{77a,77b}, F. Cerutti ^{18a}, B. Cervato ¹⁴⁴, A. Cervelli ^{24b}, G. Cesarini ⁵⁴, S.A. Cetin ⁸³,
 D. Chakraborty ¹¹⁸, J. Chan ^{18a}, W.Y. Chan ¹⁵⁶, J.D. Chapman ³³, E. Chapon ¹³⁸,
 B. Chargeishvili ^{152b}, D.G. Charlton ²¹, M. Chatterjee ²⁰, C. Chauhan ¹³⁶, Y. Che ^{114a},
 S. Chekanov ⁶, S.V. Chekulaev ^{159a}, G.A. Chelkov ^{39,a}, A. Chen ¹⁰⁸, B. Chen ¹⁵⁴, B. Chen ¹⁶⁸,
 H. Chen ^{114a}, H. Chen ³⁰, J. Chen ^{63c}, J. Chen ¹⁴⁵, M. Chen ¹²⁹, S. Chen ¹⁵⁶, S.J. Chen ^{114a},
 X. Chen ^{63c}, X. Chen ^{15,ab}, Y. Chen ^{63a}, C.L. Cheng ¹⁷³, H.C. Cheng ^{65a}, S. Cheong ¹⁴⁶,
 A. Cheplakov ³⁹, E. Cheremushkina ⁴⁹, E. Cherepanova ¹¹⁷, R. Cherkaoui El Moursli ^{36e},
 E. Cheu ⁷, K. Cheung ⁶⁶, L. Chevalier ¹³⁸, V. Chiarella ⁵⁴, G. Chiarelli ^{75a}, N. Chiedde ¹⁰⁴,
 G. Chiodini ^{71a}, A.S. Chisholm ²¹, A. Chitan ^{28b}, M. Chitishvili ¹⁶⁶, M.V. Chizhov ³⁹,

K. Choi ¹¹, Y. Chou ¹⁴¹, E.Y.S. Chow ¹¹⁶, K.L. Chu ¹⁷², M.C. Chu ^{65a}, X. Chu ^{14,114c},
 Z. Chubinidze ⁵⁴, J. Chudoba ¹³⁴, J.J. Chwastowski ⁸⁸, D. Cieri ¹¹², K.M. Ciesla ^{87a},
 V. Cindro ⁹⁵, A. Ciocio ^{18a}, F. Cirotto ^{73a,73b}, Z.H. Citron ¹⁷², M. Citterio ^{72a}, D.A. Ciubotaru ^{28b},
 A. Clark ⁵⁷, P.J. Clark ⁵³, N. Clarke Hall ⁹⁸, C. Clarry ¹⁵⁸, J.M. Clavijo Columbie ⁴⁹,
 S.E. Clawson ⁴⁹, C. Clement ^{48a,48b}, Y. Coadou ¹⁰⁴, M. Cobal ^{70a,70c}, A. Coccaro ^{58b},
 R.F. Coelho Barrue ^{133a}, R. Coelho Lopes De Sa ¹⁰⁵, S. Coelli ^{72a}, B. Cole ⁴², J. Collot ⁶¹,
 P. Conde Muiño ^{133a,133g}, M.P. Connell ^{34c}, S.H. Connell ^{34c}, E.I. Conroy ¹²⁹, F. Conventi ^{73a,ad},
 H.G. Cooke ²¹, A.M. Cooper-Sarkar ¹²⁹, F.A. Corchia ^{24b,24a}, A. Cordeiro Oudot Choi ¹³⁰,
 L.D. Corpe ⁴¹, M. Corradi ^{76a,76b}, F. Corriveau ^{106,w}, A. Cortes-Gonzalez ¹⁹, M.J. Costa ¹⁶⁶,
 F. Costanza ⁴, D. Costanzo ¹⁴², B.M. Cote ¹²², J. Couthures ⁴, G. Cowan ⁹⁷, K. Cranmer ¹⁷³,
 D. Cremonini ^{24b,24a}, S. Crépe-Renaudin ⁶¹, F. Crescioli ¹³⁰, M. Cristinziani ¹⁴⁴,
 M. Cristoforetti ^{79a,79b}, V. Croft ¹¹⁷, J.E. Crosby ¹²⁴, G. Crosetti ^{44b,44a}, A. Cueto ¹⁰¹, H. Cui ⁹⁸,
 Z. Cui ⁷, W.R. Cunningham ⁶⁰, F. Curcio ¹⁶⁶, J.R. Curran ⁵³, P. Czodrowski ³⁷,
 M.J. Da Cunha Sargedas De Sousa ^{58b,58a}, J.V. Da Fonseca Pinto ^{84b}, C. Da Via ¹⁰³,
 W. Dabrowski ^{87a}, T. Dado ³⁷, S. Dahbi ¹⁵¹, T. Dai ¹⁰⁸, D. Dal Santo ²⁰, C. Dallapiccola ¹⁰⁵,
 M. Dam ⁴³, G. D'amen ³⁰, V. D'Amico ¹¹¹, J. Damp ¹⁰², J.R. Dandoy ³⁵, D. Dannheim ³⁷,
 M. Danninger ¹⁴⁵, V. Dao ¹⁴⁸, G. Darbo ^{58b}, S.J. Das ^{30,ae}, F. Dattola ⁴⁹, S. D'Auria ^{72a,72b},
 A. D'avano ^{73a,73b}, C. David ^{34a}, T. Davidek ¹³⁶, I. Dawson ⁹⁶, H.A. Day-hall ¹³⁵, K. De ⁸,
 R. De Asmundis ^{73a}, N. De Biase ⁴⁹, S. De Castro ^{24b,24a}, N. De Groot ¹¹⁶, P. de Jong ¹¹⁷,
 H. De la Torre ¹¹⁸, A. De Maria ^{114a}, A. De Salvo ^{76a}, U. De Sanctis ^{77a,77b}, F. De Santis ^{71a,71b},
 A. De Santo ¹⁴⁹, J.B. De Vivie De Regie ⁶¹, D.V. Dedovich ³⁹, J. Degens ⁹⁴, A.M. Deiana ⁴⁵,
 F. Del Corso ^{24b,24a}, J. Del Peso ¹⁰¹, F. Del Rio ^{64a}, L. Delagrangé ¹³⁰, F. Deliot ¹³⁸,
 C.M. Delitzsch ⁵⁰, M. Della Pietra ^{73a,73b}, D. Della Volpe ⁵⁷, A. Dell'Acqua ³⁷,
 L. Dell'Asta ^{72a,72b}, M. Delmastro ⁴, P.A. Delsart ⁶¹, S. Demers ¹⁷⁵, M. Demichev ³⁹,
 S.P. Denisov ³⁸, L. D'Eramo ⁴¹, D. Derendarz ⁸⁸, F. Derue ¹³⁰, P. Dervan ⁹⁴, K. Desch ²⁵,
 C. Deutsch ²⁵, F.A. Di Bello ^{58b,58a}, A. Di Ciaccio ^{77a,77b}, L. Di Ciaccio ⁴,
 A. Di Domenico ^{76a,76b}, C. Di Donato ^{73a,73b}, A. Di Girolamo ³⁷, G. Di Gregorio ³⁷,
 A. Di Luca ^{79a,79b}, B. Di Micco ^{78a,78b}, R. Di Nardo ^{78a,78b}, K.F. Di Petrillo ⁴⁰,
 M. Diamantopoulou ³⁵, F.A. Dias ¹¹⁷, T. Dias Do Vale ¹⁴⁵, M.A. Diaz ^{140a,140b},
 F.G. Diaz Capriles ²⁵, A.R. Didenko ³⁹, M. Didenko ¹⁶⁶, E.B. Diehl ¹⁰⁸, S. Díez Cornell ⁴⁹,
 C. Díez Pardos ¹⁴⁴, C. Dimitriadi ¹⁶⁴, A. Dimitrievska ²¹, J. Dingfelder ²⁵, T. Dingley ¹²⁹,
 I-M. Dinu ^{28b}, S.J. Dittmeier ^{64b}, F. Dittus ³⁷, M. Divisek ¹³⁶, F. Djama ¹⁰⁴, T. Djobava ^{152b},
 C. Doglioni ^{103,100}, A. Dohnalova ^{29a}, J. Dolejsi ¹³⁶, Z. Dolezal ¹³⁶, K. Domijan ^{87a},
 K.M. Dona ⁴⁰, M. Donadelli ^{84d}, B. Dong ¹⁰⁹, J. Donini ⁴¹, A. D'Onofrio ^{73a,73b},
 M. D'Onofrio ⁹⁴, J. Dopke ¹³⁷, A. Doria ^{73a}, N. Dos Santos Fernandes ^{133a}, P. Dougan ¹⁰³,
 M.T. Dova ⁹², A.T. Doyle ⁶⁰, M.A. Dragnet ¹²⁹, E. Dreyer ¹⁷², I. Drivas-koulouris ¹⁰,
 M. Drnevich ¹²⁰, M. Drozdova ⁵⁷, D. Du ^{63a}, T.A. du Pree ¹¹⁷, F. Dubinin ³⁸, M. Dubovsky ^{29a},
 E. Duchovni ¹⁷², G. Duckeck ¹¹¹, O.A. Ducu ^{28b}, D. Duda ⁵³, A. Dudarev ³⁷, E.R. Duden ²⁷,
 M. D'uffizi ¹⁰³, L. Duflost ⁶⁷, M. Dührssen ³⁷, I. Duminica ^{28g}, A.E. Dumitriu ^{28b},
 M. Dunford ^{64a}, S. Dungs ⁵⁰, K. Dunne ^{48a,48b}, A. Duperrin ¹⁰⁴, H. Duran Yildiz ^{3a},
 M. Düren ⁵⁹, A. Durglishvili ^{152b}, B.L. Dwyer ¹¹⁸, G.I. Dyckes ^{18a}, M. Dyndal ^{87a},
 B.S. Dziedzic ³⁷, Z.O. Earnshaw ¹⁴⁹, G.H. Eberwein ¹²⁹, B. Eckerova ^{29a}, S. Eggebrecht ⁵⁶,
 E. Egidio Purcino De Souza ^{84e}, L.F. Ehrke ⁵⁷, G. Eigen ¹⁷, K. Einsweiler ^{18a}, T. Ekelof ¹⁶⁴,
 P.A. Ekman ¹⁰⁰, S. El Farkh ^{36b}, Y. El Ghazali ^{63a}, H. El Jarrari ³⁷, A. El Moussaouy ^{36a},
 V. Ellajosyula ¹⁶⁴, M. Ellert ¹⁶⁴, F. Ellinghaus ¹⁷⁴, N. Ellis ³⁷, J. Elmsheuser ³⁰, M. Elsayy ^{119a},
 M. Elsing ³⁷, D. Emelianov ¹³⁷, Y. Enari ⁸⁵, I. Ene ^{18a}, S. Epari ¹³, P.A. Erland ⁸⁸,
 D. Ernani Martins Neto ⁸⁸, M. Errenst ¹⁷⁴, M. Escalier ⁶⁷, C. Escobar ¹⁶⁶, E. Etzion ¹⁵⁴,

G. Evans [ID133a](#), H. Evans [ID69](#), L.S. Evans [ID97](#), A. Ezhilov [ID38](#), S. Ezzarqtouni [ID36a](#), F. Fabbri [ID24b,24a](#), L. Fabbri [ID24b,24a](#), G. Facini [ID98](#), V. Fadeyev [ID139](#), R.M. Fakhrutdinov [ID38](#), D. Fakoudis [ID102](#), S. Falciano [ID76a](#), L.F. Falda Ulhoa Coelho [ID37](#), F. Fallavollita [ID112](#), G. Falsetti [ID44b,44a](#), J. Faltova [ID136](#), C. Fan [ID165](#), Y. Fan [ID14](#), Y. Fang [ID14,114c](#), M. Fanti [ID72a,72b](#), M. Faraj [ID70a,70b](#), Z. Farazpay [ID99](#), A. Farbin [ID8](#), A. Farilla [ID78a](#), T. Farooque [ID109](#), S.M. Farrington [ID53](#), F. Fassi [ID36e](#), D. Fassouliotis [ID9](#), M. Faucci Giannelli [ID77a,77b](#), W.J. Fawcett [ID33](#), L. Fayard [ID67](#), P. Federic [ID136](#), P. Federicova [ID134](#), O.L. Fedin [ID38,a](#), M. Feickert [ID173](#), L. Feligioni [ID104](#), D.E. Fellers [ID126](#), C. Feng [ID63b](#), Z. Feng [ID117](#), M.J. Fenton [ID162](#), L. Ferencz [ID49](#), R.A.M. Ferguson [ID93](#), S.I. Fernandez Luengo [ID140f](#), P. Fernandez Martinez [ID13](#), M.J.V. Fernoux [ID104](#), J. Ferrando [ID93](#), A. Ferrari [ID164](#), P. Ferrari [ID117,116](#), R. Ferrari [ID74a](#), D. Ferrere [ID57](#), C. Ferretti [ID108](#), D. Fiacco [ID76a,76b](#), F. Fiedler [ID102](#), P. Fiedler [ID135](#), A. Filipčič [ID95](#), E.K. Filmer [ID1](#), F. Filthaut [ID116](#), M.C.N. Fiolhais [ID133a,133c,c](#), L. Fiorini [ID166](#), W.C. Fisher [ID109](#), T. Fitschen [ID103](#), P.M. Fitzhugh [ID138](#), I. Fleck [ID144](#), P. Fleischmann [ID108](#), T. Flick [ID174](#), M. Flores [ID34d,z](#), L.R. Flores Castillo [ID65a](#), L. Flores Sanz De Acedo [ID37](#), F.M. Follega [ID79a,79b](#), N. Fomin [ID33](#), J.H. Foo [ID158](#), A. Formica [ID138](#), A.C. Forti [ID103](#), E. Fortin [ID37](#), A.W. Fortman [ID18a](#), M.G. Foti [ID18a](#), L. Fountas [ID9,j](#), D. Fournier [ID67](#), H. Fox [ID93](#), P. Francavilla [ID75a,75b](#), S. Francescato [ID62](#), S. Franchellucci [ID57](#), M. Franchini [ID24b,24a](#), S. Franchino [ID64a](#), D. Francis [ID37](#), L. Franco [ID116](#), V. Franco Lima [ID37](#), L. Franconi [ID49](#), M. Franklin [ID62](#), G. Frattari [ID27](#), Y.Y. Frid [ID154](#), J. Friend [ID60](#), N. Fritzsche [ID37](#), A. Froch [ID55](#), D. Froidevaux [ID37](#), J.A. Frost [ID129](#), Y. Fu [ID63a](#), S. Fuenzalida Garrido [ID140f](#), M. Fujimoto [ID104](#), K.Y. Fung [ID65a](#), E. Furtado De Simas Filho [ID84e](#), M. Furukawa [ID156](#), J. Fuster [ID166](#), A. Gaa [ID56](#), A. Gabrielli [ID24b,24a](#), A. Gabrielli [ID158](#), P. Gadow [ID37](#), G. Gagliardi [ID58b,58a](#), L.G. Gagnon [ID18a](#), S. Gaid [ID163](#), S. Galantzan [ID154](#), E.J. Gallas [ID129](#), B.J. Gallop [ID137](#), K.K. Gan [ID122](#), S. Ganguly [ID156](#), Y. Gao [ID53](#), F.M. Garay Walls [ID140a,140b](#), B. Garcia [ID30](#), C. García [ID166](#), A. Garcia Alonso [ID117](#), A.G. Garcia Caffaro [ID175](#), J.E. García Navarro [ID166](#), M. Garcia-Sciveres [ID18a](#), G.L. Gardner [ID131](#), R.W. Gardner [ID40](#), N. Garelli [ID161](#), D. Garg [ID81](#), R.B. Garg [ID146](#), J.M. Gargan [ID53](#), C.A. Garner [ID158](#), C.M. Garvey [ID34a](#), V.K. Gassmann [ID161](#), G. Gaudio [ID74a](#), V. Gautam [ID13](#), P. Gauzzi [ID76a,76b](#), J. Gavranovic [ID95](#), I.L. Gavrilenko [ID38](#), A. Gavrilyuk [ID38](#), C. Gay [ID167](#), G. Gaycken [ID126](#), E.N. Gazis [ID10](#), A.A. Geanta [ID28b](#), C.M. Gee [ID139](#), A. Gekow [ID122](#), C. Gemme [ID58b](#), M.H. Genest [ID61](#), A.D. Gentry [ID115](#), S. George [ID97](#), W.F. George [ID21](#), T. Geralis [ID47](#), P. Gessinger-Befurt [ID37](#), M.E. Geyik [ID174](#), M. Ghani [ID170](#), K. Ghorbanian [ID96](#), A. Ghosal [ID144](#), A. Ghosh [ID162](#), A. Ghosh [ID7](#), B. Giacobbe [ID24b](#), S. Giagu [ID76a,76b](#), T. Giani [ID117](#), A. Giannini [ID63a](#), S.M. Gibson [ID97](#), M. Gignac [ID139](#), D.T. Gil [ID87b](#), A.K. Gilbert [ID87a](#), B.J. Gilbert [ID42](#), D. Gillberg [ID35](#), G. Gilles [ID117](#), L. Ginabat [ID130](#), D.M. Gingrich [ID2,ac](#), M.P. Giordani [ID70a,70c](#), P.F. Giraud [ID138](#), G. Giugliarelli [ID70a,70c](#), D. Giugni [ID72a](#), F. Giuli [ID37](#), I. Gkialas [ID9,j](#), L.K. Gladilin [ID38](#), C. Glasman [ID101](#), G.R. Gledhill [ID126](#), G. Glemža [ID49](#), M. Glisic [ID126](#), I. Gnesi [ID44b,e](#), Y. Go [ID30](#), M. Goblirsch-Kolb [ID37](#), B. Gocke [ID50](#), D. Godin [ID110](#), B. Gokturk [ID22a](#), S. Goldfarb [ID107](#), T. Golling [ID57](#), M.G.D. Gololo [ID34g](#), D. Golubkov [ID38](#), J.P. Gombas [ID109](#), A. Gomes [ID133a,133b](#), G. Gomes Da Silva [ID144](#), A.J. Gomez Delegido [ID166](#), R. Gonçalves [ID133a](#), L. Gonella [ID21](#), A. Gongadze [ID152c](#), F. Gonnella [ID21](#), J.L. Gonski [ID146](#), R.Y. González Andana [ID53](#), S. González de la Hoz [ID166](#), R. Gonzalez Lopez [ID94](#), C. Gonzalez Renteria [ID18a](#), M.V. Gonzalez Rodrigues [ID49](#), R. Gonzalez Suarez [ID164](#), S. Gonzalez-Sevilla [ID57](#), L. Goossens [ID37](#), B. Gorini [ID37](#), E. Gorini [ID71a,71b](#), A. Gorišek [ID95](#), T.C. Gosart [ID131](#), A.T. Goshaw [ID52](#), M.I. Gostkin [ID39](#), S. Goswami [ID124](#), C.A. Gottardo [ID37](#), S.A. Gotz [ID111](#), M. Gouighri [ID36b](#), V. Goumarre [ID49](#), A.G. Goussiou [ID141](#), N. Govender [ID34c](#), R.P. Grabarczyk [ID129](#), I. Grabowska-Bold [ID87a](#), K. Graham [ID35](#), E. Gramstad [ID128](#), S. Grancagnolo [ID71a,71b](#), C.M. Grant [ID1,138](#), P.M. Gravila [ID28f](#), F.G. Gravili [ID71a,71b](#), H.M. Gray [ID18a](#), M. Greco [ID71a,71b](#), M.J. Green [ID1](#), C. Grefe [ID25](#), A.S. Grefsrud [ID17](#), I.M. Gregor [ID49](#), K.T. Greif [ID162](#), P. Grenier [ID146](#), S.G. Grewe [ID112](#), A.A. Grillo [ID139](#), K. Grimm [ID32](#), S. Grinstein [ID13,s](#), J.-F. Grivaz [ID67](#), E. Gross [ID172](#), J. Grosse-Knetter [ID56](#), J.C. Grundy [ID129](#), L. Guan [ID108](#), J.G.R. Guerrero Rojas [ID166](#),

G. Guerrieri ^{id37}, R. Gugel ^{id102}, J.A.M. Guhit ^{id108}, A. Guida ^{id19}, E. Guilloton ^{id170}, S. Guindon ^{id37}, F. Guo ^{id14,114c}, J. Guo ^{id63c}, L. Guo ^{id49}, Y. Guo ^{id108}, R. Gupta ^{id132}, S. Gurbuz ^{id25}, S.S. Gurdasani ^{id55}, G. Gustavino ^{id76a,76b}, P. Gutierrez ^{id123}, L.F. Gutierrez Zagazeta ^{id131}, M. Gutsche ^{id51}, C. Gutschow ^{id98}, C. Gwenlan ^{id129}, C.B. Gwilliam ^{id94}, E.S. Haaland ^{id128}, A. Haas ^{id120}, M. Habedank ^{id49}, C. Haber ^{id18a}, H.K. Hadavand ^{id8}, A. Hadeef ^{id51}, S. Hadzic ^{id112}, A.I. Hagan ^{id93}, J.J. Hahn ^{id144}, E.H. Haines ^{id98}, M. Haleem ^{id169}, J. Haley ^{id124}, J.J. Hall ^{id142}, G.D. Hallewell ^{id104}, L. Halser ^{id20}, K. Hamano ^{id168}, M. Hamer ^{id25}, G.N. Hamity ^{id53}, E.J. Hampshire ^{id97}, J. Han ^{id63b}, K. Han ^{id63a}, L. Han ^{id114a}, L. Han ^{id63a}, S. Han ^{id18a}, Y.F. Han ^{id158}, K. Hanagaki ^{id85}, M. Hance ^{id139}, D.A. Hangal ^{id42}, H. Hanif ^{id145}, M.D. Hank ^{id131}, J.B. Hansen ^{id43}, P.H. Hansen ^{id43}, D. Harada ^{id57}, T. Harenberg ^{id174}, S. Harkusha ^{id38}, M.L. Harris ^{id105}, Y.T. Harris ^{id129}, J. Harrison ^{id13}, N.M. Harrison ^{id122}, P.F. Harrison ^{id170}, N.M. Hartman ^{id112}, N.M. Hartmann ^{id111}, R.Z. Hasan ^{id97,137}, Y. Hasegawa ^{id143}, F. Haslbeck ^{id129}, S. Hassan ^{id17}, R. Hauser ^{id109}, C.M. Hawkes ^{id21}, R.J. Hawkings ^{id37}, Y. Hayashi ^{id156}, D. Hayden ^{id109}, C. Hayes ^{id108}, R.L. Hayes ^{id117}, C.P. Hays ^{id129}, J.M. Hays ^{id96}, H.S. Hayward ^{id94}, F. He ^{id63a}, M. He ^{id14,114c}, Y. He ^{id49}, Y. He ^{id98}, N.B. Heatley ^{id96}, V. Hedberg ^{id100}, A.L. Heggelund ^{id128}, N.D. Hehir ^{id96,*}, C. Heidegger ^{id55}, K.K. Heidegger ^{id55}, J. Heilman ^{id35}, S. Heim ^{id49}, T. Heim ^{id18a}, J.G. Heinlein ^{id131}, J.J. Heinrich ^{id126}, L. Heinrich ^{id112,aa}, J. Hejbal ^{id134}, A. Held ^{id173}, S. Hellesund ^{id17}, C.M. Helling ^{id167}, S. Hellman ^{id48a,48b}, R.C.W. Henderson ^{id93}, L. Henkelmann ^{id33}, A.M. Henriques Correia ^{id37}, H. Herde ^{id100}, Y. Hernández Jiménez ^{id148}, L.M. Herrmann ^{id25}, T. Herrmann ^{id51}, G. Herten ^{id55}, R. Hertenberger ^{id111}, L. Hervas ^{id37}, M.E. Hesping ^{id102}, N.P. Hessey ^{id159a}, M. Hidaoui ^{id36b}, N. Hidic ^{id136}, E. Hill ^{id158}, S.J. Hillier ^{id21}, J.R. Hinds ^{id109}, F. Hinterkeuser ^{id25}, M. Hirose ^{id127}, S. Hirose ^{id160}, D. Hirschbuehl ^{id174}, T.G. Hitchings ^{id103}, B. Hiti ^{id95}, J. Hobbs ^{id148}, R. Hobincu ^{id28e}, N. Hod ^{id172}, M.C. Hodgkinson ^{id142}, B.H. Hodgkinson ^{id129}, A. Hoecker ^{id37}, D.D. Hofer ^{id108}, J. Hofer ^{id49}, T. Holm ^{id25}, M. Holzbock ^{id37}, L.B.A.H. Hommels ^{id33}, B.P. Honan ^{id103}, J.J. Hong ^{id69}, J. Hong ^{id63c}, T.M. Hong ^{id132}, B.H. Hooberman ^{id165}, W.H. Hopkins ^{id6}, M.C. Hoppesch ^{id165}, Y. Horii ^{id113}, S. Hou ^{id151}, A.S. Howard ^{id95}, J. Howarth ^{id60}, J. Hoya ^{id6}, M. Hrabovsky ^{id125}, A. Hrynevich ^{id49}, T. Hryn'ova ^{id4}, P.J. Hsu ^{id66}, S.-C. Hsu ^{id141}, T. Hsu ^{id67}, M. Hu ^{id18a}, Q. Hu ^{id63a}, S. Huang ^{id65b}, X. Huang ^{id14,114c}, Y. Huang ^{id142}, Y. Huang ^{id102}, Y. Huang ^{id14}, Z. Huang ^{id103}, Z. Hubacek ^{id135}, M. Huebner ^{id25}, F. Huegging ^{id25}, T.B. Huffman ^{id129}, C.A. Hugli ^{id49}, M. Huhtinen ^{id37}, S.K. Huiberts ^{id17}, R. Hulsken ^{id106}, N. Huseynov ^{id12,g}, J. Huston ^{id109}, J. Huth ^{id62}, R. Hyneman ^{id146}, G. Iacobucci ^{id57}, G. Iakovidis ^{id30}, L. Iconomidou-Fayard ^{id67}, J.P. Iddon ^{id37}, P. Iengo ^{id73a,73b}, R. Iguchi ^{id156}, Y. Iiyama ^{id156}, T. Iizawa ^{id129}, Y. Ikegami ^{id85}, N. Ilic ^{id158}, H. Imam ^{id84c}, M. Ince Lezki ^{id57}, T. Ingebretsen Carlson ^{id48a,48b}, J.M. Inglis ^{id96}, G. Introzzi ^{id74a,74b}, M. Iodice ^{id78a}, V. Ippolito ^{id76a,76b}, R.K. Irwin ^{id94}, M. Ishino ^{id156}, W. Islam ^{id173}, C. Issever ^{id19,49}, S. Istin ^{id22a,ag}, H. Ito ^{id171}, R. Iuppa ^{id79a,79b}, A. Ivina ^{id172}, J.M. Izen ^{id46}, V. Izzo ^{id73a}, P. Jacka ^{id134}, P. Jackson ^{id1}, C.S. Jagfeld ^{id111}, G. Jain ^{id159a}, P. Jain ^{id49}, K. Jakobs ^{id55}, T. Jakoubek ^{id172}, J. Jamieson ^{id60}, W. Jang ^{id156}, M. Javurkova ^{id105}, P. Jawahar ^{id103}, L. Jeanty ^{id126}, J. Jejelava ^{id152a,y}, P. Jenni ^{id55,f}, C.E. Jessiman ^{id35}, C. Jia ^{id63b}, J. Jia ^{id148}, X. Jia ^{id14,114c}, Z. Jia ^{id114a}, C. Jiang ^{id53}, S. Jiggins ^{id49}, J. Jimenez Pena ^{id13}, S. Jin ^{id114a}, A. Jinaru ^{id28b}, O. Jinnouchi ^{id157}, P. Johansson ^{id142}, K.A. Johns ^{id7}, J.W. Johnson ^{id139}, F.A. Jolly ^{id49}, D.M. Jones ^{id149}, E. Jones ^{id49}, K.S. Jones ^{id8}, P. Jones ^{id33}, R.W.L. Jones ^{id93}, T.J. Jones ^{id94}, H.L. Joos ^{id56,37}, R. Joshi ^{id122}, J. Jovicevic ^{id16}, X. Ju ^{id18a}, J.J. Junggeburth ^{id105}, T. Junkermann ^{id64a}, A. Juste Rozas ^{id13,s}, M.K. Juzek ^{id88}, S. Kabana ^{id140e}, A. Kaczmarek ^{id88}, M. Kado ^{id112}, H. Kagan ^{id122}, M. Kagan ^{id146}, A. Kahn ^{id131}, C. Kahra ^{id102}, T. Kaji ^{id156}, E. Kajomovitz ^{id153}, N. Kakati ^{id172}, I. Kalaitzidou ^{id55}, C.W. Kalderon ^{id30}, N.J. Kang ^{id139}, D. Kar ^{id34g}, K. Karava ^{id129}, M.J. Kareem ^{id159b}, E. Karentzos ^{id55}, O. Karkout ^{id117}, S.N. Karpov ^{id39}, Z.M. Karpova ^{id39}, V. Kartvelishvili ^{id93}, A.N. Karyukhin ^{id38}, E. Kasimi ^{id155}, J. Katzy ^{id49}, S. Kaur ^{id35}, K. Kawade ^{id143}, M.P. Kawale ^{id123}, C. Kawamoto ^{id89}, T. Kawamoto ^{id63a},

E.F. Kay [ID37](#), F.I. Kaya [ID161](#), S. Kazakos [ID109](#), V.F. Kazanin [ID38](#), Y. Ke [ID148](#), J.M. Keaveney [ID34a](#),
 R. Keeler [ID168](#), G.V. Kehris [ID62](#), J.S. Keller [ID35](#), A.S. Kelly⁹⁸, J.J. Kempster [ID149](#), P.D. Kennedy [ID102](#),
 O. Kepka [ID134](#), B.P. Kerridge [ID137](#), S. Kersten [ID174](#), B.P. Kerševan [ID95](#), L. Keszeghova [ID29a](#),
 S. Ketabchi Haghghat [ID158](#), R.A. Khan [ID132](#), A. Khanov [ID124](#), A.G. Kharlamov [ID38](#), T. Kharlamova [ID38](#),
 E.E. Khoda [ID141](#), M. Kholodenko [ID133a](#), T.J. Khoo [ID19](#), G. Khoriali [ID169](#), J. Khubua [ID152b,*](#),
 Y.A.R. Khwaira [ID130](#), B. Kibirige^{34g}, D. Kim [ID6](#), D.W. Kim [ID48a,48b](#), Y.K. Kim [ID40](#), N. Kimura [ID98](#),
 M.K. Kingston [ID56](#), A. Kirchhoff [ID56](#), C. Kirfel [ID25](#), F. Kirfel [ID25](#), J. Kirk [ID137](#), A.E. Kiryunin [ID112](#),
 C. Kitsaki [ID10](#), O. Kivernyk [ID25](#), M. Klassen [ID161](#), C. Klein [ID35](#), L. Klein [ID169](#), M.H. Klein [ID45](#),
 S.B. Klein [ID57](#), U. Klein [ID94](#), P. Klimek [ID37](#), A. Klimentov [ID30](#), T. Klioutchnikova [ID37](#), P. Kluit [ID117](#),
 S. Kluth [ID112](#), E. Kneringer [ID80](#), T.M. Knight [ID158](#), A. Knue [ID50](#), D. Kobylanskii [ID172](#), S.F. Koch [ID129](#),
 M. Kocian [ID146](#), P. Kodyš [ID136](#), D.M. Koeck [ID126](#), P.T. Koenig [ID25](#), T. Koffas [ID35](#), O. Kolay [ID51](#),
 I. Koletsou [ID4](#), T. Komarek [ID88](#), K. Köneke [ID55](#), A.X.Y. Kong [ID1](#), T. Kono [ID121](#), N. Konstantinidis [ID98](#),
 P. Kontaxakis [ID57](#), B. Konya [ID100](#), R. Kopeliansky [ID42](#), S. Koperny [ID87a](#), K. Korcyl [ID88](#),
 K. Kordas [ID155,d](#), A. Korn [ID98](#), S. Korn [ID56](#), I. Korolkov [ID13](#), N. Korotkova [ID38](#), B. Kortman [ID117](#),
 O. Kortner [ID112](#), S. Kortner [ID112](#), W.H. Kostecka [ID118](#), V.V. Kostyukhin [ID144](#), A. Kotsokechagia [ID37](#),
 A. Kotwal [ID52](#), A. Koulouris [ID37](#), A. Kourkoumeli-Charalampidi [ID74a,74b](#), C. Kourkoumelis [ID9](#),
 E. Kourlitis [ID112,aa](#), O. Kovanda [ID126](#), R. Kowalewski [ID168](#), W. Kozanecki [ID138](#), A.S. Kozhin [ID38](#),
 V.A. Kramarenko [ID38](#), G. Kramberger [ID95](#), P. Kramer [ID102](#), M.W. Krasny [ID130](#), A. Krasznahorkay [ID37](#),
 A.C. Kraus [ID118](#), J.W. Kraus [ID174](#), J.A. Kremer [ID49](#), T. Kresse [ID51](#), L. Kretschmann [ID174](#),
 J. Kretschmar [ID94](#), K. Kreul [ID19](#), P. Krieger [ID158](#), M. Krivos [ID136](#), K. Krizka [ID21](#), K. Kroeninger [ID50](#),
 H. Kroha [ID112](#), J. Kroll [ID134](#), J. Kroll [ID131](#), K.S. Krowpman [ID109](#), U. Kruchonak [ID39](#), H. Krüger [ID25](#),
 N. Krumnack⁸², M.C. Kruse [ID52](#), O. Kuchinskaia [ID38](#), S. Kuday [ID3a](#), S. Kuehn [ID37](#), R. Kuesters [ID55](#),
 T. Kuhl [ID49](#), V. Kukhtin [ID39](#), Y. Kulchitsky [ID38,a](#), S. Kuleshov [ID140d,140b](#), M. Kumar [ID34g](#),
 N. Kumari [ID49](#), P. Kumari [ID159b](#), A. Kupco [ID134](#), T. Kupfer⁵⁰, A. Kupich [ID38](#), O. Kuprash [ID55](#),
 H. Kurashige [ID86](#), L.L. Kurchaninov [ID159a](#), O. Kurdysh [ID67](#), Y.A. Kurochkin [ID38](#), A. Kurova [ID38](#),
 M. Kuze [ID157](#), A.K. Kvam [ID105](#), J. Kvita [ID125](#), T. Kwan [ID106](#), N.G. Kyriacou [ID108](#), L.A.O. Laatu [ID104](#),
 C. Lacasta [ID166](#), F. Lacava [ID76a,76b](#), H. Lacker [ID19](#), D. Lacour [ID130](#), N.N. Lad [ID98](#), E. Ladygin [ID39](#),
 A. Lafarge [ID41](#), B. Laforge [ID130](#), T. Lagouri [ID175](#), F.Z. Lahbabi [ID36a](#), S. Lai [ID56](#), J.E. Lambert [ID168](#),
 S. Lammers [ID69](#), W. Lampl [ID7](#), C. Lampoudis [ID155,d](#), G. Lamprinoudis¹⁰², A.N. Lancaster [ID118](#),
 E. Lançon [ID30](#), U. Landgraf [ID55](#), M.P.J. Landon [ID96](#), V.S. Lang [ID55](#), O.K.B. Langrekken [ID128](#),
 A.J. Lankford [ID162](#), F. Lanni [ID37](#), K. Lantzsch [ID25](#), A. Lanza [ID74a](#), J.F. Laporte [ID138](#), T. Lari [ID72a](#),
 F. Lasagni Manghi [ID24b](#), M. Lassnig [ID37](#), V. Latonova [ID134](#), A. Laurier [ID153](#), S.D. Lawlor [ID142](#),
 Z. Lawrence [ID103](#), R. Lazaridou¹⁷⁰, M. Lazzaroni [ID72a,72b](#), B. Le¹⁰³, E.M. Le Boulicaut [ID52](#),
 L.T. Le Pottier [ID18a](#), B. Leban [ID24b,24a](#), A. Lebedev [ID82](#), M. LeBlanc [ID103](#), F. Ledroit-Guillon [ID61](#),
 S.C. Lee [ID151](#), S. Lee [ID48a,48b](#), T.F. Lee [ID94](#), L.L. Leeuw [ID34c](#), H.P. Lefebvre [ID97](#), M. Lefebvre [ID168](#),
 C. Leggett [ID18a](#), G. Lehmann Miotto [ID37](#), M. Leigh [ID57](#), W.A. Leight [ID105](#), W. Leinonen [ID116](#),
 A. Leisos [ID155,r](#), M.A.L. Leite [ID84c](#), C.E. Leitgeb [ID19](#), R. Leitner [ID136](#), K.J.C. Leney [ID45](#), T. Lenz [ID25](#),
 S. Leone [ID75a](#), C. Leonidopoulos [ID53](#), A. Leopold [ID147](#), R. Les [ID109](#), C.G. Lester [ID33](#),
 M. Levchenko [ID38](#), J. Levêque [ID4](#), L.J. Levinson [ID172](#), G. Levrini [ID24b,24a](#), M.P. Lewicki [ID88](#),
 C. Lewis [ID141](#), D.J. Lewis [ID4](#), A. Li [ID5](#), B. Li [ID63b](#), C. Li^{63a}, C-Q. Li [ID112](#), H. Li [ID63a](#), H. Li [ID63b](#),
 H. Li [ID114a](#), H. Li [ID15](#), H. Li [ID63b](#), J. Li [ID63c](#), K. Li [ID141](#), L. Li [ID63c](#), M. Li [ID14,114c](#), S. Li [ID14,114c](#),
 S. Li [ID63d,63c](#), T. Li [ID5](#), X. Li [ID106](#), Z. Li [ID129](#), Z. Li [ID156](#), Z. Li [ID14,114c](#), Z. Li [ID63a](#), S. Liang [ID14,114c](#),
 Z. Liang [ID14](#), M. Liberatore [ID138](#), B. Liberti [ID77a](#), K. Lie [ID65c](#), J. Lieber Marin [ID84e](#), H. Lien [ID69](#),
 H. Lin [ID108](#), K. Lin [ID109](#), R.E. Lindley [ID7](#), J.H. Lindon [ID2](#), J. Ling [ID62](#), E. Lipeles [ID131](#),
 A. Lipniacka [ID17](#), A. Lister [ID167](#), J.D. Little [ID69](#), B. Liu [ID14](#), B.X. Liu [ID114b](#), D. Liu [ID63d,63c](#),
 E.H.L. Liu [ID21](#), J.B. Liu [ID63a](#), J.K.K. Liu [ID33](#), K. Liu [ID63d](#), K. Liu [ID63d,63c](#), M. Liu [ID63a](#), M.Y. Liu [ID63a](#),
 P. Liu [ID14](#), Q. Liu [ID63d,141,63c](#), X. Liu [ID63a](#), X. Liu [ID63b](#), Y. Liu [ID114b,114c](#), Y.L. Liu [ID63b](#), Y.W. Liu [ID63a](#),





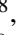



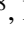




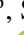
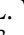
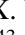





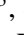
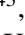




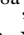
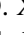





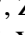

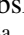
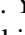
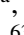


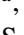
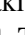
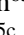


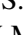
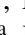
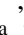



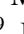

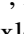
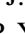
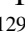
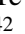


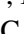

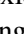
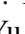
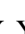
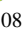
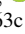
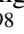

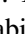



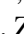



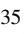

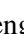
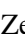
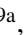

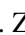
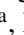


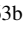


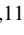


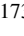

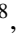


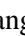
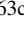
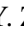

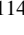


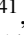


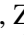
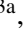

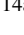
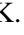
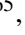

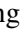
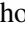
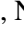
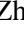
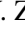
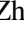
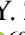
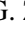
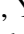
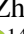











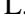





S.L. Lloyd ⁹⁶, E.M. Lobodzinska ⁴⁹, P. Loch ⁷, T. Lohse ¹⁹, K. Lohwasser ¹⁴², E. Loiacono ⁴⁹,
 M. Lokajicek ^{134,*}, J.D. Lomas ²¹, J.D. Long ¹⁶⁵, I. Longarini ¹⁶², R. Longo ¹⁶⁵,
 I. Lopez Paz ⁶⁸, A. Lopez Solis ⁴⁹, N.A. Lopez-canelas ⁷, N. Lorenzo Martinez ⁴, A.M. Lory ¹¹¹,
 M. Losada ^{119a}, G. Löschecke Centeno ¹⁴⁹, O. Loseva ³⁸, X. Lou ^{48a,48b}, X. Lou ^{14,114c},
 A. Lounis ⁶⁷, P.A. Love ⁹³, G. Lu ^{14,114c}, M. Lu ⁶⁷, S. Lu ¹³¹, Y.J. Lu ⁶⁶, H.J. Lubatti ¹⁴¹,
 C. Luci ^{76a,76b}, F.L. Lucio Alves ^{114a}, F. Luehring ⁶⁹, I. Luise ¹⁴⁸, O. Lukianchuk ⁶⁷,
 O. Lundberg ¹⁴⁷, B. Lund-Jensen ^{147,*}, N.A. Luongo ⁶, M.S. Lutz ³⁷, A.B. Lux ²⁶, D. Lynn ³⁰,
 R. Lysak ¹³⁴, E. Lytken ¹⁰⁰, V. Lyubushkin ³⁹, T. Lyubushkina ³⁹, M.M. Lyukova ¹⁴⁸,
 M.Firdaus M. Soberi ⁵³, H. Ma ³⁰, K. Ma ^{63a}, L.L. Ma ^{63b}, W. Ma ^{63a}, Y. Ma ¹²⁴,
 J.C. MacDonald ¹⁰², P.C. Machado De Abreu Farias ^{84e}, R. Madar ⁴¹, T. Madula ⁹⁸, J. Maeda ⁸⁶,
 T. Maeno ³⁰, H. Maguire ¹⁴², V. Maiboroda ¹³⁸, A. Maio ^{133a,133b,133d}, K. Maj ^{87a},
 O. Majersky ⁴⁹, S. Majewski ¹²⁶, N. Makovec ⁶⁷, V. Maksimovic ¹⁶, B. Malaescu ¹³⁰,
 Pa. Malecki ⁸⁸, V.P. Maleev ³⁸, F. Malek ^{61,n}, M. Mali ⁹⁵, D. Malito ⁹⁷, U. Mallik ⁸¹,
 S. Maltezos ¹⁰, S. Malyukov ³⁹, J. Mamuzic ¹³, G. Mancini ⁵⁴, M.N. Mancini ²⁷, G. Manco ^{74a,74b},
 J.P. Mandalia ⁹⁶, S.S. Mandarray ¹⁴⁹, I. Mandić ⁹⁵, L. Manhaes de Andrade Filho ^{84a},
 I.M. Maniatis ¹⁷², J. Manjarres Ramos ⁹¹, D.C. Mankad ¹⁷², A. Mann ¹¹¹, S. Manzoni ³⁷,
 L. Mao ^{63c}, X. Mapekula ^{34c}, A. Marantis ^{155,r}, G. Marchiori ⁵, M. Marcisovsky ¹³⁴,
 C. Marcon ^{72a}, M. Marinescu ²¹, S. Marium ⁴⁹, M. Marjanovic ¹²³, A. Markhoos ⁵⁵,
 M. Markovitch ⁶⁷, E.J. Marshall ⁹³, Z. Marshall ^{18a}, S. Marti-Garcia ¹⁶⁶, J. Martin ⁹⁸,
 T.A. Martin ¹³⁷, V.J. Martin ⁵³, B. Martin dit Latour ¹⁷, L. Martinelli ^{76a,76b}, M. Martinez ^{13,s},
 P. Martinez Agullo ¹⁶⁶, V.I. Martinez Outschoorn ¹⁰⁵, P. Martinez Suarez ¹³, S. Martin-Haugh ¹³⁷,
 G. Martinovicova ¹³⁶, V.S. Martoiu ^{28b}, A.C. Martyniuk ⁹⁸, A. Marzin ³⁷, D. Mascione ^{79a,79b},
 L. Masetti ¹⁰², J. Masik ¹⁰³, A.L. Maslennikov ³⁸, P. Massarotti ^{73a,73b}, P. Mastrandrea ^{75a,75b},
 A. Mastroberardino ^{44b,44a}, T. Masubuchi ¹²⁷, T. Mathisen ¹⁶⁴, J. Matousek ¹³⁶, J. Maurer ^{28b},
 A.J. Maury ⁶⁷, B. Maček ⁹⁵, D.A. Maximov ³⁸, A.E. May ¹⁰³, R. Mazini ¹⁵¹, I. Maznas ¹¹⁸,
 M. Mazza ¹⁰⁹, S.M. Mazza ¹³⁹, E. Mazzeo ^{72a,72b}, C. Mc Ginn ³⁰, J.P. Mc Gowan ¹⁶⁸,
 S.P. Mc Kee ¹⁰⁸, C.C. McCracken ¹⁶⁷, E.F. McDonald ¹⁰⁷, A.E. McDougall ¹¹⁷,
 J.A. Mcfayden ¹⁴⁹, R.P. McGovern ¹³¹, R.P. McKenzie ^{34g}, T.C. Mclachlan ⁴⁹, D.J. Mclaughlin ⁹⁸,
 S.J. McMahon ¹³⁷, C.M. Mcpartland ⁹⁴, R.A. McPherson ^{168,w}, S. Mehlhase ¹¹¹, A. Mehta ⁹⁴,
 D. Melini ¹⁶⁶, B.R. Mellado Garcia ^{34g}, A.H. Melo ⁵⁶, F. Meloni ⁴⁹,
 A.M. Mendes Jacques Da Costa ¹⁰³, H.Y. Meng ¹⁵⁸, L. Meng ⁹³, S. Menke ¹¹², M. Mentink ³⁷,
 E. Meoni ^{44b,44a}, G. Mercado ¹¹⁸, S. Merianos ¹⁵⁵, C. Merlassino ^{70a,70c}, L. Merola ^{73a,73b},
 C. Meroni ^{72a,72b}, J. Metcalfe ⁶, A.S. Mete ⁶, E. Meuser ¹⁰², C. Meyer ⁶⁹, J-P. Meyer ¹³⁸,
 R.P. Middleton ¹³⁷, L. Mijović ⁵³, G. Mikenberg ¹⁷², M. Mikestikova ¹³⁴, M. Mikuž ⁹⁵,
 H. Mildner ¹⁰², A. Milic ³⁷, D.W. Miller ⁴⁰, E.H. Miller ¹⁴⁶, L.S. Miller ³⁵, A. Milov ¹⁷²,
 D.A. Milstead ^{48a,48b}, T. Min ^{114a}, A.A. Minaenko ³⁸, I.A. Minashvili ^{152b}, L. Mince ⁶⁰,
 A.I. Mincer ¹²⁰, B. Mindur ^{87a}, M. Mineev ³⁹, Y. Mino ⁸⁹, L.M. Mir ¹³, M. Miralles Lopez ⁶⁰,
 M. Mironova ^{18a}, M.C. Missio ¹¹⁶, A. Mitra ¹⁷⁰, V.A. Mitsou ¹⁶⁶, Y. Mitsumori ¹¹³, O. Miu ¹⁵⁸,
 P.S. Miyagawa ⁹⁶, T. Mkrtychyan ^{64a}, M. Mlinarevic ⁹⁸, T. Mlinarevic ⁹⁸, M. Mlynarikova ³⁷,
 S. Mobius ²⁰, P. Mogg ¹¹¹, M.H. Mohamed Farook ¹¹⁵, A.F. Mohammed ^{14,114c}, S. Mohapatra ⁴²,
 G. Mokgatitswane ^{34g}, L. Moleri ¹⁷², B. Mondal ¹⁴⁴, S. Mondal ¹³⁵, K. Mönig ⁴⁹,
 E. Monnier ¹⁰⁴, L. Monsonis Romero ¹⁶⁶, J. Montejo Berlingen ¹³, A. Montella ^{48a,48b},
 M. Montella ¹²², F. Montekali ^{78a,78b}, F. Monticelli ⁹², S. Monzani ^{70a,70c}, A. Morancho Tarda ⁴³,
 N. Morange ⁶⁷, A.L. Moreira De Carvalho ⁴⁹, M. Moreno Llácer ¹⁶⁶, C. Moreno Martinez ⁵⁷,
 P. Morettini ^{58b}, S. Morgenstern ³⁷, M. Morii ⁶², M. Morinaga ¹⁵⁶, F. Morodei ^{76a,76b},
 L. Morvaj ³⁷, P. Moschovakos ³⁷, B. Moser ¹²⁹, M. Mosidze ^{152b}, T. Moskalets ⁴⁵,
 P. Moskvitina ¹¹⁶, J. Moss ^{32,k}, P. Moszkowicz ^{87a}, A. Moussa ^{36d}, E.J.W. Moyses ¹⁰⁵,

O. Mtintsilana ^{34g}, S. Muanza ¹⁰⁴, J. Mueller ¹³², D. Muenstermann ⁹³, R. Müller ³⁷, G.A. Mullier ¹⁶⁴, A.J. Mullin³³, J.J. Mullin¹³¹, D.P. Mungo ¹⁵⁸, D. Munoz Perez ¹⁶⁶, F.J. Munoz Sanchez ¹⁰³, M. Murin ¹⁰³, W.J. Murray ^{170,137}, M. Muškinja ⁹⁵, C. Mwewa ³⁰, A.G. Myagkov ^{38,a}, A.J. Myers ⁸, G. Myers ¹⁰⁸, M. Myska ¹³⁵, B.P. Nachman ^{18a}, O. Nackenhorst ⁵⁰, K. Nagai ¹²⁹, K. Nagano ⁸⁵, J.L. Nagle ^{30,ae}, E. Nagy ¹⁰⁴, A.M. Nairz ³⁷, Y. Nakahama ⁸⁵, K. Nakamura ⁸⁵, K. Nakkalil ⁵, H. Nanjo ¹²⁷, E.A. Narayanan ¹¹⁵, I. Naryshkin ³⁸, L. Nasella ^{72a,72b}, M. Naseri ³⁵, S. Nasri ^{119b}, C. Nass ²⁵, G. Navarro ^{23a}, J. Navarro-Gonzalez ¹⁶⁶, R. Nayak ¹⁵⁴, A. Nayaz ¹⁹, P.Y. Nechaeva ³⁸, S. Nechaeva ^{24b,24a}, F. Nechansky ⁴⁹, L. Nedic ¹²⁹, T.J. Neep ²¹, A. Negri ^{74a,74b}, M. Negrini ^{24b}, C. Nellist ¹¹⁷, C. Nelson ¹⁰⁶, K. Nelson ¹⁰⁸, S. Nemecek ¹³⁴, M. Nessi ^{37,h}, M.S. Neubauer ¹⁶⁵, F. Neuhaus ¹⁰², J. Neundorff ⁴⁹, P.R. Newman ²¹, C.W. Ng ¹³², Y.W.Y. Ng ⁴⁹, B. Ngair ^{119a}, H.D.N. Nguyen ¹¹⁰, R.B. Nickerson ¹²⁹, R. Nicolaidou ¹³⁸, J. Nielsen ¹³⁹, M. Niemeyer ⁵⁶, J. Niermann ⁵⁶, N. Nikipforou ³⁷, V. Nikolaenko ^{38,a}, I. Nikolic-Audit ¹³⁰, K. Nikolopoulos ²¹, P. Nilsson ³⁰, I. Ninca ⁴⁹, G. Ninio ¹⁵⁴, A. Nisati ^{76a}, N. Nishu ², R. Nisius ¹¹², J-E. Nitschke ⁵¹, E.K. Nkadimeng ^{34g}, T. Nobe ¹⁵⁶, T. Nommensen ¹⁵⁰, M.B. Norfolk ¹⁴², B.J. Norman ³⁵, M. Noury ^{36a}, J. Novak ⁹⁵, T. Novak ⁹⁵, L. Novotny ¹³⁵, R. Novotny ¹¹⁵, L. Nozka ¹²⁵, K. Ntekas ¹⁶², N.M.J. Nunes De Moura Junior ^{84b}, J. Ocariz ¹³⁰, A. Ochi ⁸⁶, I. Ochoa ^{133a}, S. Oerdek ^{49,t}, J.T. Offermann ⁴⁰, A. Ogrodnik ¹³⁶, A. Oh ¹⁰³, C.C. Ohm ¹⁴⁷, H. Oide ⁸⁵, R. Oishi ¹⁵⁶, M.L. Ojeda ⁴⁹, Y. Okumura ¹⁵⁶, L.F. Oleiro Seabra ^{133a}, I. Oleksiyuk ⁵⁷, S.A. Olivares Pino ^{140d}, G. Oliveira Correa ¹³, D. Oliveira Damazio ³⁰, J.L. Oliver ¹⁶², Ö.O. Öncel ⁵⁵, A.P. O'Neill ²⁰, A. Onofre ^{133a,133e}, P.U.E. Onyisi ¹¹, M.J. Oreglia ⁴⁰, G.E. Orellana ⁹², D. Orestano ^{78a,78b}, N. Orlando ¹³, R.S. Orr ¹⁵⁸, L.M. Osojnak ¹³¹, R. Ospanov ^{63a}, G. Otero y Garzon ³¹, H. Otono ⁹⁰, P.S. Ott ^{64a}, G.J. Ottino ^{18a}, M. Ouchrif ^{36d}, F. Ould-Saada ¹²⁸, T. Ovsiannikova ¹⁴¹, M. Owen ⁶⁰, R.E. Owen ¹³⁷, V.E. Ozcan ^{22a}, F. Ozturk ⁸⁸, N. Ozturk ⁸, S. Ozturk ⁸³, H.A. Pacey ¹²⁹, A. Pacheco Pages ¹³, C. Padilla Aranda ¹³, G. Padovano ^{76a,76b}, S. Pagan Griso ^{18a}, G. Palacino ⁶⁹, A. Palazzo ^{71a,71b}, J. Pampel ²⁵, J. Pan ¹⁷⁵, T. Pan ^{65a}, D.K. Panchal ¹¹, C.E. Pandini ¹¹⁷, J.G. Panduro Vazquez ¹³⁷, H.D. Pandya ¹, H. Pang ¹⁵, P. Pani ⁴⁹, G. Panizzo ^{70a,70c}, L. Panwar ¹³⁰, L. Paolozzi ⁵⁷, S. Parajuli ¹⁶⁵, A. Paramonov ⁶, C. Paraskevopoulos ⁵⁴, D. Paredes Hernandez ^{65b}, A. Pareti ^{74a,74b}, K.R. Park ⁴², T.H. Park ¹⁵⁸, M.A. Parker ³³, F. Parodi ^{58b,58a}, E.W. Parrish ¹¹⁸, V.A. Parrish ⁵³, J.A. Parsons ⁴², U. Parzefall ⁵⁵, B. Pascual Dias ¹¹⁰, L. Pascual Dominguez ¹⁰¹, E. Pasqualucci ^{76a}, S. Passaggio ^{58b}, F. Pastore ⁹⁷, P. Patel ⁸⁸, U.M. Patel ⁵², J.R. Pater ¹⁰³, T. Pauly ³⁷, C.I. Pazos ¹⁶¹, J. Pearkes ¹⁴⁶, M. Pedersen ¹²⁸, R. Pedro ^{133a}, S.V. Peleganchuk ³⁸, O. Penc ³⁷, E.A. Pender ⁵³, S. Peng ¹⁵, G.D. Penn ¹⁷⁵, K.E. Penski ¹¹¹, M. Penzin ³⁸, B.S. Peralva ^{84d}, A.P. Pereira Peixoto ¹⁴¹, L. Pereira Sanchez ¹⁴⁶, D.V. Perepelitsa ^{30,ae}, G. Perera ¹⁰⁵, E. Perez Codina ^{159a}, M. Perganti ¹⁰, H. Pernegger ³⁷, S. Perrella ^{76a,76b}, O. Perrin ⁴¹, K. Peters ⁴⁹, R.F.Y. Peters ¹⁰³, B.A. Petersen ³⁷, T.C. Petersen ⁴³, E. Petit ¹⁰⁴, V. Petousis ¹³⁵, C. Petridou ^{155,d}, T. Petru ¹³⁶, A. Petrukhin ¹⁴⁴, M. Pettee ^{18a}, A. Petukhov ³⁸, K. Petukhova ³⁷, R. Pezoa ^{140f}, L. Pezzotti ³⁷, G. Pezzullo ¹⁷⁵, T.M. Pham ¹⁷³, T. Pham ¹⁰⁷, P.W. Phillips ¹³⁷, G. Piacquadio ¹⁴⁸, E. Pianori ^{18a}, F. Piazza ¹²⁶, R. Piegai ³¹, D. Pietreanu ^{28b}, A.D. Pilkington ¹⁰³, M. Pinamonti ^{70a,70c}, J.L. Pinfeld ², B.C. Pinheiro Pereira ^{133a}, A.E. Pinto Pinoargote ^{138,138}, L. Pintucci ^{70a,70c}, K.M. Piper ¹⁴⁹, A. Pirttikoski ⁵⁷, D.A. Pizzi ³⁵, L. Pizzimento ^{65b}, A. Pizzini ¹¹⁷, M.-A. Pleier ³⁰, V. Pleskot ¹³⁶, E. Plotnikova³⁹, G. Poddar ⁹⁶, R. Poettgen ¹⁰⁰, L. Poggioli ¹³⁰, I. Pokharel ⁵⁶, S. Polacek ¹³⁶, G. Polesello ^{74a}, A. Poley ^{145,159a}, A. Polini ^{24b}, C.S. Pollard ¹⁷⁰, Z.B. Pollock ¹²², E. Pompa Pacchi ^{76a,76b}, N.I. Pond ⁹⁸, D. Ponomarenko ¹¹⁶, L. Pontecorvo ³⁷, S. Popa ^{28a}, G.A. Popeneciu ^{28d}, A. Poreba ³⁷, D.M. Portillo Quintero ^{159a}, S. Pospisil ¹³⁵, M.A. Postill ¹⁴², P. Postolache ^{28c},

K. Potamianos [id170](#), P.A. Potepa [id87a](#), I.N. Potrap [id39](#), C.J. Potter [id33](#), H. Potti [id150](#), J. Poveda [id166](#),
 M.E. Pozo Astigarraga [id37](#), A. Prades Ibanez [id77a,77b](#), J. Pretel [id168](#), D. Price [id103](#), M. Primavera [id71a](#),
 L. Primomo [id70a,70c](#), M.A. Principe Martin [id101](#), R. Privara [id125](#), T. Procter [id60](#), M.L. Proffitt [id141](#),
 N. Proklova [id131](#), K. Prokofiev [id65c](#), G. Proto [id112](#), J. Proudfoot [id6](#), M. Przybycien [id87a](#),
 W.W. Przygoda [id87b](#), A. Psallidas [id47](#), J.E. Puddefoot [id142](#), D. Pudzha [id55](#), D. Pyatiizbyantseva [id38](#),
 J. Qian [id108](#), D. Qichen [id103](#), Y. Qin [id13](#), T. Qiu [id53](#), A. Quadt [id56](#), M. Queitsch-Maitland [id103](#),
 G. Quetant [id57](#), R.P. Quinn [id167](#), G. Rabanal Bolanos [id62](#), D. Rafanoharana [id55](#), F. Raffaelli [id77a,77b](#),
 F. Ragusa [id72a,72b](#), J.L. Rainbolt [id40](#), J.A. Raine [id57](#), S. Rajagopalan [id30](#), E. Ramakoti [id38](#),
 L. Rambelli [id58b,58a](#), I.A. Ramirez-Berend [id35](#), K. Ran [id49,114c](#), D.S. Rankin [id131](#), N.P. Rapheeha [id34g](#),
 H. Rasheed [id28b](#), V. Raskina [id130](#), D.F. Rassloff [id64a](#), A. Rastogi [id18a](#), S. Rave [id102](#), S. Ravera [id58b,58a](#),
 B. Ravina [id56](#), I. Ravinovich [id172](#), M. Raymond [id37](#), A.L. Read [id128](#), N.P. Readioff [id142](#),
 D.M. Rebuzzi [id74a,74b](#), G. Redlinger [id30](#), A.S. Reed [id112](#), K. Reeves [id27](#), J.A. Reidelsturz [id174](#),
 D. Reikher [id126](#), A. Rej [id50](#), C. Rembser [id37](#), M. Renda [id28b](#), F. Renner [id49](#), A.G. Rennie [id162](#),
 A.L. Rescia [id49](#), S. Resconi [id72a](#), M. Ressegotti [id58b,58a](#), S. Rettie [id37](#), J.G. Reyes Rivera [id109](#),
 E. Reynolds [id18a](#), O.L. Rezanova [id38](#), P. Reznicek [id136](#), H. Riani [id36d](#), N. Ribaric [id93](#), E. Ricci [id79a,79b](#),
 R. Richter [id112](#), S. Richter [id48a,48b](#), E. Richter-Was [id87b](#), M. Ridel [id130](#), S. Ridouani [id36d](#), P. Rieck [id120](#),
 P. Riedler [id37](#), E.M. Riefel [id48a,48b](#), J.O. Rieger [id117](#), M. Rijssenbeek [id148](#), M. Rimoldi [id37](#),
 L. Rinaldi [id24b,24a](#), P. Rincke [id56,164](#), T.T. Rinn [id30](#), M.P. Rinnagel [id111](#), G. Ripellino [id164](#), I. Riu [id13](#),
 J.C. Rivera Vergara [id168](#), F. Rizatdinova [id124](#), E. Rizvi [id96](#), B.R. Roberts [id18a](#), S.S. Roberts [id139](#),
 S.H. Robertson [id106,w](#), D. Robinson [id33](#), M. Robles Manzano [id102](#), A. Robson [id60](#), A. Rocchi [id77a,77b](#),
 C. Roda [id75a,75b](#), S. Rodriguez Bosca [id37](#), Y. Rodriguez Garcia [id23a](#), A. Rodriguez Rodriguez [id55](#),
 A.M. Rodríguez Vera [id118](#), S. Roe [id37](#), J.T. Roemer [id37](#), A.R. Roepe-Gier [id139](#), O. Røhne [id128](#),
 R.A. Rojas [id105](#), C.P.A. Roland [id130](#), J. Roloff [id30](#), A. Romaniouk [id38](#), E. Romano [id74a,74b](#),
 M. Romano [id24b](#), A.C. Romero Hernandez [id165](#), N. Rompotis [id94](#), L. Roos [id130](#), S. Rosati [id76a](#),
 B.J. Rosser [id40](#), E. Rossi [id129](#), E. Rossi [id73a,73b](#), L.P. Rossi [id62](#), L. Rossini [id55](#), R. Rosten [id122](#),
 M. Rotaru [id28b](#), B. Rottler [id55](#), C. Rougier [id91](#), D. Rousseau [id67](#), D. Rousso [id49](#), A. Roy [id165](#),
 S. Roy-Garand [id158](#), A. Rozanov [id104](#), Z.M.A. Rozario [id60](#), Y. Rozen [id153](#), A. Rubio Jimenez [id166](#),
 A.J. Ruby [id94](#), V.H. Ruelas Rivera [id19](#), T.A. Ruggeri [id1](#), A. Ruggiero [id129](#), A. Ruiz-Martinez [id166](#),
 A. Rummler [id37](#), Z. Rurikova [id55](#), N.A. Rusakovich [id39](#), H.L. Russell [id168](#), G. Russo [id76a,76b](#),
 J.P. Rutherford [id7](#), S. Rutherford Colmenares [id33](#), M. Rybar [id136](#), E.B. Rye [id128](#), A. Ryzhov [id45](#),
 J.A. Sabater Iglesias [id57](#), H.F.W. Sadrozinski [id139](#), F. Safai Tehrani [id76a](#), B. Safarzadeh Samani [id137](#),
 S. Saha [id1](#), M. Sahinsoy [id83](#), A. Saibel [id166](#), M. Saimpert [id138](#), M. Saito [id156](#), T. Saito [id156](#),
 A. Sala [id72a,72b](#), D. Salamani [id37](#), A. Salnikov [id146](#), J. Salt [id166](#), A. Salvador Salas [id154](#),
 D. Salvatore [id44b,44a](#), F. Salvatore [id149](#), A. Salzburger [id37](#), D. Sammel [id55](#), E. Sampson [id93](#),
 D. Sampsonidis [id155,d](#), D. Sampsonidou [id126](#), J. Sánchez [id166](#), V. Sanchez Sebastian [id166](#),
 H. Sandaker [id128](#), C.O. Sander [id49](#), J.A. Sandesara [id105](#), M. Sandhoff [id174](#), C. Sandoval [id23b](#),
 L. Sanfilippo [id64a](#), D.P.C. Sankey [id137](#), T. Sano [id89](#), A. Sansoni [id54](#), L. Santi [id37,76b](#), C. Santoni [id41](#),
 H. Santos [id133a,133b](#), A. Santra [id172](#), E. Sanzani [id24b,24a](#), K.A. Saoucha [id163](#), J.G. Saraiva [id133a,133d](#),
 J. Sardain [id7](#), O. Sasaki [id85](#), K. Sato [id160](#), C. Sauer [id64b](#), E. Sauvan [id4](#), P. Savard [id158,ac](#), R. Sawada [id156](#),
 C. Sawyer [id137](#), L. Sawyer [id99](#), C. Sbarra [id24b](#), A. Sbrizzi [id24b,24a](#), T. Scanlon [id98](#),
 J. Schaarschmidt [id141](#), U. Schäfer [id102](#), A.C. Schaffer [id67,45](#), D. Schaile [id111](#), R.D. Schamberger [id148](#),
 C. Scharf [id19](#), M.M. Schefer [id20](#), V.A. Schegelsky [id38](#), D. Scheirich [id136](#), M. Schernau [id162](#),
 C. Scheulen [id56](#), C. Schiavi [id58b,58a](#), M. Schioppa [id44b,44a](#), B. Schlag [id146,m](#), K.E. Schleicher [id55](#),
 S. Schlenker [id37](#), J. Schmeing [id174](#), M.A. Schmidt [id174](#), K. Schmieden [id102](#), C. Schmitt [id102](#),
 N. Schmitt [id102](#), S. Schmitt [id49](#), L. Schoeffel [id138](#), A. Schoening [id64b](#), P.G. Scholer [id35](#), E. Schopf [id129](#),
 M. Schott [id25](#), J. Schovancova [id37](#), S. Schramm [id57](#), T. Schroer [id57](#), H-C. Schultz-Coulon [id64a](#),
 M. Schumacher [id55](#), B.A. Schumm [id139](#), Ph. Schune [id138](#), A.J. Schuy [id141](#), H.R. Schwartz [id139](#),

A. Schwartzman ¹⁴⁶, T.A. Schwarz ¹⁰⁸, Ph. Schwemling ¹³⁸, R. Schvienhorst ¹⁰⁹,
 F.G. Sciacca ²⁰, A. Sciandra ³⁰, G. Sciolla ²⁷, F. Scuri ^{75a}, C.D. Sebastiani ⁹⁴, K. Sedlaczek ¹¹⁸,
 S.C. Seidel ¹¹⁵, A. Seiden ¹³⁹, B.D. Seidlitz ⁴², C. Seitz ⁴⁹, J.M. Seixas ^{84b}, G. Sekhniaidze ^{73a},
 L. Selem ⁶¹, N. Semprini-Cesari ^{24b,24a}, D. Sengupta ⁵⁷, V. Senthilkumar ¹⁶⁶, L. Serin ⁶⁷,
 M. Sessa ^{77a,77b}, H. Severini ¹²³, F. Sforza ^{58b,58a}, A. Sfyrla ⁵⁷, Q. Sha ¹⁴, E. Shabalina ⁵⁶,
 A.H. Shah ³³, R. Shaheen ¹⁴⁷, J.D. Shahinian ¹³¹, D. Shaked Renous ¹⁷², L.Y. Shan ¹⁴,
 M. Shapiro ^{18a}, A. Sharma ³⁷, A.S. Sharma ¹⁶⁷, P. Sharma ⁸¹, P.B. Shatalov ³⁸, K. Shaw ¹⁴⁹,
 S.M. Shaw ¹⁰³, Q. Shen ^{63c}, D.J. Sheppard ¹⁴⁵, P. Sherwood ⁹⁸, L. Shi ⁹⁸, X. Shi ¹⁴,
 S. Shimizu ⁸⁵, C.O. Shimmin ¹⁷⁵, J.D. Shinner ⁹⁷, I.P.J. Shipsey ¹²⁹, S. Shirabe ⁹⁰,
 M. Shiyakova ^{39,u}, M.J. Shochet ⁴⁰, D.R. Shope ¹²⁸, B. Shrestha ¹²³, S. Shrestha ^{122,af},
 M.J. Shroff ¹⁶⁸, P. Sicho ¹³⁴, A.M. Sickles ¹⁶⁵, E. Sideras Haddad ^{34g}, A.C. Sidley ¹¹⁷,
 A. Sidoti ^{24b}, F. Siegert ⁵¹, Dj. Sijacki ¹⁶, F. Sili ⁹², J.M. Silva ⁵³, I. Silva Ferreira ^{84b},
 M.V. Silva Oliveira ³⁰, S.B. Silverstein ^{48a}, S. Simion ⁶⁷, R. Simoniello ³⁷, E.L. Simpson ¹⁰³,
 H. Simpson ¹⁴⁹, L.R. Simpson ¹⁰⁸, N.D. Simpson ¹⁰⁰, S. Simsek ⁸³, S. Sindhu ⁵⁶, P. Sinervo ¹⁵⁸,
 S. Singh ¹⁵⁸, S. Sinha ⁴⁹, S. Sinha ¹⁰³, M. Sioli ^{24b,24a}, I. Siral ³⁷, E. Sitnikova ⁴⁹,
 J. Sjölin ^{48a,48b}, A. Skaf ⁵⁶, E. Skorda ²¹, P. Skubic ¹²³, M. Slawinska ⁸⁸, V. Smakhtin ¹⁷²,
 B.H. Smart ¹³⁷, S.Yu. Smirnov ³⁸, Y. Smirnov ³⁸, L.N. Smirnova ^{38,a}, O. Smirnova ¹⁰⁰,
 A.C. Smith ⁴², D.R. Smith ¹⁶², E.A. Smith ⁴⁰, H.A. Smith ¹²⁹, J.L. Smith ¹⁰³, R. Smith ¹⁴⁶,
 M. Smizanska ⁹³, K. Smolek ¹³⁵, A.A. Snesarev ³⁸, S.R. Snider ¹⁵⁸, H.L. Snoek ¹¹⁷,
 S. Snyder ³⁰, R. Sobie ^{168,w}, A. Soffer ¹⁵⁴, C.A. Solans Sanchez ³⁷, E.Yu. Soldatov ³⁸,
 U. Soldevila ¹⁶⁶, A.A. Solodkov ³⁸, S. Solomon ²⁷, A. Soloshenko ³⁹, K. Solovieva ⁵⁵,
 O.V. Solovyanov ⁴¹, P. Sommer ⁵¹, A. Sonay ¹³, W.Y. Song ^{159b}, A. Sopczak ¹³⁵, A.L. Soppio ⁹⁸,
 F. Sopkova ^{29b}, J.D. Sorenson ¹¹⁵, I.R. Sotarriva Alvarez ¹⁵⁷, V. Sothilingam ^{64a},
 O.J. Soto Sandoval ^{140c,140b}, S. Sottocornola ⁶⁹, R. Soualah ¹⁶³, Z. Soumami ^{36e}, D. South ⁴⁹,
 N. Soybelman ¹⁷², S. Spagnolo ^{71a,71b}, M. Spalla ¹¹², D. Sperlich ⁵⁵, G. Spigo ³⁷,
 B. Spisso ^{73a,73b}, D.P. Spiteri ⁶⁰, M. Spousta ¹³⁶, E.J. Staats ³⁵, R. Stamen ^{64a}, A. Stampekis ²¹,
 M. Standke ²⁵, E. Stanecka ⁸⁸, W. Stanek-Maslouska ⁴⁹, M.V. Stange ⁵¹, B. Stanislaus ^{18a},
 M.M. Stanitzki ⁴⁹, B. Stapf ⁴⁹, E.A. Starchenko ³⁸, G.H. Stark ¹³⁹, J. Stark ⁹¹, P. Staroba ¹³⁴,
 P. Starovoitov ^{64a}, S. Stärz ¹⁰⁶, R. Staszewski ⁸⁸, G. Stavropoulos ⁴⁷, P. Steinberg ³⁰,
 B. Stelzer ^{145,159a}, H.J. Stelzer ¹³², O. Stelzer-Chilton ^{159a}, H. Stenzel ⁵⁹, T.J. Stevenson ¹⁴⁹,
 G.A. Stewart ³⁷, J.R. Stewart ¹²⁴, M.C. Stockton ³⁷, G. Stoicea ^{28b}, M. Stolarski ^{133a},
 S. Stonjek ¹¹², A. Straessner ⁵¹, J. Strandberg ¹⁴⁷, S. Strandberg ^{48a,48b}, M. Stratmann ¹⁷⁴,
 M. Strauss ¹²³, T. Streblor ¹⁰⁴, P. Strizenec ^{29b}, R. Ströhmer ¹⁶⁹, D.M. Strom ¹²⁶,
 R. Stroynowski ⁴⁵, A. Strubig ^{48a,48b}, S.A. Stucci ³⁰, B. Stugu ¹⁷, J. Stupak ¹²³, N.A. Styles ⁴⁹,
 D. Su ¹⁴⁶, S. Su ^{63a}, W. Su ^{63d}, X. Su ^{63a}, D. Suchy ^{29a}, K. Sugizaki ¹⁵⁶, V.V. Sulin ³⁸,
 M.J. Sullivan ⁹⁴, D.M.S. Sultan ¹²⁹, L. Sultanaliyeva ³⁸, S. Sultansoy ^{3b}, T. Sumida ⁸⁹,
 S. Sun ¹⁷³, O. Sunneborn Gudnadottir ¹⁶⁴, N. Sur ¹⁰⁴, M.R. Sutton ¹⁴⁹, H. Suzuki ¹⁶⁰,
 M. Svatos ¹³⁴, M. Swiatlowski ^{159a}, T. Swirski ¹⁶⁹, I. Sykora ^{29a}, M. Sykora ¹³⁶, T. Sykora ¹³⁶,
 D. Ta ¹⁰², K. Tackmann ^{49,t}, A. Taffard ¹⁶², R. Tafirout ^{159a}, J.S. Tafoya Vargas ⁶⁷, Y. Takubo ⁸⁵,
 M. Talby ¹⁰⁴, A.A. Talyshv ³⁸, K.C. Tam ^{65b}, N.M. Tamir ¹⁵⁴, A. Tanaka ¹⁵⁶, J. Tanaka ¹⁵⁶,
 R. Tanaka ⁶⁷, M. Tanasini ¹⁴⁸, Z. Tao ¹⁶⁷, S. Tapia Araya ^{140f}, S. Tapprogge ¹⁰²,
 A. Tarek Abouelfadl Mohamed ¹⁰⁹, S. Tarem ¹⁵³, K. Tariq ¹⁴, G. Tarna ^{28b}, G.F. Tartarelli ^{72a},
 M.J. Tartarin ⁹¹, P. Tas ¹³⁶, M. Tasevsky ¹³⁴, E. Tassi ^{44b,44a}, A.C. Tate ¹⁶⁵, G. Tateno ¹⁵⁶,
 Y. Tayalati ^{36e,v}, G.N. Taylor ¹⁰⁷, W. Taylor ^{159b}, R. Teixeira De Lima ¹⁴⁶, P. Teixeira-Dias ⁹⁷,
 J.J. Teoh ¹⁵⁸, K. Terashi ¹⁵⁶, J. Terron ¹⁰¹, S. Terzo ¹³, M. Testa ⁵⁴, R.J. Teuscher ^{158,w},
 A. Thaler ⁸⁰, O. Theiner ⁵⁷, N. Themistokleous ⁵³, T. Thevenaux-Pelzer ¹⁰⁴, O. Thielmann ¹⁷⁴,
 D.W. Thomas ⁹⁷, J.P. Thomas ²¹, E.A. Thompson ^{18a}, P.D. Thompson ²¹, E. Thomson ¹³¹,

R.E. Thornberry ^{id45}, C. Tian ^{id63a}, Y. Tian ^{id56}, V. Tikhomirov ^{id38,a}, Yu.A. Tikhonov ^{id38}, S. Timoshenko ^{id38}, D. Timoshyn ^{id136}, E.X.L. Ting ^{id1}, P. Tipton ^{id175}, A. Tishelman-Charny ^{id30}, S.H. Tlou ^{id34g}, K. Todome ^{id157}, S. Todorova-Nova ^{id136}, S. Todt ^{id51}, L. Toffolin ^{id70a,70c}, M. Togawa ^{id85}, J. Tojo ^{id90}, S. Tokár ^{id29a}, K. Tokushuku ^{id85}, O. Toldaiev ^{id69}, M. Tomoto ^{id85,113}, L. Tompkins ^{id146,m}, K.W. Topolnicki ^{id87b}, E. Torrence ^{id126}, H. Torres ^{id91}, E. Torró Pastor ^{id166}, M. Toscani ^{id31}, C. Toscirci ^{id40}, M. Tost ^{id11}, D.R. Tovey ^{id142}, I.S. Trandafir ^{id28b}, T. Trefzger ^{id169}, A. Tricoli ^{id30}, I.M. Trigger ^{id159a}, S. Trincaz-Duvoid ^{id130}, D.A. Trischuk ^{id27}, B. Trocmé ^{id61}, A. Tropina ^{id39}, L. Truong ^{id34c}, M. Trzebinski ^{id88}, A. Trzupiek ^{id88}, F. Tsai ^{id148}, M. Tsai ^{id108}, A. Tsiamis ^{id155,d}, P.V. Tsiareshka ^{id38}, S. Tsigaridas ^{id159a}, A. Tsirigotis ^{id155,r}, V. Tsiskaridze ^{id158}, E.G. Tskhadadze ^{id152a}, M. Tsopoulou ^{id155}, Y. Tsujikawa ^{id89}, I.I. Tsukerman ^{id38}, V. Tsulaia ^{id18a}, S. Tsuno ^{id85}, K. Tsurii ^{id121}, D. Tsybychev ^{id148}, Y. Tu ^{id65b}, A. Tudorache ^{id28b}, V. Tudorache ^{id28b}, A.N. Tuna ^{id62}, S. Turchikhin ^{id58b,58a}, I. Turk Cakir ^{id3a}, R. Turra ^{id72a}, T. Turtuvshin ^{id39}, P.M. Tuts ^{id42}, S. Tzamarias ^{id155,d}, E. Tzovara ^{id102}, F. Ukegawa ^{id160}, P.A. Ulloa Poblete ^{id140c,140b}, E.N. Umaka ^{id30}, G. Unal ^{id37}, A. Undrus ^{id30}, G. Unel ^{id162}, J. Urban ^{id29b}, P. Urrejola ^{id140a}, G. Usai ^{id8}, R. Ushioda ^{id157}, M. Usman ^{id110}, Z. Uysal ^{id83}, V. Vacek ^{id135}, B. Vachon ^{id106}, T. Vafeiadis ^{id37}, A. Vaitkus ^{id98}, C. Valderanis ^{id111}, E. Valdes Santurio ^{id48a,48b}, M. Valente ^{id159a}, S. Valentinetti ^{id24b,24a}, A. Valero ^{id166}, E. Valiente Moreno ^{id166}, A. Vallier ^{id91}, J.A. Valls Ferrer ^{id166}, D.R. Van Arneeman ^{id117}, T.R. Van Daalen ^{id141}, A. Van Der Graaf ^{id50}, P. Van Gemmeren ^{id6}, M. Van Rijnbach ^{id37}, S. Van Stroud ^{id98}, I. Van Vulpen ^{id117}, P. Vana ^{id136}, M. Vanadia ^{id77a,77b}, W. Vandelli ^{id37}, E.R. Vandewall ^{id124}, D. Vannicola ^{id154}, L. Vannoli ^{id54}, R. Vari ^{id76a}, E.W. Varnes ^{id7}, C. Varni ^{id18b}, T. Varol ^{id151}, D. Varouchas ^{id67}, L. Varriale ^{id166}, K.E. Varvell ^{id150}, M.E. Vasile ^{id28b}, L. Vaslin ^{id85}, G.A. Vasquez ^{id168}, A. Vasyukov ^{id39}, L.M. Vaughan ^{id124}, R. Vavricka ^{id102}, T. Vazquez Schroeder ^{id37}, J. Veatch ^{id32}, V. Vecchio ^{id103}, M.J. Veen ^{id105}, I. Veliscek ^{id30}, L.M. Veloce ^{id158}, F. Veloso ^{id133a,133c}, S. Veneziano ^{id76a}, A. Ventura ^{id71a,71b}, S. Ventura Gonzalez ^{id138}, A. Verbytskyi ^{id112}, M. Verducci ^{id75a,75b}, C. Vergis ^{id96}, M. Verissimo De Araujo ^{id84b}, W. Verkerke ^{id117}, J.C. Vermeulen ^{id117}, C. Vernieri ^{id146}, M. Vessella ^{id105}, M.C. Vetterli ^{id145,ac}, A. Vgenopoulos ^{id102}, N. Viaux Maira ^{id140f}, T. Vickey ^{id142}, O.E. Vickey Boeriu ^{id142}, G.H.A. Viehhauser ^{id129}, L. Vigani ^{id64b}, M. Vigl ^{id112}, M. Villa ^{id24b,24a}, M. Villaplana Perez ^{id166}, E.M. Villhauer ^{id53}, E. Vilucchi ^{id54}, M.G. Vincter ^{id35}, A. Visibile ^{id117}, C. Vittori ^{id37}, I. Vivarelli ^{id24b,24a}, E. Voevodina ^{id112}, F. Vogel ^{id111}, J.C. Voigt ^{id51}, P. Vokac ^{id135}, Yu. Volkotrub ^{id87b}, J. Von Ahnen ^{id49}, E. Von Toerne ^{id25}, B. Vormwald ^{id37}, V. Vorobel ^{id136}, K. Vorobev ^{id38}, M. Vos ^{id166}, K. Voss ^{id144}, M. Vozak ^{id117}, L. Vozdecky ^{id123}, N. Vranjes ^{id16}, M. Vranjes Milosavljevic ^{id16}, M. Vreeswijk ^{id117}, N.K. Vu ^{id63d,63c}, R. Vuillermet ^{id37}, O. Vujinovic ^{id102}, I. Vukotic ^{id40}, S. Wada ^{id160}, C. Wagner ^{id105}, J.M. Wagner ^{id18a}, W. Wagner ^{id174}, S. Wahdan ^{id174}, H. Wahlberg ^{id92}, J. Walder ^{id137}, R. Walker ^{id111}, W. Walkowiak ^{id144}, A. Wall ^{id131}, E.J. Wallin ^{id100}, T. Wamorkar ^{id6}, A.Z. Wang ^{id139}, C. Wang ^{id102}, C. Wang ^{id11}, H. Wang ^{id18a}, J. Wang ^{id65c}, P. Wang ^{id98}, R. Wang ^{id62}, R. Wang ^{id6}, S.M. Wang ^{id151}, S. Wang ^{id63b}, S. Wang ^{id14}, T. Wang ^{id63a}, W.T. Wang ^{id81}, W. Wang ^{id14}, X. Wang ^{id114a}, X. Wang ^{id165}, X. Wang ^{id63c}, Y. Wang ^{id63d}, Y. Wang ^{id114a}, Y. Wang ^{id63a}, Z. Wang ^{id108}, Z. Wang ^{id63d,52,63c}, Z. Wang ^{id108}, A. Warburton ^{id106}, R.J. Ward ^{id21}, N. Warrack ^{id60}, S. Waterhouse ^{id97}, A.T. Watson ^{id21}, H. Watson ^{id60}, M.F. Watson ^{id21}, E. Watton ^{id60,137}, G. Watts ^{id141}, B.M. Waugh ^{id98}, J.M. Webb ^{id55}, C. Weber ^{id30}, H.A. Weber ^{id19}, M.S. Weber ^{id20}, S.M. Weber ^{id64a}, C. Wei ^{id63a}, Y. Wei ^{id55}, A.R. Weidberg ^{id129}, E.J. Weik ^{id120}, J. Weingarten ^{id50}, C. Weiser ^{id55}, C.J. Wells ^{id49}, T. Wenaus ^{id30}, B. Wendland ^{id50}, T. Wengler ^{id37}, N.S. Wenke ^{id112}, N. Wermes ^{id25}, M. Wessels ^{id64a}, A.M. Wharton ^{id93}, A.S. White ^{id62}, A. White ^{id8}, M.J. White ^{id1}, D. Whiteson ^{id162}, L. Wickremasinghe ^{id127}, W. Wiedenmann ^{id173}, M. Wielers ^{id137}, C. Wiglesworth ^{id43}, D.J. Wilbern ^{id123}, H.G. Wilkens ^{id37}, J.J.H. Wilkinson ^{id33}, D.M. Williams ^{id42}, H.H. Williams ^{id131}, S. Williams ^{id33}, S. Willocq ^{id105}, B.J. Wilson ^{id103}, P.J. Windischhofer ^{id40}, F.I. Winkel ^{id31}, F. Winklmeier ^{id126}, B.T. Winter ^{id55},

J.K. Winter ¹⁰³, M. Wittgen¹⁴⁶, M. Wobisch ⁹⁹, T. Wojtkowski⁶¹, Z. Wolffs ¹¹⁷, J. Wollrath¹⁶², M.W. Wolter ⁸⁸, H. Wolters ^{133a,133c}, M.C. Wong¹³⁹, E.L. Woodward ⁴², S.D. Worm ⁴⁹, B.K. Wosiek ⁸⁸, K.W. Woźniak ⁸⁸, S. Wozniowski ⁵⁶, K. Wraight ⁶⁰, C. Wu ²¹, M. Wu ^{114b}, M. Wu ¹¹⁶, S.L. Wu ¹⁷³, X. Wu ⁵⁷, Y. Wu ^{63a}, Z. Wu ⁴, J. Wuerzinger ^{112,aa}, T.R. Wyatt ¹⁰³, B.M. Wynne ⁵³, S. Xella ⁴³, L. Xia ^{114a}, M. Xia ¹⁵, M. Xie ^{63a}, S. Xin ^{14,114c}, A. Xiong ¹²⁶, J. Xiong ^{18a}, D. Xu ¹⁴, H. Xu ^{63a}, L. Xu ^{63a}, R. Xu ¹³¹, T. Xu ¹⁰⁸, Y. Xu ¹⁵, Z. Xu ⁵³, Z. Xu^{114a}, B. Yabsley ¹⁵⁰, S. Yacoob ^{34a}, Y. Yamaguchi ⁸⁵, E. Yamashita ¹⁵⁶, H. Yamauchi ¹⁶⁰, T. Yamazaki ^{18a}, Y. Yamazaki ⁸⁶, J. Yan^{63c}, S. Yan ⁶⁰, Z. Yan ¹⁰⁵, H.J. Yang ^{63c,63d}, H.T. Yang ^{63a}, S. Yang ^{63a}, T. Yang ^{65c}, X. Yang ³⁷, X. Yang ¹⁴, Y. Yang ⁴⁵, Y. Yang^{63a}, Z. Yang ^{63a}, W-M. Yao ^{18a}, H. Ye ^{114a}, H. Ye ⁵⁶, J. Ye ¹⁴, S. Ye ³⁰, X. Ye ^{63a}, Y. Yeh ⁹⁸, I. Yeletsikh ³⁹, B.K. Yeo ^{18b}, M.R. Yexley ⁹⁸, T.P. Yildirim ¹²⁹, P. Yin ⁴², K. Yorita ¹⁷¹, S. Younas ^{28b}, C.J.S. Young ³⁷, C. Young ¹⁴⁶, C. Yu ^{14,114c}, Y. Yu ^{63a}, J. Yuan ^{14,114c}, M. Yuan ¹⁰⁸, R. Yuan ^{63d,63c}, L. Yue ⁹⁸, M. Zaazoua ^{63a}, B. Zabinski ⁸⁸, E. Zaid⁵³, Z.K. Zak ⁸⁸, T. Zakareishvili ¹⁶⁶, S. Zambito ⁵⁷, J.A. Zamora Saa ^{140d,140b}, J. Zang ¹⁵⁶, D. Zanzi ⁵⁵, O. Zaplatilek ¹³⁵, C. Zeitnitz ¹⁷⁴, H. Zeng ¹⁴, J.C. Zeng ¹⁶⁵, D.T. Zenger Jr ²⁷, O. Zenin ³⁸, T. Ženiš ^{29a}, S. Zenz ⁹⁶, S. Zerradi ^{36a}, D. Zerwas ⁶⁷, M. Zhai ^{14,114c}, D.F. Zhang ¹⁴², J. Zhang ^{63b}, J. Zhang ⁶, K. Zhang ^{14,114c}, L. Zhang ^{63a}, L. Zhang ^{114a}, P. Zhang ^{14,114c}, R. Zhang ¹⁷³, S. Zhang ¹⁰⁸, S. Zhang ⁹¹, T. Zhang ¹⁵⁶, X. Zhang ^{63c}, X. Zhang ^{63b}, Y. Zhang ^{63c}, Y. Zhang ⁹⁸, Y. Zhang ^{114a}, Z. Zhang ^{18a}, Z. Zhang ^{63b}, Z. Zhang ⁶⁷, H. Zhao ¹⁴¹, T. Zhao ^{63b}, Y. Zhao ¹³⁹, Z. Zhao ^{63a}, Z. Zhao ^{63a}, A. Zhemchugov ³⁹, J. Zheng ^{114a}, K. Zheng ¹⁶⁵, X. Zheng ^{63a}, Z. Zheng ¹⁴⁶, D. Zhong ¹⁶⁵, B. Zhou ¹⁰⁸, H. Zhou ⁷, N. Zhou ^{63c}, Y. Zhou¹⁵, Y. Zhou ^{114a}, Y. Zhou⁷, C.G. Zhu ^{63b}, J. Zhu ¹⁰⁸, X. Zhu^{63d}, Y. Zhu ^{63c}, Y. Zhu ^{63a}, X. Zhuang ¹⁴, K. Zhukov ⁶⁹, N.I. Zimine ³⁹, J. Zinsser ^{64b}, M. Ziolkowski ¹⁴⁴, L. Živković ¹⁶, A. Zoccoli ^{24b,24a}, K. Zoch ⁶², T.G. Zorbas ¹⁴², O. Zormpa ⁴⁷, W. Zou ⁴², L. Zwalinski ³⁷.

¹Department of Physics, University of Adelaide, Adelaide; Australia.

²Department of Physics, University of Alberta, Edmonton AB; Canada.

³(^a)Department of Physics, Ankara University, Ankara; (^b)Division of Physics, TOBB University of Economics and Technology, Ankara; Türkiye.

⁴LAPP, Université Savoie Mont Blanc, CNRS/IN2P3, Annecy; France.

⁵APC, Université Paris Cité, CNRS/IN2P3, Paris; France.

⁶High Energy Physics Division, Argonne National Laboratory, Argonne IL; United States of America.

⁷Department of Physics, University of Arizona, Tucson AZ; United States of America.

⁸Department of Physics, University of Texas at Arlington, Arlington TX; United States of America.

⁹Physics Department, National and Kapodistrian University of Athens, Athens; Greece.

¹⁰Physics Department, National Technical University of Athens, Zografou; Greece.

¹¹Department of Physics, University of Texas at Austin, Austin TX; United States of America.

¹²Institute of Physics, Azerbaijan Academy of Sciences, Baku; Azerbaijan.

¹³Institut de Física d'Altes Energies (IFAE), Barcelona Institute of Science and Technology, Barcelona; Spain.

¹⁴Institute of High Energy Physics, Chinese Academy of Sciences, Beijing; China.

¹⁵Physics Department, Tsinghua University, Beijing; China.

¹⁶Institute of Physics, University of Belgrade, Belgrade; Serbia.

¹⁷Department for Physics and Technology, University of Bergen, Bergen; Norway.

¹⁸(^a)Physics Division, Lawrence Berkeley National Laboratory, Berkeley CA; (^b)University of California, Berkeley CA; United States of America.

- ¹⁹Institut für Physik, Humboldt Universität zu Berlin, Berlin; Germany.
- ²⁰Albert Einstein Center for Fundamental Physics and Laboratory for High Energy Physics, University of Bern, Bern; Switzerland.
- ²¹School of Physics and Astronomy, University of Birmingham, Birmingham; United Kingdom.
- ²²(^a) Department of Physics, Bogazici University, Istanbul; (^b) Department of Physics Engineering, Gaziantep University, Gaziantep; (^c) Department of Physics, Istanbul University, Istanbul; Türkiye.
- ²³(^a) Facultad de Ciencias y Centro de Investigaciones, Universidad Antonio Nariño, Bogotá; (^b) Departamento de Física, Universidad Nacional de Colombia, Bogotá; Colombia.
- ²⁴(^a) Dipartimento di Fisica e Astronomia A. Righi, Università di Bologna, Bologna; (^b) INFN Sezione di Bologna; Italy.
- ²⁵Physikalisches Institut, Universität Bonn, Bonn; Germany.
- ²⁶Department of Physics, Boston University, Boston MA; United States of America.
- ²⁷Department of Physics, Brandeis University, Waltham MA; United States of America.
- ²⁸(^a) Transilvania University of Brasov, Brasov; (^b) Horia Hulubei National Institute of Physics and Nuclear Engineering, Bucharest; (^c) Department of Physics, Alexandru Ioan Cuza University of Iasi, Iasi; (^d) National Institute for Research and Development of Isotopic and Molecular Technologies, Physics Department, Cluj-Napoca; (^e) National University of Science and Technology Politehnica, Bucharest; (^f) West University in Timisoara, Timisoara; (^g) Faculty of Physics, University of Bucharest, Bucharest; Romania.
- ²⁹(^a) Faculty of Mathematics, Physics and Informatics, Comenius University, Bratislava; (^b) Department of Subnuclear Physics, Institute of Experimental Physics of the Slovak Academy of Sciences, Kosice; Slovak Republic.
- ³⁰Physics Department, Brookhaven National Laboratory, Upton NY; United States of America.
- ³¹Universidad de Buenos Aires, Facultad de Ciencias Exactas y Naturales, Departamento de Física, y CONICET, Instituto de Física de Buenos Aires (IFIBA), Buenos Aires; Argentina.
- ³²California State University, CA; United States of America.
- ³³Cavendish Laboratory, University of Cambridge, Cambridge; United Kingdom.
- ³⁴(^a) Department of Physics, University of Cape Town, Cape Town; (^b) iThemba Labs, Western Cape; (^c) Department of Mechanical Engineering Science, University of Johannesburg, Johannesburg; (^d) National Institute of Physics, University of the Philippines Diliman (Philippines); (^e) University of South Africa, Department of Physics, Pretoria; (^f) University of Zululand, KwaDlangezwa; (^g) School of Physics, University of the Witwatersrand, Johannesburg; South Africa.
- ³⁵Department of Physics, Carleton University, Ottawa ON; Canada.
- ³⁶(^a) Faculté des Sciences Ain Chock, Université Hassan II de Casablanca; (^b) Faculté des Sciences, Université Ibn-Tofail, Kénitra; (^c) Faculté des Sciences Semlalia, Université Cadi Ayyad, LPHEA-Marrakech; (^d) LPMR, Faculté des Sciences, Université Mohamed Premier, Oujda; (^e) Faculté des sciences, Université Mohammed V, Rabat; (^f) Institute of Applied Physics, Mohammed VI Polytechnic University, Ben Guerir; Morocco.
- ³⁷CERN, Geneva; Switzerland.
- ³⁸Affiliated with an institute covered by a cooperation agreement with CERN.
- ³⁹Affiliated with an international laboratory covered by a cooperation agreement with CERN.
- ⁴⁰Enrico Fermi Institute, University of Chicago, Chicago IL; United States of America.
- ⁴¹LPC, Université Clermont Auvergne, CNRS/IN2P3, Clermont-Ferrand; France.
- ⁴²Nevis Laboratory, Columbia University, Irvington NY; United States of America.
- ⁴³Niels Bohr Institute, University of Copenhagen, Copenhagen; Denmark.
- ⁴⁴(^a) Dipartimento di Fisica, Università della Calabria, Rende; (^b) INFN Gruppo Collegato di Cosenza, Laboratori Nazionali di Frascati; Italy.
- ⁴⁵Physics Department, Southern Methodist University, Dallas TX; United States of America.

- ⁴⁶Physics Department, University of Texas at Dallas, Richardson TX; United States of America.
- ⁴⁷National Centre for Scientific Research "Demokritos", Agia Paraskevi; Greece.
- ⁴⁸(^a) Department of Physics, Stockholm University; (^b) Oskar Klein Centre, Stockholm; Sweden.
- ⁴⁹Deutsches Elektronen-Synchrotron DESY, Hamburg and Zeuthen; Germany.
- ⁵⁰Fakultät Physik, Technische Universität Dortmund, Dortmund; Germany.
- ⁵¹Institut für Kern- und Teilchenphysik, Technische Universität Dresden, Dresden; Germany.
- ⁵²Department of Physics, Duke University, Durham NC; United States of America.
- ⁵³SUPA - School of Physics and Astronomy, University of Edinburgh, Edinburgh; United Kingdom.
- ⁵⁴INFN e Laboratori Nazionali di Frascati, Frascati; Italy.
- ⁵⁵Physikalisches Institut, Albert-Ludwigs-Universität Freiburg, Freiburg; Germany.
- ⁵⁶II. Physikalisches Institut, Georg-August-Universität Göttingen, Göttingen; Germany.
- ⁵⁷Département de Physique Nucléaire et Corpusculaire, Université de Genève, Genève; Switzerland.
- ⁵⁸(^a) Dipartimento di Fisica, Università di Genova, Genova; (^b) INFN Sezione di Genova; Italy.
- ⁵⁹II. Physikalisches Institut, Justus-Liebig-Universität Giessen, Giessen; Germany.
- ⁶⁰SUPA - School of Physics and Astronomy, University of Glasgow, Glasgow; United Kingdom.
- ⁶¹LPSC, Université Grenoble Alpes, CNRS/IN2P3, Grenoble INP, Grenoble; France.
- ⁶²Laboratory for Particle Physics and Cosmology, Harvard University, Cambridge MA; United States of America.
- ⁶³(^a) Department of Modern Physics and State Key Laboratory of Particle Detection and Electronics, University of Science and Technology of China, Hefei; (^b) Institute of Frontier and Interdisciplinary Science and Key Laboratory of Particle Physics and Particle Irradiation (MOE), Shandong University, Qingdao; (^c) School of Physics and Astronomy, Shanghai Jiao Tong University, Key Laboratory for Particle Astrophysics and Cosmology (MOE), SKLPPC, Shanghai; (^d) Tsung-Dao Lee Institute, Shanghai; (^e) School of Physics and Microelectronics, Zhengzhou University; China.
- ⁶⁴(^a) Kirchhoff-Institut für Physik, Ruprecht-Karls-Universität Heidelberg, Heidelberg; (^b) Physikalisches Institut, Ruprecht-Karls-Universität Heidelberg, Heidelberg; Germany.
- ⁶⁵(^a) Department of Physics, Chinese University of Hong Kong, Shatin, N.T., Hong Kong; (^b) Department of Physics, University of Hong Kong, Hong Kong; (^c) Department of Physics and Institute for Advanced Study, Hong Kong University of Science and Technology, Clear Water Bay, Kowloon, Hong Kong; China.
- ⁶⁶Department of Physics, National Tsing Hua University, Hsinchu; Taiwan.
- ⁶⁷IJCLab, Université Paris-Saclay, CNRS/IN2P3, 91405, Orsay; France.
- ⁶⁸Centro Nacional de Microelectrónica (IMB-CNM-CSIC), Barcelona; Spain.
- ⁶⁹Department of Physics, Indiana University, Bloomington IN; United States of America.
- ⁷⁰(^a) INFN Gruppo Collegato di Udine, Sezione di Trieste, Udine; (^b) ICTP, Trieste; (^c) Dipartimento Politecnico di Ingegneria e Architettura, Università di Udine, Udine; Italy.
- ⁷¹(^a) INFN Sezione di Lecce; (^b) Dipartimento di Matematica e Fisica, Università del Salento, Lecce; Italy.
- ⁷²(^a) INFN Sezione di Milano; (^b) Dipartimento di Fisica, Università di Milano, Milano; Italy.
- ⁷³(^a) INFN Sezione di Napoli; (^b) Dipartimento di Fisica, Università di Napoli, Napoli; Italy.
- ⁷⁴(^a) INFN Sezione di Pavia; (^b) Dipartimento di Fisica, Università di Pavia, Pavia; Italy.
- ⁷⁵(^a) INFN Sezione di Pisa; (^b) Dipartimento di Fisica E. Fermi, Università di Pisa, Pisa; Italy.
- ⁷⁶(^a) INFN Sezione di Roma; (^b) Dipartimento di Fisica, Sapienza Università di Roma, Roma; Italy.
- ⁷⁷(^a) INFN Sezione di Roma Tor Vergata; (^b) Dipartimento di Fisica, Università di Roma Tor Vergata, Roma; Italy.
- ⁷⁸(^a) INFN Sezione di Roma Tre; (^b) Dipartimento di Matematica e Fisica, Università Roma Tre, Roma; Italy.
- ⁷⁹(^a) INFN-TIFPA; (^b) Università degli Studi di Trento, Trento; Italy.
- ⁸⁰Universität Innsbruck, Department of Astro and Particle Physics, Innsbruck; Austria.

- ⁸¹University of Iowa, Iowa City IA; United States of America.
- ⁸²Department of Physics and Astronomy, Iowa State University, Ames IA; United States of America.
- ⁸³Istinye University, Sariyer, Istanbul; Türkiye.
- ⁸⁴(^a) Departamento de Engenharia Elétrica, Universidade Federal de Juiz de Fora (UFJF), Juiz de Fora; (^b) Universidade Federal do Rio De Janeiro COPPE/EE/IF, Rio de Janeiro; (^c) Instituto de Física, Universidade de São Paulo, São Paulo; (^d) Rio de Janeiro State University, Rio de Janeiro; (^e) Federal University of Bahia, Bahia; Brazil.
- ⁸⁵KEK, High Energy Accelerator Research Organization, Tsukuba; Japan.
- ⁸⁶Graduate School of Science, Kobe University, Kobe; Japan.
- ⁸⁷(^a) AGH University of Krakow, Faculty of Physics and Applied Computer Science, Krakow; (^b) Marian Smoluchowski Institute of Physics, Jagiellonian University, Krakow; Poland.
- ⁸⁸Institute of Nuclear Physics Polish Academy of Sciences, Krakow; Poland.
- ⁸⁹Faculty of Science, Kyoto University, Kyoto; Japan.
- ⁹⁰Research Center for Advanced Particle Physics and Department of Physics, Kyushu University, Fukuoka ; Japan.
- ⁹¹L2IT, Université de Toulouse, CNRS/IN2P3, UPS, Toulouse; France.
- ⁹²Instituto de Física La Plata, Universidad Nacional de La Plata and CONICET, La Plata; Argentina.
- ⁹³Physics Department, Lancaster University, Lancaster; United Kingdom.
- ⁹⁴Oliver Lodge Laboratory, University of Liverpool, Liverpool; United Kingdom.
- ⁹⁵Department of Experimental Particle Physics, Jožef Stefan Institute and Department of Physics, University of Ljubljana, Ljubljana; Slovenia.
- ⁹⁶School of Physics and Astronomy, Queen Mary University of London, London; United Kingdom.
- ⁹⁷Department of Physics, Royal Holloway University of London, Egham; United Kingdom.
- ⁹⁸Department of Physics and Astronomy, University College London, London; United Kingdom.
- ⁹⁹Louisiana Tech University, Ruston LA; United States of America.
- ¹⁰⁰Fysiska institutionen, Lunds universitet, Lund; Sweden.
- ¹⁰¹Departamento de Física Teórica C-15 and CIAFF, Universidad Autónoma de Madrid, Madrid; Spain.
- ¹⁰²Institut für Physik, Universität Mainz, Mainz; Germany.
- ¹⁰³School of Physics and Astronomy, University of Manchester, Manchester; United Kingdom.
- ¹⁰⁴CPPM, Aix-Marseille Université, CNRS/IN2P3, Marseille; France.
- ¹⁰⁵Department of Physics, University of Massachusetts, Amherst MA; United States of America.
- ¹⁰⁶Department of Physics, McGill University, Montreal QC; Canada.
- ¹⁰⁷School of Physics, University of Melbourne, Victoria; Australia.
- ¹⁰⁸Department of Physics, University of Michigan, Ann Arbor MI; United States of America.
- ¹⁰⁹Department of Physics and Astronomy, Michigan State University, East Lansing MI; United States of America.
- ¹¹⁰Group of Particle Physics, University of Montreal, Montreal QC; Canada.
- ¹¹¹Fakultät für Physik, Ludwig-Maximilians-Universität München, München; Germany.
- ¹¹²Max-Planck-Institut für Physik (Werner-Heisenberg-Institut), München; Germany.
- ¹¹³Graduate School of Science and Kobayashi-Maskawa Institute, Nagoya University, Nagoya; Japan.
- ¹¹⁴(^a) Department of Physics, Nanjing University, Nanjing; (^b) School of Science, Shenzhen Campus of Sun Yat-sen University; (^c) University of Chinese Academy of Science (UCAS), Beijing; China.
- ¹¹⁵Department of Physics and Astronomy, University of New Mexico, Albuquerque NM; United States of America.
- ¹¹⁶Institute for Mathematics, Astrophysics and Particle Physics, Radboud University/Nikhef, Nijmegen; Netherlands.
- ¹¹⁷Nikhef National Institute for Subatomic Physics and University of Amsterdam, Amsterdam;

Netherlands.

¹¹⁸Department of Physics, Northern Illinois University, DeKalb IL; United States of America.

¹¹⁹^(a)New York University Abu Dhabi, Abu Dhabi;^(b)United Arab Emirates University, Al Ain; United Arab Emirates.

¹²⁰Department of Physics, New York University, New York NY; United States of America.

¹²¹Ochanomizu University, Otsuka, Bunkyo-ku, Tokyo; Japan.

¹²²Ohio State University, Columbus OH; United States of America.

¹²³Homer L. Dodge Department of Physics and Astronomy, University of Oklahoma, Norman OK; United States of America.

¹²⁴Department of Physics, Oklahoma State University, Stillwater OK; United States of America.

¹²⁵Palacký University, Joint Laboratory of Optics, Olomouc; Czech Republic.

¹²⁶Institute for Fundamental Science, University of Oregon, Eugene, OR; United States of America.

¹²⁷Graduate School of Science, Osaka University, Osaka; Japan.

¹²⁸Department of Physics, University of Oslo, Oslo; Norway.

¹²⁹Department of Physics, Oxford University, Oxford; United Kingdom.

¹³⁰LPNHE, Sorbonne Université, Université Paris Cité, CNRS/IN2P3, Paris; France.

¹³¹Department of Physics, University of Pennsylvania, Philadelphia PA; United States of America.

¹³²Department of Physics and Astronomy, University of Pittsburgh, Pittsburgh PA; United States of America.

¹³³^(a)Laboratório de Instrumentação e Física Experimental de Partículas - LIP, Lisboa;^(b)Departamento de Física, Faculdade de Ciências, Universidade de Lisboa, Lisboa;^(c)Departamento de Física, Universidade de Coimbra, Coimbra;^(d)Centro de Física Nuclear da Universidade de Lisboa, Lisboa;^(e)Departamento de Física, Universidade do Minho, Braga;^(f)Departamento de Física Teórica y del Cosmos, Universidad de Granada, Granada (Spain);^(g)Departamento de Física, Instituto Superior Técnico, Universidade de Lisboa, Lisboa; Portugal.

¹³⁴Institute of Physics of the Czech Academy of Sciences, Prague; Czech Republic.

¹³⁵Czech Technical University in Prague, Prague; Czech Republic.

¹³⁶Charles University, Faculty of Mathematics and Physics, Prague; Czech Republic.

¹³⁷Particle Physics Department, Rutherford Appleton Laboratory, Didcot; United Kingdom.

¹³⁸IRFU, CEA, Université Paris-Saclay, Gif-sur-Yvette; France.

¹³⁹Santa Cruz Institute for Particle Physics, University of California Santa Cruz, Santa Cruz CA; United States of America.

¹⁴⁰^(a)Departamento de Física, Pontificia Universidad Católica de Chile, Santiago;^(b)Millennium Institute for Subatomic physics at high energy frontier (SAPHIR), Santiago;^(c)Instituto de Investigación Multidisciplinario en Ciencia y Tecnología, y Departamento de Física, Universidad de La Serena;^(d)Universidad Andres Bello, Department of Physics, Santiago;^(e)Instituto de Alta Investigación, Universidad de Tarapacá, Arica;^(f)Departamento de Física, Universidad Técnica Federico Santa María, Valparaíso; Chile.

¹⁴¹Department of Physics, University of Washington, Seattle WA; United States of America.

¹⁴²Department of Physics and Astronomy, University of Sheffield, Sheffield; United Kingdom.

¹⁴³Department of Physics, Shinshu University, Nagano; Japan.

¹⁴⁴Department Physik, Universität Siegen, Siegen; Germany.

¹⁴⁵Department of Physics, Simon Fraser University, Burnaby BC; Canada.

¹⁴⁶SLAC National Accelerator Laboratory, Stanford CA; United States of America.

¹⁴⁷Department of Physics, Royal Institute of Technology, Stockholm; Sweden.

¹⁴⁸Departments of Physics and Astronomy, Stony Brook University, Stony Brook NY; United States of America.

- ¹⁴⁹Department of Physics and Astronomy, University of Sussex, Brighton; United Kingdom.
- ¹⁵⁰School of Physics, University of Sydney, Sydney; Australia.
- ¹⁵¹Institute of Physics, Academia Sinica, Taipei; Taiwan.
- ¹⁵²(^a) E. Andronikashvili Institute of Physics, Iv. Javakhishvili Tbilisi State University, Tbilisi; (^b) High Energy Physics Institute, Tbilisi State University, Tbilisi; (^c) University of Georgia, Tbilisi; Georgia.
- ¹⁵³Department of Physics, Technion, Israel Institute of Technology, Haifa; Israel.
- ¹⁵⁴Raymond and Beverly Sackler School of Physics and Astronomy, Tel Aviv University, Tel Aviv; Israel.
- ¹⁵⁵Department of Physics, Aristotle University of Thessaloniki, Thessaloniki; Greece.
- ¹⁵⁶International Center for Elementary Particle Physics and Department of Physics, University of Tokyo, Tokyo; Japan.
- ¹⁵⁷Department of Physics, Tokyo Institute of Technology, Tokyo; Japan.
- ¹⁵⁸Department of Physics, University of Toronto, Toronto ON; Canada.
- ¹⁵⁹(^a) TRIUMF, Vancouver BC; (^b) Department of Physics and Astronomy, York University, Toronto ON; Canada.
- ¹⁶⁰Division of Physics and Tomonaga Center for the History of the Universe, Faculty of Pure and Applied Sciences, University of Tsukuba, Tsukuba; Japan.
- ¹⁶¹Department of Physics and Astronomy, Tufts University, Medford MA; United States of America.
- ¹⁶²Department of Physics and Astronomy, University of California Irvine, Irvine CA; United States of America.
- ¹⁶³University of Sharjah, Sharjah; United Arab Emirates.
- ¹⁶⁴Department of Physics and Astronomy, University of Uppsala, Uppsala; Sweden.
- ¹⁶⁵Department of Physics, University of Illinois, Urbana IL; United States of America.
- ¹⁶⁶Instituto de Física Corpuscular (IFIC), Centro Mixto Universidad de Valencia - CSIC, Valencia; Spain.
- ¹⁶⁷Department of Physics, University of British Columbia, Vancouver BC; Canada.
- ¹⁶⁸Department of Physics and Astronomy, University of Victoria, Victoria BC; Canada.
- ¹⁶⁹Fakultät für Physik und Astronomie, Julius-Maximilians-Universität Würzburg, Würzburg; Germany.
- ¹⁷⁰Department of Physics, University of Warwick, Coventry; United Kingdom.
- ¹⁷¹Waseda University, Tokyo; Japan.
- ¹⁷²Department of Particle Physics and Astrophysics, Weizmann Institute of Science, Rehovot; Israel.
- ¹⁷³Department of Physics, University of Wisconsin, Madison WI; United States of America.
- ¹⁷⁴Fakultät für Mathematik und Naturwissenschaften, Fachgruppe Physik, Bergische Universität Wuppertal, Wuppertal; Germany.
- ¹⁷⁵Department of Physics, Yale University, New Haven CT; United States of America.
- ^a Also Affiliated with an institute covered by a cooperation agreement with CERN.
- ^b Also at An-Najah National University, Nablus; Palestine.
- ^c Also at Borough of Manhattan Community College, City University of New York, New York NY; United States of America.
- ^d Also at Center for Interdisciplinary Research and Innovation (CIRI-AUTH), Thessaloniki; Greece.
- ^e Also at Centro Studi e Ricerche Enrico Fermi; Italy.
- ^f Also at CERN, Geneva; Switzerland.
- ^g Also at CMD-AC UNEC Research Center, Azerbaijan State University of Economics (UNEC); Azerbaijan.
- ^h Also at Département de Physique Nucléaire et Corpusculaire, Université de Genève, Genève; Switzerland.
- ⁱ Also at Departament de Física de la Universitat Autònoma de Barcelona, Barcelona; Spain.
- ^j Also at Department of Financial and Management Engineering, University of the Aegean, Chios; Greece.
- ^k Also at Department of Physics, California State University, Sacramento; United States of America.

- ^l Also at Department of Physics, King's College London, London; United Kingdom.
- ^m Also at Department of Physics, Stanford University, Stanford CA; United States of America.
- ⁿ Also at Department of Physics, Stellenbosch University; South Africa.
- ^o Also at Department of Physics, University of Fribourg, Fribourg; Switzerland.
- ^p Also at Department of Physics, University of Thessaly; Greece.
- ^q Also at Department of Physics, Westmont College, Santa Barbara; United States of America.
- ^r Also at Hellenic Open University, Patras; Greece.
- ^s Also at Institutio Catalana de Recerca i Estudis Avancats, ICREA, Barcelona; Spain.
- ^t Also at Institut für Experimentalphysik, Universität Hamburg, Hamburg; Germany.
- ^u Also at Institute for Nuclear Research and Nuclear Energy (INRNE) of the Bulgarian Academy of Sciences, Sofia; Bulgaria.
- ^v Also at Institute of Applied Physics, Mohammed VI Polytechnic University, Ben Guerir; Morocco.
- ^w Also at Institute of Particle Physics (IPP); Canada.
- ^x Also at Institute of Physics, Azerbaijan Academy of Sciences, Baku; Azerbaijan.
- ^y Also at Institute of Theoretical Physics, Ilia State University, Tbilisi; Georgia.
- ^z Also at National Institute of Physics, University of the Philippines Diliman (Philippines); Philippines.
- ^{aa} Also at Technical University of Munich, Munich; Germany.
- ^{ab} Also at The Collaborative Innovation Center of Quantum Matter (CICQM), Beijing; China.
- ^{ac} Also at TRIUMF, Vancouver BC; Canada.
- ^{ad} Also at Università di Napoli Parthenope, Napoli; Italy.
- ^{ae} Also at University of Colorado Boulder, Department of Physics, Colorado; United States of America.
- ^{af} Also at Washington College, Chestertown, MD; United States of America.
- ^{ag} Also at Yeditepe University, Physics Department, Istanbul; Türkiye.
- * Deceased